Understanding the spread and eradication of novel zoonotic diseases through the study of a compartmental epidemiological model

A Master's Thesis by
Mats Lindström

With many thanks to my supervisor
Éva Kisdi

University of Helsinki
Department of Science
Faculty of Mathematics and Statistics

October 30, 2020

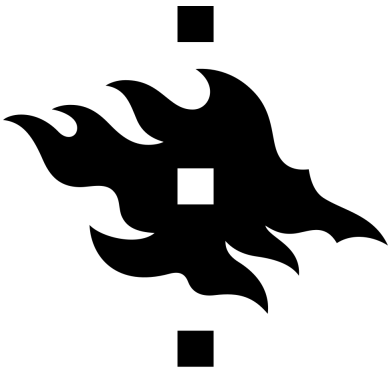

HELSINGIN YLIOPISTO
HELSINGFORS UNIVERSITET
UNIVERSITY OF HELSINKI

HELSINGIN YLIOPISTO — HELSINGFORS UNIVERSITET — UNIVERSITY OF HELSINKI

Tiedekunta/Osasto — Fakultet/Sektion — Faculty	Laitos — Institution — Department
Faculty of Science	Department of Mathematics and Statistics

Tekijä — Författare — Author
Mats Johan Wilhelm Lindström

Työn nimi — Arbetets titel — Title
Understanding the spread and eradication of novel zoonotic diseases through the study of a compartmental epidemiological model

Oppiaine — Läroämne — Subject
Mathematics

Työn laji — Arbetets art — Level	Aika — Datum — Month and year	Sivumäärä — Sidoantal — Number of pages
Pro gradu -thesis	October 2020	111

Tiivistelmä — Referat — Abstract

Studying the spread of diseases through mathematical models provides an excellent tool for understanding and predicting epidemiological phenomena in the real world. In particular, understanding which actions facilitate the containment and eventual eradication of a pathogen in a host population is of central importance. In this thesis we present and study a compartmental epidemiological model that exhibits rich dynamical behaviours. The model that we study is a generalisation of the commonly known SIR-model and similar to the SEIR-model, as it incorporates a compartment for asymptomatic carriers of the pathogen.

We begin the analysis in section 2, where we examine the most basic modelling assumptions of this thesis and present our model together with the aforementioned SIR- and SEIR-models for comparison.

In section 3 we give a brief introduction to the analytic and numerical methods used in the analysis of our model. The analytic methods include defining the state space and phase space as well as a rundown of linear stability analysis. We conclude the section by presenting the numerical algorithm by which stable limit cycles appearing in the demographic dynamics of the model are found.

In section 4 we delve into the demographic analysis of our model. We begin by introducing the basic reproduction number, R_0. After this we study the equilibria of the system, with an emphasis on the equilibria that admit a biological interpretation. We then proceed with the bifurcation analysis, finding conditions for forwards and backwards transcritical bifurcations and showing that a backwards bifurcation implies the existence of a biologically meaningful saddle-node bifurcation. Finally, we conclude section 4 by studying examples of the demographic dynamics and bifurcation patterns. Here we also see examples of Hopf bifurcations giving rise to stable limit cycles.

In section 5 we introduce the mechanisms of evolution for the pathogen and host. We present models that describe the dynamics of a rare mutant in an established resident population and study under which conditions a mutant can invade and eventually replace the resident population in an invasion-replacement event.

In section 6 we expand on the preceding section by looking at the long term dynamics of evolution as it proceeds through successive invasion-replacement events. In a major result of this section, we connect the evolutionary dynamics to the bifurcation analysis when we identify the existence of a biologically meaningful saddle-node bifurcation as a necessary condition for the eradication of the pathogen through evolutionary means. Moreover, we provide examples of host and pathogen evolution. In particular, we showcase situations where the pathogen eradicates itself through evolutionary suicide.

Section 7 concludes the thesis with a discussion around the central results and further research questions. Finally, the appendix collects a variety of results that were excluded from the main part of the thesis.

Avainsanat — Nyckelord — Keywords
mathematical modelling, compartmental epidemiological model, adaptive dynamics

Säilytyspaikka — Förvaringsställe — Where deposited
Electronic thesis archive E-thesis

Muita tietoja — Övriga uppgifter — Additional information

Abstract

Within the last century humanity has grown significantly more numerous and more globally connected than ever before in its history. Together with the increased risks of climate change, we are more susceptible than ever to major epidemics and pandemics caused by novel zoonotic diseases. For these reasons it is not only important understand under which conditions novel pathogens are able to invade and spread in a host population but also to understand how these pathogens can be eradicated following an invasion event.

In this thesis we present and study the demographic and evolutionary dynamics of a compartmental epidemiological model that includes a compartment for asymptomatic individuals, who require a second infection to become symptomatic and infectious. We show that the model exhibits a wide variety of demographic dynamical behaviour, all of which can be evolutionarily attracting configurations under simple evolutionary considerations. The model is an extreme simplification of the real world and excludes relevant information such as age and spatial structures of the population at hand.

The aim of this thesis is to obtain a general understanding of how varying certain parameters on one hand allows a pathogen to invade a host population and, on the other hand, allows the host to eradicate an established pathogen, in particular, through the process of evolution.

Contents

1 Introduction

As the climate changes, the environmental conditions shift and become unstable. The increased frequency of natural disasters and extreme weathers in turn put humanity under increased stresses [13]. This translates to humans being more susceptible to new zoonotic pathogens. Indeed, in recent decades the world has seen several novel pandemics and epidemics appear all around the world. Notable among these are the 2009 swine flu pandemic, the 2002-2004 SARS outbreak, the 2015-2016 zika virus epidemic and the currently ongoing COVID-19 pandemic. Many, if not all, of these are zoonotic diseases, meaning they have at some point switched from a non-human host to humans.

When a pathogen switches hosts, it finds itself in a foreign environment. As a consequence, little is known about its ability to effectively spread and infect further hosts. Moreover, the new environment puts the pathogen under heavy evolutionary pressures. A study published in September of 2020 estimated that a total of 20% of those who contracted SARS-CoV-2, the zoonotic coronavirus behind the COVID-19 pandemic, remained asymptomatic throughout the infection [17], while another study published in July of 2020 identified six distinct strains of SARS-CoV-2 [18]. These six strains (including the original strain) accounted for 95% of the sequenced genomes. In particular, only 7% of the sequenced genomes belonged to the original strain that set off the pandemic.

In this thesis we present and study a particular compartmental epidemiological model with constant parameters that exhibits rich dynamical behaviour. The model incorporates asymptomatic individuals that require a double infection to become infectious themselves. Moreover, on top of the demographic dynamics, we formulate a model of evolution and study how the pathogen and host evolve on a larger timescale.

The model of this thesis is very simple in its description, and is as such not well suited for making real-world predictions. Despite the disconnect with reality, we nevertheless motivate and interpret our findings in a biological context. The aim of this thesis is to obtain a general understanding of how varying certain parameters on one hand allows the pathogen to invade a host population and, on the other hand, allows the host to eradicate an established pathogen. In gaining this understanding, we also show that our model presents an excellent foundation for the more targeted study of real-world epidemiological phenomena.

We begin the analysis in section 2 by considering basic assumptions and presenting the model of this thesis together with the more commonly known SIR- and SEIR-models for comparison.

Section 3 provides a brief introduction to the analytic methods of this thesis as well as walk-through of the numerical methods used in this thesis.

In section 4 we look at the demographic dynamics of the model, in particular we

study the diverse bifurcation patters of the model through analysis and examples and show that the model exhibits limit cycles.

Section 5 introduces the mechanisms by which the host and pathogen evolve, and finally, in section 6 we study the long term evolutionary dynamics as the host and pathogen are allowed to evolve, with a particular focus on conditions that allow for the eradication of the pathogen through evolutionary means.

2 Basic assumptions and model description

In this section we present the model that we will be working with along with the basic modelling assumptions that form the foundation of our results.

2.1 Demographic model assumptions

Before presenting the model that we will be working with, we explain some of the most basic assumptions underlying the model. As is always the case with modelling, one must simplify reality, hence sacrificing some of it in the process. As explained in [1], the assumptions we make are commonly used in epidemiological models, hence their use is warranted at least in the sense that results can be compared to other similar models. The main purpose of the assumptions is to allow us invoke the law of large numbers so we can disregard some probabilistic considerations that would otherwise have to be taken into account. These assumptions are as follows:

A1. The population size is infinite.

A2. The population is well mixed.

Basically, the law of large numbers states that as a random event (such as a coin flip) is repeated many times, the average of the outcomes approaches the expected value of the event. Indeed, flip a coin twice: you expect it to land heads once, but instead it does so twice. Surprising? Not really. Now flip the coin two million times. If it lands heads two million times, historians will write about it for centuries to come. However, as the law of large numbers dictates, you count the number of heads and, indeed, the number of heads turns out to be somewhere around the one million mark. In other words, we notice that

$$\lim_{\#\text{flips}\to\infty} \frac{\#\text{heads}}{\#\text{flips}} = \mathbb{P}(\text{heads}) = 0.5.$$

The population in our model will not be flipping coins but will nonetheless be subject to other random events. To use the law of large numbers as a good approximation, we must guarantee that these random events are repeated often, hence assumption **A1**. Because the absolute population size is assumed to be infinite, we will talk

about population *densities* rather than absolute numbers of individuals as the density can remain a finite number while allowing for infinite populations.

Some of the random events that our population is subject to are tied to interactions between individuals. This is where assumption **A2** comes in. A well mixed population simply means that the probability that a chosen individual comes into contact with another individual is uniformly spread throughout the entire population; there are no hierarchical or spatial considerations that would give rise to localised patterns of interactions. In our epidemiological context, this means that a person that becomes infected with a pathogen will not go home and remain there, thus only infecting their closest relatives. Instead they will continue to glide through the entire population coming into contact with others in a truly uniformly random fashion. Hence, assumption **A2** guarantees that the law of large numbers does not fail because of localised structures that interrupt the independence or repetition of these random events.

With these simplifying assumptions in the back of our minds we are thus qualified to use the law of large numbers as a good approximation. This in turn lets us move from a probabilistic model to a deterministic one. Indeed, if the *probability* of an event is k, then we will see that the *fraction* of individuals affected by this event will be k; probabilities on an individual level translate to fractions on the population level.

2.2 Evolutionary model assumptions

In addition to the demographic analysis of our model, we shall allow both the host and the pathogen populations to evolve within the framework of the theory of adaptive dynamics as presented and described in [3].

As is with the demographic dynamics, we need to simplify matters with a few assumptions lest we become lost in a hopeless mess of complexity. These assumptions are not specific to our model, rather, they are among the underlying assumptions behind the theory of adaptive dynamics.

AD1. Individuals reproduce asexually and the offspring is phenotypically identical to its parent.

AD2. Mutations are a sufficiently rare occurrence.

AD3. Mutation steps are very small.

By the *phenotype* we refer to the observable characteristics of individuals, as opposed to the *genotype* which refers to the genetic make up [8]. For evolution to proceed we must allow for the occasional mutation to occur. In these cases the offspring is *not*

identical to its parent. Rather, the idea of the first assumption, **AD1**, guarantees that as a mutation arises in a resident population, the mutant population is reproductively *isolated* from the resident population. While the pathogen is asexually reproducing, this is admittedly a bold assumption to make for the host. However, it allows us to greatly simplify the evolutionary analysis as the novel mutant and pre-existing resident populations exist as two discrete and separate sub-populations.

In fact, in section 5.3, where we present the mechanisms of pathogen evolution, we lessen the importance of this assumption to an extent in the sense that we allow for a single host individual to carry two different pathogen strains. Although the two pathogen strains, namely the pre-existing resident and the novel mutant, are reproductively isolated, their *effective* phenotype is a mix of the resident and mutant strains. Allowing these mixed strains to arise, we very quickly find ourselves hanging off the cliff of impossible complexity. This is however remedied by the fact that the host only experiences the effective phenotype of the mixed strain, which behaves well even though the evolutionary dynamics of the underlying individual pathogen strains become undefined as the evolutionary attractor is approached.

The second assumption, **AD2**, allows us to make two simplifying conclusions. The first one being that only one mutation occurs at any one time. Hence we only need to consider the resident-mutant dynamics of a single mutant in the resident population. Furthermore, whenever an invasive mutant appears and manages to outcompete the resident, hence establishing itself as the new resident, we assume that this new resident has reached its demographic attractor before a new mutation occurs. This way we may always assume that the resident is at its demographic attractor when a new mutation appears in the population. In addition to this, on the exceedingly long time-scale of the evolutionary dynamics, we don't need to concern ourselves with the transient demographic dynamics, only the demographic attractors are of relevance. Hence, the evolutionary dynamics are entirely determined by the selection pressures that prevail at the demographic attractors.

Although mutations occur all the time on a genetic level, as an observed phenomenon evolution tends to be an extremely slow process and populations remain seemingly unchanged on the demographical time-scale of generations. Indeed, phenotypic characteristics such as the structure and purpose of limbs change very slowly and are often only observable through the fossil record. In this sense, this assumption is particularly well founded in reality as we study evolution of the host population through phenotypic changes.

Finally, assumption **AD3** allows us to disregard the sudden appearance of vastly different mutants in comparison to the resident. Although we do not explicitly assume that mutation steps are infinitesimal, we will suppose that they are sufficiently small. What this means is that, as the mutant is very similar to the resident, we can

use various arguments of continuity as needed to simplify the evolutionary analysis.

2.3 The classic SIR- and SEIR-models

The model we will be studying in this thesis is similar to the well known SEIR-model, as well as a generalisation of the SIR-model [1]. For this reason, before presenting the model of this thesis, we familiarise ourselves with the commonly known SIR- and SEIR-models for comparison. For convenience and readability, we write N for the *total population density*. Indeed, for the SIR-model we then obtain $N = S + I + R$, while for the SEIR-model we obtain $N = S + E + I + R$. This convention will also be used for the model that is subject to analysis in this thesis.

The SIR-model. The SIR-model (with logistic vitality dynamics) is as follows:

$$\begin{aligned}\frac{dS}{dt} &= (a - cN)N - \beta IS - \mu S,\\ \frac{dI}{dt} &= \beta IS - (\alpha + \mu + \nu)I,\\ \frac{dR}{dt} &= \nu I - \mu R.\end{aligned}$$

Here S stands for the sub-population density of *susceptible* individuals; the density of those who may contract the disease. The first equation describes how this sub-population changes with time. The first term $(a - cN)N$ describes the logistic population growth, where $(a - cN)$ is the density dependent birth rate. Indeed, all new born individuals are automatically susceptible. When the total population is low, then cN^2 is negligible and the population grows exponentially, as dictated by the exponential growth rate, a. As N increases the effect of cN^2 becomes stronger, and so the exponential growth is slowed down until eventually the two terms are equal and no more births occur. In the absence of a pathogen only susceptibles exist, hence we have $N = S$, in this case the population grows until the growth rate $a - cN$ is balanced out by the death rate μ. In this case the total population density stabilises at $(a - \mu)/c$, since this is where the derivative of S with respect to time vanishes. Note that this implies that $a - \mu > 0$, something that we will assume throughout this thesis.

When a pathogen is present other terms affecting the population dynamics appear. The parameter β describes the *transmission rate per density* of the pathogen. Hence the term $-\beta IS$ which describes the removal of susceptibles at a rate βI. Here I stands for the sub-population density of the infectious individuals. Indeed, each infected susceptible individual becomes an infectious individual, and so we begin describing the change of the infectious individuals, I, with the term $+\beta IS$. In addition to simply dying due to the background death-rate, μ, an infectious individual carries an additional risk of death. This added death rate is called the *virulence* and

is denoted by α. Furthermore, we do not wish to be all doom and gloom, so we allow the infectious individuals a chance to recover. This recovery rate is given by ν.

Finally, the evolution of the recovered sub-population density, R, is described by the last equation. Indeed, every individual that was lost from the infectious state due to recovery will enter the recovered state, hence the term νI. Furthermore, the recovered individuals stay recovered for the rest of their life and so the only way to exit this state is through the sweet release of death after a hard and disease-filled life, hence the term μR. There exist models in which the recovered individuals might lose their immunity and thus transition back into the susceptible state. These models are referred to as SIRS-models, but we shall not dwell on those models in this thesis.

The SEIR-model. Next we present the SEIR-model. In this model many of the terms will be the same as in the SIR-model, so we will mainly focus on what is different. The SEIR-model (with logistic vitality dynamics) is described by the following differential equations: Here N is the total population density, while S gives the density of the sub-population of susceptible individuals, E the exposed individuals, I the infectious individuals and R the recovered individuals. With this in mind, we obtain the following system of differential equations:

$$\begin{aligned}
\frac{dS}{dt} &= (a - cN)N - \beta IS - \mu S, \\
\frac{dE}{dt} &= \beta IS - \theta E - \mu E, \\
\frac{dI}{dt} &= \theta E - (\alpha + \mu + \nu)I, \\
\frac{dR}{dt} &= \nu I - \mu R.
\end{aligned}$$

The most obvious difference to the SIR-model is that now we have an entirely new equation. This equation describes how the sub-population density of the *exposed* individuals changes with time. The exposed individuals are to be interpreted as individuals who have been infected by the pathogen, but are not yet infectious themselves. This latency period between getting infected and becoming infectious is given by the transition rate θ. Indeed, every individual that exits the exposed state through this process must enter the infectious state, hence the term $+\theta E$ in the equation describing infectious individuals. Since, upon infection, a susceptible *must* pass through the latency period before becoming infectious, the term $+\beta IS$ now resides in the equation describing the exposed individuals. Of course, exposed individuals can also die due to the background death rate, hence the term $-\mu E$. Otherwise, everything remains the same in comparison to the SIR-model.

2.4 The model of this thesis

Now we may present the model that is the centre of focus in this thesis. The differential equations describing this model are as follows:

$$\begin{aligned}
\frac{dS}{dt} &= (a - cN)N + \nu_E E - \mu S - \beta^T IS, \\
\frac{dE}{dt} &= (1-k)\beta^T SI - \beta^T EI - \nu_E E - \mu E, \\
\frac{dI}{dt} &= \beta^T (kS + E)I - (\alpha + \mu + \nu_I)I, \\
\frac{dR}{dt} &= \nu_I I - \mu R, \\
\frac{dN}{dt} &= (a - \mu - cN)N - \alpha I.
\end{aligned} \tag{1}$$

While the last equation, $\frac{dN}{dt}$, is redundant, we include it for future reference. In fact, while it is often convenient to talk about the model in terms of the susceptible sub-population, S, much of the analysis and the numerics of this thesis have all been performed by replacing the dynamics of S with the dynamics of N. Henceforth, this system of differential equations will be referred to as *the system*.

We begin by describing the sub-population density of exposed individuals, denoted by E. In contrast to the SEIR-model presented above, the exposed individuals do not capture the concept of a latency period between getting infected and becoming infectious. Instead, the exposed individuals capture the concept of a *weak* infection, in which a susceptible individual does not necessarily become infectious upon infection; these individuals need to be infected twice within a short period of time to become infectious individuals.

Just as an infectious individual can recover, the exposed individual can recover as well. However, there is a difference in the recovery mechanism here. An exposed individual recovers due to a response from the *innate immune system*, which does not grant long-term immunity to the disease, while an infectious individual must recover due to the *adaptive immune system*, which we assume will grand life-long immunity towards the pathogen.

The innate immune system leads to recovery mainly through the workings of the phagocytic cells that engulf the pathogen and break it down. This immune response is general and works the same way regardless of the pathogen, hence no immunity is obtained. Conversely, the adaptive immune system acts by producing antibodies which bind to the pathogen and block its ability to proliferate in the host. The production of specific antibodies against a specific pathogen is a targeted response. Once the host has developed the right antibodies for a specific pathogen, successive infections are quickly suppressed due to the fast and effective response from the adaptive immune system. Hence, immunity has been obtained [8].

With these considerations, we obtain the two separate recovery rates, namely ν_E for the exposed individuals and ν_I for the infectious individuals. As can be seen, any exposed individuals lost through recovery are accounted for in the equation describing the susceptible sub-population, while any infectious individuals lost through recovery are accounted for in the equation describing the recovered individuals.

The parameter k. Another striking difference to the SEIR-model is the appearance of a parameter k in the equations. As it turns out, this parameter is of central importance in the results of this thesis, hence we devote extra attention to it here.

Looking closely, we see that the loss term in the S-equation, $-\beta^T IS$, due to infection, is compensated for by the terms $+(1-k)\beta^T SI$ in the E-equation and $+k\beta^T SI$ in the I-equation. Indeed, k describes the probability that a susceptible individual becomes infectious upon a single transmission of the disease. Hence, taking into account the law of large numbers, this translates into fractions; a fraction $(1-k)$ of those infected transition into the exposed state, while the remaining fraction, k, of those infected transition straight into the infectious state.

In this thesis, the interpretation behind k is quite multifaceted. For the most part, we will discuss it as a parameter that relates a stressful environment to an increased susceptibility of the host. On the other hand, k can just as well be taken as a parameter that represents a sort of infectivity of the pathogen. For example, abnormally high precipitation levels can bring about floods and increased humidity levels in a region. Flooding deteriorates sanitary conditions, increasing host susceptibility, and the increased humidity might facilitate the spread of a pathogen, increasing pathogen infectivity. The combined effect of this is a higher k. Furthermore, k can be taken as a variable parameter, reflecting deliberate actions against the pathogen or simply the evolution of a novel pathogen as it adapts to a new host. For example, wearing a mask and ensuring good hand hygiene generally reduces the exposure to pathogen particles, bringing down k. On the contrary, a virus that has undergone a mutation that enables it to switch to a novel host might initially have trouble establishing itself in this new host environment. However, as it evolves it becomes more adapted to this new host, increasing k as a result.

Naturally, more detailed model formulations that better capture the complex reality of epidemiological dynamics would take these considerations into account as separate parameters of the model, rather than combining them under the single parameter k, as we have done. Moreover, the fact that k is entirely independent of the transmission rates is a major simplification in our thesis and not something one would expect in any realistic considerations. In particular, this means that both host and pathogen evolution will not have an effect on k, a direct counterpoint to the last aforementioned interpretation.

The parameter β is the transmission rate. The superscript, T, stands for "total"

and will be explained shortly. As can be seen, once an individual is exposed and becomes infected another time there can only be one outcome; all of the exposed individuals that exit the exposed state due to infection, as described by the term $-\beta^T EI$, are compensated for in the I-equation.

Other than this, the rest is identical the other models. Growth is logistic and described by $(a-cN)N$ and everyone is subject to the same background death rate, μ, while infectious individuals are further subject to the added death rate brought on by the disease, as described by the virulence, α. Furthermore, as a final remark, we require that $a-\mu > 0$, that is, the exponential birth rate is always greater than the death rate, otherwise the demographic landscape would be rather dull indeed; the change in the total population size, $\frac{dN}{dt}$, would be negative for all population sizes, and so the only outcome of the dynamics would be immediate extinction.

Evolutionary parameters. The most central parameters to this thesis are the *transmission rates* of the pathogen. Hence, let us go into a little more detail regarding these parameters.

Above, we were introduced to only one transmission rate, namely β^T. However, β^T hides within it two other transmission rates, these are the *host* transmission rate, β^H, and the *pathogen* transmission rate, β^P. These combine to form the *total* transmission rate, β^T. Indeed, we define

$$\beta^H := rq^H, \quad \beta^P := q^P, \quad \beta^T := \beta^H\beta^P = rq^Hq^P.$$

The quantities q^i are probabilities, where q^H is the probability that the host immune system is unable to prevent infection upon a contact, while q^P is the probability that the pathogen is given off by the infecting host in the first place. Note that the pathogen transmission rate is *not* actually a rate, it is just a probability. We only call it the pathogen transmission rate in accordance with the other transmission rates. Finally, r is the contact rate of the individuals in the host population. And so, upon an infectious contact, β^H is determined by the host that is *receiving* the pathogen, while β^P is determined by the pathogen being carried by the *infecting* host. Hence, β^H is a trait carried by the host and β^P is a trait carried by the pathogen. Furthermore, we see that β^P is restricted to the interval $[0,1]$, while β^H is bounded by the contact rate, and so we make no restrictions on β^H other than require it to be non-negative. Finally, for a contact to be successful, that is, result in an infection, the host needs to receive the pathogen *and* the pathogen needs to establish itself once it has been received, hence why we multiply these probabilities with the contact rate to obtain the total transmission rate, β^T.

Since the transmission rates are *evolutionary parameters*, they will later be subject to evolution as per the theory of adaptive dynamics [3]. To give the evolutionary dynamics a realistic context, we couple the transmission rates with the exponential

birth rate, a, and the virulence, α. Indeed, we declare that $a(\beta^H)$ is a strictly increasing function of the host transmission rate, β^H, while $\alpha(\beta^P)$ is a strictly increasing function of the pathogen transmission rate, β^P. The idea here is that as the host invests more resources into the immune system (lower q^H), less resources and energy are available for reproducing. Alternatively, lowering the contact rate in response to a pathogen, leaves less opportunities for reproducing. Similarly, we suppose that a pathogen with a high transmission rate is also more deadly: for example, a virus that is aggressively reproducing within its host is more likely to be given off by the host (higher q^P), however the host is more easily overwhelmed by the aggressive pathogen and so it is more likely to succumb to the disease. Furthermore, as was mentioned, we require that $a(\beta^H) > \mu$ for all $\beta^H \in [0, \infty)$. Henceforth, we suppress the argument from the functions a and α in an effort to keep expressions somewhat more readable as they sometimes become quite long and complicated.

3 Analytic and numerical methods

This section provides a brief introduction to the basic analysis of systems of differential equations. The contents of this section are by no means general in their scope, rather we only present the tools and methods needed for our specific needs.

We begin by introducing the framework in which we may conveniently discuss the solutions to the system (1). After this we present the method of *linear stability analysis* and finally we explain the numerical method by which limit cycles of the system are found.

3.1 State space and phase space

As can be seen, the population of our model consists of four different sub-population, namely those denoted by S, E, I and R. The densities of these sub-populations can be written as a vector $(S, E, I, R) \in \mathbb{R}^4$, which we refer to as the state of the system. Accordingly, let us call $\mathbb{R}^4$ the *state space* of the system, since any point in this space corresponds to a state of the system and the state of the system will remain in this space as it evolves through time. Note that we disregard the biological interpretation of the population here, naturally we can not have negative population densities.

On the state space we may define a vector field as follows:

$$\begin{aligned} &V : \mathbb{R}^4 \to \mathbb{R}^4, \\ &V_p := V(p) = \left(\dot{S}(p), \dot{E}(p), \dot{I}(p), \dot{R}(p)\right), \end{aligned}$$

where p is a point in the state space. Here the dot over the sub-population densities indicates the time derivative. Hence, the vector field V is determined by the differential equations in (1). Note that the time derivatives of the sub-population densities

are not explicitly functions of time, in other words, the system is *autonomous*. Hence, while we consider the sub-population densities as functions of time, their respective derivatives are considered to be functions of the sub-population densities themselves.

The *phase space* of the system is the set $\{(p, V_p) \in \mathbb{R}^4 \times \mathbb{R}^4\}$. Each point in the phase space can be interpreted as a state of the system, p, and its velocity and direction as it changes in time, V_p. Since at each point, (p, V_p), of the phase space, the second component, V_p, is entirely determined by the point p in the state space, we may *identify* the phase space with the state space. Henceforth, we speak of the phase space in terms of the state space with the implicit knowledge that to each point p is associated the vector V_p.

Remark 1. Note that the distinction between state space and phase space here is entirely artificial, one could simply take the vectors V_p as part of the description of the state of the system. However, since not every point of $\mathbb{R}^4 \times \mathbb{R}^4$ corresponds to a state of the system (1), we are restricted in our movement in this space. Hence, we choose to make the distinction and think of the state space as $\mathbb{R}^4$, where we are free to move and every point corresponds to a valid state of the system, and then to consider the phase space as the full description of the system where every state p comes with the vector V_p attached.

A path in the phase space, $p(t)$, is an *orbit* if it satisfies the condition that $p'(t) = V_p$ for all $t \in [0, \infty)$. Indeed, the orbit starting at a point p_0 is exactly the solution to the initial value problem

$$\begin{aligned} p'(t) &= V_p, \\ p(0) &= p_0. \end{aligned}$$

In other words, the orbits are the solutions to the system (1).

In our analysis, we will often restrict ourselves to a two-dimensional subset of the phase space, called a *phase plane*. Furthermore, due to our biological context, we are really only concerned with the subset $\mathbb{R}^4_+ = [0, \infty)^4$ of the phase space.

The set of points in the phase space, where the i^{th} component of V_p vanishes is referred to as the i-isocline. For example, the S-isocline is the set

$$\{(p, V_p) \mid \dot{S}(p) = 0\}.$$

Evidently, the isoclines are obtained by setting the respective derivatives in (1) equal to 0.

Note that the points $\hat{p}$, where $V_{\hat{p}} = 0$, are located where the isoclines all intersect. Note that 0 in this context is the four dimensional zero-vector, not the real number 0; a convention we will use throughout this thesis. The orbits of these points are stationary, that is, $\hat{p}'(t) = 0$ for all times t. In other words, the state of the system remains constant in time. These states are known as *steady states*, or as we will refer

to them, *equilibria* of the system. Next, we turn our focus to these equilibria and present the method of analysing the qualitative aspects of these equilibria through linear stability analysis.

3.2 Linear stability analysis

Here we present a brief introduction to the method of linear stability analysis. The purpose of linear stability analysis is to study the stability of equilibria against small perturbations in the system. An equilibrium is said to be asymptotically stable when small perturbations of the system at the equilibrium asymptotically converge to 0. Conversely, an equilibrium is unstable when these perturbations grow and the state of the system wanders away from the equilibrium. Here we only treat a special case of the linear stability analysis, that is we assume that the Jacobian matrix of the system is diagonalisable, however the results that we obtain hold for the general case as well. For the full treatment of linear stability analysis, see for example [9].

Suppose we have a system of differential equations defined by

$$\dot{p}(t) = f(p), \tag{2}$$

where $p(t) \in \mathbb{R}^n$ and $f \in C^1(\mathbb{R}^n,\ \mathbb{R}^n)$. Furthermore, suppose $\hat{p}$ is an equilibrium of the system, that is, $f(\hat{p}) = 0$. A natural question to ask is what happens to the system if we perturb the state $\hat{p}$? Will the system converge back to $\hat{p}$ or will it wander off to some other part of the phase space, perhaps to some other equilibrium point?

To answer these questions we linearise the system around the state $\hat{p}$. That is, we perform a first order Taylor expansion of (2) around the point $\hat{p}$. We obtain

$$\dot{p}(t) = f(\hat{p}) + J_f(\hat{p})(p - \hat{p}).$$

Here $J_f(\hat{p})$ is the Jacobian matrix of f evaluated at the state $\hat{p}$. Moreover, note that $f(\hat{p}) = 0$ by our assumption that $\hat{p}$ is an equilibrium. Hence, writing $\Delta p := p - \hat{p}$ and noting that $\Delta\dot{p}(t) = \dot{p}(t)$, we obtain

$$\Delta\dot{p}(t) = J_f(\hat{p})\Delta p. \tag{3}$$

By the Hartman-Grobman theorem, the dynamics of this linearised system are equivalent to the dynamics of (2), provided that the perturbation, Δp, is sufficiently small. Now, suppose $J_f(\hat{p})$ admits an eigenbasis (for a more thorough treatment, see [9]), we may write

$$\Delta p(t) = \sum_i u^i(t) u_i,$$

where u_i is the i^{th} eigenvector of $J_f(\hat{p})$ and $u^i(t)$ is the i^{th} *time dependent* component of $\Delta p(t)$. With this we may formulate (3) in the eigenbasis, obtaining

$$\dot{u}^i(t) = \lambda_i u^i(t).$$

Where λ_i are the eigenvalues corresponding to the eigenvectors u_i. Hence, the solution, $\Delta p(t)$, is given by

$$\Delta p(t) = \sum_i u^i(0) e^{\lambda_i t} u_i.$$

From this we may immediately conclude the following:

$$\mathrm{Re}(\lambda_i) < 0 \text{ for all } i \quad \Rightarrow \quad \lim_{t\to\infty} \Delta p(t) = 0.$$

Indeed, we see that the perturbation, Δp eventually vanishes and the system converges back to the equilibrium, $\hat{p}$. We say that $\hat{p}$ is asymptotically stable. On the other hand, supposing $\mathrm{Re}(\lambda_i) > 0$ for some i, then the perturbation does not vanish, consequently, we say that $\hat{p}$ is unstable. In this case no further conclusions can be made; when the perturbation grows the linear approximation around $\hat{p}$ becomes inaccurate.

When $\mathrm{Re}(\lambda_i) = 0$ for some i, interesting phenomena occur; the qualitative properties of the equilibrium changes when $\mathrm{Re}(\lambda_i)$ changes sign. These phenomena are referred to as *bifurcations* of the system. In this thesis, we will perform the bifurcation analysis mainly by studying the isoclines of the system rather than the eigenvalues of the Jacobian matrix. Nevertheless, there exists the so called Hopf bifurcation, whose existence can not be inferred from the isoclines. This bifurcation occurs when a complex conjugate pair of eigenvalues, λ_i and $\bar{\lambda}_i$, of the Jacobian matrix at an equilibrium satisfy the following conditions:

$$\mathrm{Re}(\lambda_i) = 0 \quad \text{and} \quad \mathrm{Im}(\lambda_i) \neq 0,$$

that is, the eigenvalue λ_i and its conjugate pair are purely imaginary. In this case stable limit cycles can appear around the equilibrium. A stable limit cycle is an orbit, $p(t)$, that is not an equilibrium and has the property that $p(0) = p(\Pi)$ for some period $\Pi > 0$ [10].

Due to the difficulty of analysing the 4×4 Jacobian matrix of our model, we have disregarded the analytic study of the Hopf bifurcations in this thesis. However, the resulting limit cycles following a Hopf bifurcation are of great interest, and so in the next section we describe the numerical algorithm used to find these limit cycles.

3.3 Finding stable limit cycles

We conclude section 3 by presenting the numerical methods by which limit cycles of the system are found.

The very first step in the algorithm is to solve the equilibrium and check the corresponding eigenvalues of the Jacobian matrix. If the real part of every eigenvalue is negative, then the equilibrium is deemed asymptotically stable and the algorithm terminates. If the equilibrium is unstable, then the process of finding limit cycles begins.

To find the limit cycle we select an initial point, from which to begin the search. Indeed, we can not use the equilibrium as an initial point, so we make a small perturbation in the exposed sub-population. Thus, we follow the orbit of the point $(N, E, I, R) = (\hat{N}, \hat{E} + 0.001, \hat{I}, \hat{R})$ up to time $t_0 = 10^5$. That is, we define the initial point of the search as

$$F_0 = F(t_0) = (N(t_0), E(t_0), I(t_0), R(t_0)), \quad F(0) = (\hat{N}, \hat{E} + 0.001, \hat{I}, \hat{R}),$$

where F is the solution to the system (1) with the specified initial condition. Naturally, this approach is very simplistic and relies entirely on the assumption that the initial point $F(0)$ in the vicinity of the equilibrium converges fairly close to the limit cycle in t_0 units of time.

At this point, provided that $R_0^P \leq 1$, it might happen that the orbit $F(t)$ has wandered too close to the disease free equilibrium, thus converging to $\hat{N}_{\text{free}}$. To avoid this, the algorithm keeps track of $F(t)$ for all $t \in [0, t_0]$, if at any point during this time $I(t) < 10^{-5}$ while $R_0^P \leq 1$, then it is assumed that the orbit is converging toward the disease free equilibrium and the process is terminated. Indeed, we require that $R_0^P \leq 1$, since otherwise it is known that $\hat{N}_{\text{free}}$ is not attracting, hence the orbit can not converge to the disease free equilibrium.

Supposing everything works out, we wish to keep following the orbit of F, all the while keeping track of $I(t)$. Assuming that the orbit is cyclical, we should reach a time t_1 where $I(t_1) = I(t_0)$ and $\dot{I}(t_1) < 0$ (given that $\dot{I}(t_0) < 0$, otherwise flip the inequality). This would imply, assuming that we are converging towards the limit cycle, that we would have completed one revolution on our ever more cyclical orbit and returned somewhere near the point F_0. We define

$$F_1 = F(t_1),$$

and reiterate the process. In this way we obtain a sequence of points, F_n, each hopefully closer and closer to the limit cycle.

In essence, the process of finding repeating revolutions on the limit cycle boils down to checking when the point $I(t_0)$ is crossed from above (or below). The problem here is that the orbit is 4-dimensional, and so $I(t_0)$ might be crossed multiple times before a revolution is complete. In other words, the orbit might fold on itself when projected to lower dimensions. This algorithm only accounts for cases where the projected orbit has at most one fold; any more and it will fail to detect the limit cycle.

Between each iteration, there is a check on whether or not the distance between two consecutive points F_n and F_{n-1} is short enough. Indeed, if it happens that

$$\|F_n - F_{n-1}\|_\infty < 10^{-5},$$

then the process terminates and returns a pair (F_n, Π), where F_n is a point on the limit cycle and $\Pi = t_n - t_{n-1}$ is the period of the cycle. In addition to this, in the case that there is a fold in the projected orbit, the algorithm *also* checks whether or not

$$\|F_n - F_{n-2}\|_\infty < 10^{-5}$$

is satisfied. If this is the case, then the period is $\Pi = t_n - t_{n-2}$. Of course, if the first inequality is satisfied, then the second one is never checked. Here $\|\cdot\|_\infty$ is the usual maximum norm.

Due to numerical instabilities at very low sub-population densities we include an additional fail-safe when $R_0^P > 1$. In this case, should any of sub-population densities obtain negative values, the process is terminated. This check is performed at every step throughout the algorithm. Finally, in the case that something catastrophic happens and the orbit escapes all the fail-safes above but does not converge, the sequence F_n is allowed to go only up to $n = 100$. If at this index we still have $\|F_{100} - F_{99}\|_\infty \geq 10^{-5}$ and $\|F_{100} - F_{98}\|_\infty \geq 10^{-5}$, then the results are discarded and the algorithm assumes that no limit cycle exists; the entire process terminates. For example, possible chaotic dynamics are ruled out by this final fail-safe.

All things considered, these checks are not perfect. However, their nature is such that while some stable limit cycles might (and most likely do) go undetected, no false positives will be detected.

Remark 2. It should be noted that in the examples of this thesis that require the use of the above described algorithm, a deliberate effort was made to choose the parameters in such a way that any of the fail-safes would not be triggered. That said, close to the regions where the limit cycles destabilised, it was often the case that the cycle would begin folding on itself when projected to the (N, I)-phase plane, thus the reader can expect there to be some loss of detection. However, the folding of the limit cycle and the subsequent loss of stability was so rapid that only checking for one fold was deemed a good enough compromise.

4 Demographic analysis

In this section, as well as following sections, we will make use of the following identities obtained from the isoclines of the system. They will henceforth be referred to

as the *isocline identities*.

$$\beta^T \hat{I} + \mu + \nu_E = \frac{(1-k)\beta^T \hat{S}\hat{I}}{\hat{E}}, \tag{4}$$

$$\nu_E \hat{E} = (\beta^T \hat{I} + \mu)\hat{S} - (a - c\hat{N})\hat{N}, \tag{5}$$

$$\hat{I} + \hat{R} = \frac{\mu + \nu_I}{\mu}\hat{I} \tag{6}$$

$$\beta^T(k\hat{S} + \hat{E}) = \alpha + \mu + \nu_I \tag{7}$$

$$\beta^T \hat{I} + k(\mu + \nu_E) = \frac{(1-k)\hat{I}(\alpha + \mu + \nu_I)}{\hat{E}}. \tag{8}$$

These identities were obtained by setting all of the differential equations in (1) equal to 0. Hence, the identities hold at every equilibrium of the system and can consequently be used to greatly simplify complicated expressions. In particular, this will become apparent when we discuss the basic reproduction number of the host in the following section.

4.1 The basic reproduction number

When studying the dynamics of infectious diseases, one of the most important quantities describing the behaviour of the dynamics is the *basic reproduction number*, denoted by R_0. This quantity describes the expected number of new infectious individuals produced by an initially infectious individual that enters a disease-free population, otherwise known as a *virgin* population.

In the virgin population every individual belongs to the susceptible compartment, S. In addition, the state of the system is of the form $(N, 0, 0, 0)$, where N is the total population density, hence the population dynamics live on a one-dimensional subspace of the phase space. When the virgin population is at an equilibrium, we denote the total population density of this disease-free equilibrium as $\hat{N}_{\text{free}}$. Moreover, we also refer to the equilibrium itself as $\hat{N}_{\text{free}}$, much like we refer to the zero-vector by the real number 0. The detailed analysis of the disease-free system can be found in section 8.1 of the Appendix.

If $R_0 > 1$ the disease is expected to spread, while if $R_0 < 1$ it is expected to decline and eventually disappear without causing a significant epidemic [1].

Although R_0 is usually defined in the terms above, it can also be applied in a more general context than that of infectious disease dynamics. Namely, it can be taken as the expected number of offspring an individual will produce during its lifetime. With this interpretation we can use R_0 to analyse both the pathogen dynamics as well as the evolutionary dynamics of the host. The basic reproduction numbers for these populations will be denoted R_0^P and R_0^H, respectively.

4.1.1 The basic reproduction number of the pathogen

To find R_0^P, we must know the rate at which a single infectious individual produces new infectious individuals in a virgin population. The total number of infectious contacts per unit of time made by a single infectious individual in a virgin population is $\beta^T \hat{N}_{\text{free}}$, however, not all of these infectious contacts count toward R_0^P. Recall the model assumptions **A1** and **A2**. The population being well mixed implies that the probability that a single infectious individual meets a selected individual twice is roughly $1/n^2$, where n is the total number of individuals in the population. And the second assumption, that the population is very large, makes this probability, $1/n^2$, very small. So, if at a successful transmission of the pathogen the receiving host does not immediately become infectious, but instead transitions into the exposed state, E, then we assume that they will recover well before they ever meet another infectious individual; their total number being so small in comparison to the number of susceptibles. For this reason, we must multiply $\beta^T \hat{N}_{\text{free}}$ with the fraction k, thus disregarding the possibility that an individual becomes infectious through double infection. In conclusion, the rate at which a single infectious individual produces new infectious individuals in a virgin population is $k\beta^T \hat{N}_{\text{free}}$.

Furthermore, in order to obtain how many new infectious individuals are produced by a single infectious individual in total, we must know the expected time that an individual remains infectious. An infectious individual exits the infectious state after a random time, which is exponentially distributed. The parameter of this exponential distribution is the sum of the individual exit rates, $\alpha+\mu+\nu_I$, and so the expected time to exit is the reciprocal of the parameter of the distribution, namely

$$\frac{1}{\alpha + \mu + \nu_I}.$$

Multiplying the rate of producing new infectious individuals with the expected time to remain infectious, we obtain the basic reproduction number of the pathogen:

$$R_0^P = \frac{\beta^T k \hat{N}_{\text{free}}}{\alpha + \mu + \nu_I}. \tag{9}$$

From this we see that when $k = 0$, that is, double infection is required *every* time for a susceptible individual to become infectious, then $R_0^P = 0$ for any parameters. Indeed, this implies that no matter how high the transmission rates are, an initially rare pathogen can never invade a virgin population. On the other hand, as we will see, stable endemic equilibria can still exist at $k = 0$. The process by which these equilibria arise in a biological context must however be explained through other means than the simple invasion of an initially rare pathogen. Indeed, the fact that $R_0^P = 0$ when the population is virgin does not exclude the fact that R_0^P could obtain higher values when the population is not virgin.

Assume that the pathogen is present in the population. How does the environment look from the perspective of a single infectious individual now? Once again, by assumptions **A1** and **A2**, we only count those individuals that become infectious upon one single successful contact toward R_0^P. But this time, since the pathogen is already present, we expect to see some individuals in the exposed state as well! Indeed, all the exposed individuals become infectious upon a single successful transmission of the pathogen, as does a fraction k of the susceptible sub-population. With this in mind, we obtain the following expression for R_0^P:

$$\tilde{R}_0^P := \frac{\beta^T(kS + E)}{\alpha + \mu + \nu_I}.$$

Notice that at equilibrium, we may use isocline identity (7) to our advantage, in which case we obtain

$$\hat{R}_0^P := \frac{\beta^T(k\hat{S} + \hat{E})}{\alpha + \mu + \nu_I} = 1.$$

Indeed, this is what we would expect, since at equilibrium the number of infected individuals should not be changing. Since $R_0^P < 1$ implies decline and $R_0^P > 1$ implies growth, we expect to see exactly $R_0^P = 1$. Notice that we have used the *tilde* ($\tilde{}$) to indicate R_0^P at *any* state in the phase space and the *hat* ($\hat{}$) to indicate R_0^P at an equilibrium.

This sub-population density of the individuals that become infectious upon a single successful transmission of the pathogen (at equilibrium) turns out to be of critical importance in the evolutionary analysis of the pathogen, hence we give it a name. We call the quantity $k\hat{S} + \hat{E}$ the sub-population of the *immediately infectable individuals* and denote it by $\hat{E}_0$. We obtain

$$\hat{E}_0 = k\hat{S} + \hat{E} = \frac{\alpha + \mu + \nu_I}{\beta^T}. \tag{10}$$

4.1.2 The basic reproduction number of the host

While the basic idea behind the basic reproduction number of the host is exactly the same as for the pathogen, the terms involved in the calculation are somewhat more complicated. Once again, we obtain R_0^H by multiplying the birth rate of a singe individual by its expected lifetime. Thankfully, the birth rate remains the same throughout the different stages of life, and is simply given by the term $a - cN$. Note that this time the concept of a *virgin* environment is not applicable, as it was for the pathogen. For this reason, we don't differentiate between $\tilde{R}_0^H$ and R_0^H in the same way that we did in the previous section. However, $\hat{R}_0^H$ is still relevant, and as we will see, $\hat{R}_0^H = 1$ holds for the host as well.

The expected lifetime $\mathcal{L}$ is implicitly given by

$$\mathcal{L} = T_S + P_{SE}\left(T_E + P_{ES}\mathcal{L} + P_{EI}(T_I + P_{IR}T_R)\right) + P_{SI}(T_I + P_{IR}T_R),$$

where T_i is the expected time an individual spends in state i and P_{ij} is the probability that an individual will transition from state i to state j.

Notice that if an exposed individual recovers and enters back into the susceptible state, it is still expected to live for $\mathcal{L}$ time, hence the term $P_{SE}P_{ES}\mathcal{L}$ in the above equation. Solving this equation for $\mathcal{L}$ gives

$$\mathcal{L} = \frac{T_S + P_{SE}\left(T_E + P_{EI}(T_I + P_{IR}T_R)\right) + P_{SI}(T_I + P_{IR}T_R)}{1 - P_{SE}P_{ES}}.$$

Now, R_0^H is given by $R_0^H = (a - cN)\mathcal{L}$, which expands into

$$R_0^H = (a - cN)\frac{T_S + P_{SE}\left(T_E + P_{EI}(T_I + P_{IR}T_R)\right) + P_{SI}(T_I + P_{IR}T_R)}{1 - P_{SE}P_{ES}}. \tag{11}$$

The expected times T_i and probabilities P_{ij} are as follows

$$\begin{aligned}
&T_S = \frac{1}{\beta^T I + \mu}, \quad T_E = \frac{1}{\beta^T I + \mu + \nu_E}, \quad T_I = \frac{1}{\alpha + \mu + \nu_I}, \quad T_R = \frac{1}{\mu} \\
&P_{SE} = \frac{(1-k)\beta^T I}{\beta^T I + \mu}, \quad P_{SI} = \frac{k\beta^T I}{\beta^T I + \mu}, \quad P_{ES} = \frac{\nu_E}{\beta^T I + \mu + \nu_E}, \\
&P_{EI} = \frac{\beta^T I}{\beta^T I + \mu + \nu_E}, \quad P_{IR} = \frac{\nu_I}{\alpha + \mu + \nu_I}.
\end{aligned}$$

Which, when substituted into (11), gives us

$$\begin{aligned}
R_0^H = (a - cN)\Bigg(&\frac{(2-k)\beta^T I + \mu + \nu_E}{(\beta^T I + \mu)(\beta^T I + \mu + \nu_E) - (1-k)\beta^T I\nu_E} \\
&+ \frac{\beta^T I(\beta^T I + k(\mu + \nu_E))}{(\alpha + \mu + \nu_I)\left((\beta^T I + \mu)(\beta^T I + \mu + \nu_E) - (1-k)\beta^T I\nu_E\right)} \\
&+ \frac{\beta^T I\nu_I(\beta^T I + k(\mu + \nu_E))}{\mu(\alpha + \mu + \nu_I)\left((\beta^T I + \mu)(\beta^T I + \mu + \nu_E) - (1-k)\beta^T I\nu_E\right)}\Bigg) \\
&= \frac{(a - cN)}{\mu(\alpha + \mu + \nu_I)}\frac{P}{T},
\end{aligned} \tag{12}$$

where

$$\begin{aligned}
P &= \mu(\alpha + \mu + \nu_I)\left((2-k)\beta^T I + \mu + \nu_E\right) + \beta^T I\left(\beta^T I + k(\mu + \nu_E)\right)(\mu + \nu_I), \\
T &= (\beta^T I + \mu)(\beta^T I + \mu + \nu_E) - (1-k)\beta^T I\nu_E.
\end{aligned}$$

Notice that for any possible values of the model parameters, we have $P > 0$ and $T > 0$.

Similarly to the pathogen, at equilibrium the sub-population densities should remain unchanged. In terms of R_0^H this translates to $R_0^H = 1$, since otherwise the population would be growing for $R_0^H > 1$ or declining for $R_0^H < 1$. Let us check that this is indeed the case.

In the case that the equilibrated host is disease-free, the expected lifetime is $\mathcal{L} = 1/\mu$, and so we obtain

$$\hat{R}_0^H = \frac{(a - c\hat{N}_{\text{free}})}{\mu} = \frac{a - (a - \mu)}{\mu} = 1.$$

In the case where host is at an endemic equilibrium, we obtain with help from the isocline identities:

$$P_{SE}P_{ES} = \frac{\nu_E \hat{E}}{(\beta^T \hat{I} + \mu)\hat{S}} = \frac{(\beta^T \hat{I} + \mu)\hat{S} - (a - c\hat{N})\hat{N}}{(\beta^T \hat{I} + \mu)\hat{S}} = 1 - \frac{(a - c\hat{N})\hat{N}}{(\beta^T \hat{I} + \mu)\hat{S}}.$$

And so

$$1 - P_{SE}P_{ES} = \frac{(a - c\hat{N})\hat{N}}{(\beta^T \hat{I} + \mu)\hat{S}}.$$

Moreover, using the short hand notation

$$\mathcal{T} := T_S + P_{SE}\left(T_E + P_{EI}(T_I + P_{IR}T_R)\right) + P_{SI}(T_I + P_{IR}T_R),$$

we have

$$\begin{aligned}
\mathcal{T} &= \frac{1}{\beta^T \hat{I} + \mu}\left(1 + \frac{\hat{E}}{\hat{S}}\left[1 + \frac{\beta^T \hat{I}(\mu + \nu_I)}{(\alpha + \mu + \nu_I)\mu}\right] + \frac{k\beta^T \hat{I}(\mu + \nu_I)}{(\alpha + \mu + \nu_I)\mu}\right) \\
&= \frac{1}{(\beta^T \hat{I} + \mu)\hat{S}}\left(\hat{S} + \hat{E} + \frac{\hat{E}\beta^T(\mu + \nu_I)\hat{I} + k\beta^T \hat{S}(\mu + \nu_I)\hat{I}}{(\alpha + \mu + \nu_I)\mu}\right) \\
&= \frac{1}{(\beta^T \hat{I} + \mu)\hat{S}}\left(\hat{S} + \hat{E} + (\hat{I} + \hat{R})\frac{\beta^T(k\hat{S} + \hat{E})}{\alpha + \mu + \nu_I}\right) = \frac{\hat{N}}{(\beta^T \hat{I} + \mu)\hat{S}}.
\end{aligned}$$

And so the expected lifetime, $\mathcal{L}$, becomes

$$\mathcal{L} = \frac{\mathcal{T}}{1 - P_{SE}P_{ES}} = \frac{\frac{\hat{N}}{(\beta^T \hat{I} + \mu)\hat{S}}}{\frac{(a - c\hat{N})\hat{N}}{(\beta^T \hat{I} + \mu)\hat{S}}} = \frac{1}{a - c\hat{N}}.$$

Indeed, this makes sense. At equilibrium, the birth rate must equal the death rate. Hence, the expected lifetime, which is given by the reciprocal of the death rate, is then the same as the reciprocal of the birth rate.

Finally, we obtain

$$\hat{R}_0^H = (a - c\hat{N})\mathcal{L} = \frac{a - c\hat{N}}{a - c\hat{N}} = 1, \tag{13}$$

which is what we wanted.

4.2 The endemic equilibria of the system

Along with the trivial and disease-free equilibria, $\hat{N} = 0$ and $\hat{N}_{\text{free}}$, respectively, the system can have a number of other equilibria as well. However, not all of these equilibria are ever biologically meaningful; some of them always lie in a region of the phase space that gives negative sub-population densities. In this section we study which regions of the phase space and which parts of the related isoclines are relevant to our biological interpretation of the model. Furthermore, we show that there always exists $\beta^H \in (0, \infty)$ such that endemic equilibria exist when all other parameters are kept unchanged.

4.2.1 The biologically meaningful region

In the absence of a disease the system becomes a one dimensional logistic model described by the differential equation

$$\frac{dN}{dt} = (a - \mu - cN)N.$$

Recall that $a - \mu > 0$ always holds, hence this system has an unstable equilibrium at $\hat{N} = 0$ and a stable globally attracting equilibrium at $\hat{N} = (a - \mu)/c$ (see 8.1 of the Appendix for the details). This latter equilibrium is the disease-free equilibrium, denoted $\hat{N}_{\text{free}}$ and named so because it is the demographically attracting population density in the absence of a pathogen. At the disease-free equilibrium the growth-rate of the population matches the death-rate, and so we obtain

$$a - c\hat{N}_{\text{free}} = \mu.$$

Expanding back into the four dimensional phase space, we speak of the disease-free equilibrium as being the point $(S, E, I, R) = (\hat{N}_{\text{free}}, 0, 0, 0)$ which we denote as $\hat{N}_{\text{free}}$ as well. In general, equilibrium population densities of the system are indicated by a hat ($\hat{}$) over the respective population density.

Next, we define a subset of the phase space:

$$\mathcal{N} := \{(S, E, I, R) \in \mathbb{R}_+^4 \mid a - cN \geq 0\}.$$

We shall refer to the set $\mathcal{N}$ as the *biologically meaningful region* of the model. Indeed, to be biologically meaningful, each sub-population density must be non-negative, and the birth rate of the population, $a - cN$, must be non negative as well.

Next we show that orbits starting in the biologically meaningful region is *forward invariant*, that is, orbits starting in $\mathcal{N}$ remain indefinitely in $\mathcal{N}$.

Theorem 1. *The biologically meaningful region, $\mathcal{N}$, is forward invariant.*

Proof. For this proof we introduce the shorthand notation $\dot{p}_i$ to denote the i^{th} component of V_p. That is, if p is a state of the system, then

$$(\dot{p}_1, \dot{p}_2, \dot{p}_3, \dot{p}_4) := \left(\dot{S}(p), \dot{E}(p), \dot{I}(p), \dot{R}(p)\right).$$

We prove the theorem by showing that for every point p on the boundary of $\mathcal{N}$, V_p never points out of $\mathcal{N}$.

First, let $p = (p_1, p_2, p_3, p_4) \in \mathcal{N}$ be such that $a - cN = 0$. Then we must have $\dot{N} < 0$, but this means that V_p is pointing into a region where $a - cN > 0$. If $p_i > 0$ for all i, then V_p points into the interior of $\mathcal{N}$. What remains is to check that when $p_i = 0$ for some i, we are guaranteed that V_p does not point out of $\mathcal{N}$.

So, suppose $p \in \mathcal{N}$ is such that $p_i = 0$ for some i. Then it is easy to see from (1) that $\dot{p}_i \geq 0$. In particular, the fact that $a - cN \geq 0$ guarantees that $\dot{p}_1 = \dot{S} \geq 0$ when $S = 0$. Hence, we conclude that if an orbit passes a point p on the boundary of $\mathcal{N}$, then V_p will either point into the interior of $\mathcal{N}$ or along the boundary of $\mathcal{N}$. This proves the claim of the theorem. □

From Theoreom 1 we immediately obtain two corrolaries:

Corollary 1. *No demographic attractors can exist in $\mathbb{R}^4_+ \setminus \mathcal{N}$.*

Proof. Evidently, $\dot{N} < 0$ always in $\mathbb{R}^4_+ \setminus \mathcal{N}$, hence orbits can not remain indefinitely in this region. □

Corollary 2. *The biologically meaningful region $\mathcal{N}$ must always contain a demographically attracting orbit.* □

Remark 3. Although no examples of chaotic orbits in $\mathcal{N}$ are showcased in this thesis, we do not exclude their existence. We shall refer to the equilibria within $\mathcal{N}$, for which $\hat{I} > 0$, as the *endemic* equilibria. Next, we show that endemic equilibria always exist for all possible parameters, given that one is allowed to vary the host transmission rate, β^H.

4.2.2 The existence of endemic equilibria

It is easy to see that if $\hat{I} = 0$, then the only equilibria of the system are the trivial and disease-free equilibria. Supposing instead that $\hat{I} \neq 0$, we obtain the following expressions from the isoclines of the system:

$$\begin{aligned}
\hat{I}_N &= \frac{(a - \mu - c\hat{N})\hat{N}}{\alpha}, \quad \text{whenever} \quad \alpha > 0, \\
\hat{N}_N &= 0 \text{ or } \hat{N}_{\text{free}}, \quad \text{if} \quad \alpha = 0, \\
\hat{E}_E &= \frac{(1-k)\beta^T(\hat{N} - \frac{(\mu+\nu_I)\hat{I}}{\mu})\hat{I}}{(2-k)\beta^T\hat{I} + \nu_E + \mu}, \\
\hat{E}_I &= \frac{(\alpha + \mu + \nu_I) - k\beta^T\hat{N}}{\beta^T(1-k)} + \frac{k(\mu+\nu_I)\hat{I}}{\mu(1-k)}.
\end{aligned} \tag{14}$$

The subscripts on the left hand sides refer to the isocline from which the equation was obtained, i.e. $\hat{E}_I$ was obtained from the I-isocline. Moreover, $\hat{R}$ has been replaced by $\nu_I\hat{I}/\mu$, as obtained from the R-isocline. Since $\hat{I}_N$ requires that $\alpha > 0$, whenever it is considered in any analysis, the implicit assumption is that $\alpha > 0$.

When the system is assumed to be at an equilibrium, the corresponding sub-population densities are obtained by solving these equations. In particular, we must satisfy $\hat{E}_E = \hat{E}_I$, from which we obtain the following polynomial equation:

$$\begin{aligned}
(\beta^T)^2(\mu+\nu_I)\hat{I}^2 + \left[\mu\left(2(\alpha+\mu+\nu_I) - k\alpha - \beta^T\hat{N}\right) + k\nu_E(\mu+\nu_I)\right]\beta^T\hat{I} \\
+ \mu(\nu_E+\mu)\left(\alpha + \mu + \nu_I - k\beta^T\hat{N}\right) = 0.
\end{aligned} \tag{15}$$

This can be solved for $\hat{I}$, and the roots, $\hat{I}^{\pm}_{EI}$, of this polynomial are given by the expression

$$\hat{I}^{\pm}_{EI} = \frac{-B \pm \sqrt{B^2 - A}}{2\beta^T(\mu+\nu_I)}, \tag{16}$$

where

$$\begin{aligned}
A &= 4\mu(\mu+\nu_I)(\mu+\nu_E)(\alpha+\mu+\nu_I - k\beta^T\hat{N}), \\
B &= \mu\left(2(\alpha+\mu+\nu_I) - k\alpha - \beta^T\hat{N}\right) + k\nu_E(\mu+\nu_I).
\end{aligned}$$

Now we have eliminated $\hat{E}$ from the equations to be solved, and so what remains is to solve the equation

$$\hat{I}_N = \hat{I}^{\pm}_{EI}, \quad \text{whenever} \quad \alpha > 0, \tag{17}$$

to obtain the sub-population densities.

Note that $\hat{I}^{\pm}_{EI}(\hat{N})$ gives two values for each $\hat{N}$, namely $\hat{I}^{+}_{EI}(\hat{N})$ and $\hat{I}^{-}_{EI}(\hat{N})$. On the other hand, $\hat{I}_N(\hat{N})$ is unique for each $\hat{N}$. For this reason, solutions to (17) are

total population densities, each of which correspond to a unique equilibrium of the system and so the analysis of the equilibria will often be done through the study of the equilibrium total population density, which we often denote $\hat{N}_e$. Whenever $\hat{I} > 0$ these equilibria will be endemic equilibria, as Theorem 2 below will show.

Remark 4. Although the above equations were obtained by supposing $\hat{I} \neq 0$. If we now suppose that $\hat{I} = 0$ and use these equations, we see that $\hat{I}_N = 0$ demands that $\hat{N} = \hat{N}_{\text{free}}$. Furthermore, for one of the roots given by $\hat{I}^{\pm}_{EI}$ to equal 0, we must demand that $A = 0$. This happens when

$$\alpha + \mu + \nu_I - k\beta^T \hat{N} = 0,$$

or in other words, when $R_0^P = 1$. And so we conclude that when $R_0^P = 1$ one of the solutions to equation (17) is in fact the disease-free equilibrium, $\hat{N}_{\text{free}}$. We will return to this later in the analysis.

In the special case that $\alpha = 0$, the equilibria are given by

$$\hat{I}^{\pm}_{EI}(0) \quad \text{and} \quad \hat{I}^{\pm}_{EI}(\hat{N}_{\text{free}}),$$

but we shall not concern ourselves with this special case.

Next we present some useful concepts and quantities for the analysis. It will be useful to think of $\hat{I}^{\pm}_{EI}$ and $\hat{I}_N$ as curves in the $(\hat{N}, \hat{I})$-phase plane. Although $\hat{I}^{\pm}_{EI}$ is not strictly an isocline by our definition, it serves the same purpose and so we shall refer to it too as an isocline. The *interior* of $\hat{I}_N$ is the set

$$\{(\hat{N}, \hat{I}) \mid \hat{I} < \hat{I}_N(\hat{N})\},$$

that is, those points that lie under the curve $\hat{I}_N$. The *positive* and *negative* interiors are the sets

$$\{(\hat{N}, \hat{I}) \mid 0 < \hat{I} < \hat{I}_N(\hat{N})\} \quad \text{and} \quad \{(\hat{N}, \hat{I}) \mid \hat{I} < \min(0, \hat{I}_N(\hat{N})\},$$

respectively. Note that $\hat{I}_N(\hat{N}) > 0$ only when $\hat{N} \in (0, \hat{N}_{\text{free}})$. Recall that our biological interpretation of the model demands that all considered equilibria have non-negative sub-population densities. For this reason we present the following simple, yet important, result:

Theorem 2. *Let $\hat{N}_e$ be a solution to $\hat{I}_N = \hat{I}^{\pm}_{EI}$. If $0 < \hat{N}_e < \hat{N}_{free}$, then the equilibrium corresponding to $\hat{N}_e$ is an endemic equilibrium. If $\hat{N}_{free} < \hat{N}_e$, then the corresponding equilibrium is a negative equilibrium.*

Proof. Suppose $0 < \hat{N}_e < \hat{N}_{\text{free}}$ and let $(\hat{S}_e, \hat{E}_e, \hat{I}_e, \hat{R}_e)$ be the equilibrium corresponding to $\hat{N}_e$. Then it is evident that $\hat{I}_e > 0$. Furthermore, from the isocline

identities (8) and (4), respectively, we obtain

$$\hat{E}_e = \frac{(1-k)\hat{I}_e(\alpha+\mu+\nu_I)}{\beta^T\hat{I}_e + k(\mu+\nu_E)} > 0,$$
$$\hat{S}_e = \frac{\hat{E}_e(\beta^T\hat{I}_e+\mu+\nu_E)}{(1-k)\beta^T\hat{I}_e} > 0.$$

Finally, from the R-isocline we obtain

$$\hat{R}_e = \frac{\nu_I\hat{I}_e}{\mu} > 0.$$

□

Recall that a negative equilibrium is such that at least one of the sub-population densities is negative. Much of the analysis in this section boils down to checking on which side of $\hat{N}_{\text{free}}$ a solution, $\hat{N}_e$, exists.

Regarding $\hat{I}^{\pm}_{EI}$ we shall refer to $\hat{I}^{+}_{EI}$ as the *upper arm* of $\hat{I}^{\pm}_{EI}$. Similarly, $\hat{I}^{-}_{EI}$ will be referred to as the *lower arm*.

Since $\hat{I}^{\pm}_{EI}$ is considered to be a function of $\hat{N}$ we shall require its derivative with respect to $\hat{N}$, which is

$$\frac{d\hat{I}^{\pm}_{EI}}{d\hat{N}} = \frac{-B'}{2\beta^T(\mu+\nu_I)} \pm \frac{2BB'-A'}{4\beta^T(\mu+\nu_I)\sqrt{B^2-A}}. \tag{18}$$

Here we've considered A and B as functions of $\hat{N}$ and will continue to do so in the rest of the bifurcation analysis. Notice that A' and B' are both constants. Furthermore, B' is always negative and A' is negative whenever $k > 0$. In the special case where $k = 0$, we have $A' = 0$.

We denote by $\hat{N}_A$ the value for which $A(\hat{N}) = 0$ and similarly $\hat{N}_B$ for the corresponding vanishing point of B. Indeed, $\hat{N}_A$ exists only when $k > 0$. The values of these vanishing points are given by

$$\hat{N}_A = \frac{\alpha+\mu+\nu_I}{k\beta^T}, \quad \text{whenever} \quad k > 0,$$
$$\hat{N}_B = \frac{\mu(2-k)\alpha + (\mu+\nu_I)(2\mu+k\nu_E)}{\mu\beta^T}.$$

Finally, we make use of the real roots of the discriminant, $B^2 - A$, as encountered in $\hat{I}^{\pm}_{EI}$. The discriminant is a parabola that opens upwards, and as we will soon show, it always has real roots. We denote the lesser root by $\hat{N}_{D-}$ and the greater root by $\hat{N}_D$. We leave out the sign from the greater root as we will soon show that the lesser root, $\hat{N}_{D-}$, is completely irrelevant in a biological context.

Lemma 1. *There exists $\hat{N} \in \mathbb{R}$ such that $B(\hat{N})^2 - A(\hat{N}) = 0$.*

Proof. First, we look for the minimum of $B^2 - A$. The derivative is $2BB' - A'$, and by setting this equal to 0 we obtain an equation linear in $\hat{N}$. Solving this we find the point where $B^2 - A$ obtains its minimum, denote this point by $\hat{N}_0$. We have

$$\hat{N}_0 = \frac{2\mu(\alpha + \mu + \nu_I) - k\alpha\mu - 2k\mu^2 - k\mu\nu_E - 2k\mu\nu_I - k\nu_E\nu_I}{\beta^T \mu}.$$

Now, a direct computation yields

$$B(\hat{N}_0)^2 - A(\hat{N}_0) = -4(1-k)^2\mu(\mu + \nu_E)(\mu + \nu_I)(\alpha + \mu + \nu_I).$$

Evidently, for $k < 1$ the minimum is always negative, while at $k = 1$ the minimum is 0 and in this special case we have $\hat{N}_0 = \hat{N}_{D-} = \hat{N}_D$. □

Now that we are convinced that $\hat{N}_D$ always exists, we show that in the biological context we need not concern ourselves with $\hat{N} < \hat{N}_D$.

Theorem 3. *There can not exist an endemic equilibrium for any $\hat{N} < \hat{N}_D$.*

Proof. From Theorem 2, we see that for an equilibrium to be endemic it is enough to require that the sub-population density of the infectious individuals is positive.

Note that if $\hat{N}_{D-} < \hat{N}_D$, then $\hat{I}_{EI}^{\pm}$ obtains complex values for all $\hat{N} \in (\hat{N}_{D-}, \hat{N}_D)$. Biologically meaningful sub-population densities are not complex-valued, hence we study the values that $\hat{I}_{EI}^{\pm}$ obtains when $\hat{N} \leq \hat{N}_{D-}$.

Evidently, $A(\hat{N}_{D-}) \geq 0$. Furthermore, because A is decreasing, the lesser root must always exist where the derivative of B^2 is non-positive, hence $B(\hat{N}_{D-}) \geq 0$. This implies that $-B \leq 0$ and $\sqrt{B^2 - A} \leq |B|$ for all $\hat{N} \leq \hat{N}_{D-}$. Thus, we find that

$$\hat{I}_{EI}^{+} = \frac{-B + \sqrt{B^2 - A}}{2\beta^T(\mu + \nu_I)} \leq 0, \quad \text{for all} \quad \hat{N} \leq \hat{N}_{D-}.$$

Furthermore, it is always so that $\hat{I}_{EI}^{-} \leq \hat{I}_{EI}^{+}$, hence $\hat{I}_{EI}^{\pm}$ must obtain non-positive values for all $\hat{N} \leq \hat{N}_{D-}$. This proves the claim. □

With the result of Theorem 3, we can henceforth restrict ourselves to only consider $\hat{N} \in [\hat{N}_D, \infty)$.

Theorem 3 only talks about the non-existence of endemic equilibria. But what about the existence? In what follows we show that for any possible parameters, we can set β^H such that at least one endemic equilibrium exists. To begin, we present a few useful lemmas.

Lemma 2. *For all $\hat{N} \in [\hat{N}_D, \infty)$, $\hat{I}_{EI}^{+}$ is strictly increasing, while $\hat{I}_{EI}^{-}$ is strictly decreasing.*

Proof. Recall the derivative of $\hat{I}_{EI}^{\pm}$:

$$\frac{d\hat{I}_{EI}^{\pm}}{d\hat{N}} = \frac{-B'}{2\beta^T(\mu+\nu_I)} \pm \frac{2BB'-A'}{4\beta^T(\mu+\nu_I)\sqrt{B^2-A}}.$$

The first term is a positive constant, but what about the second term?

Recall that $\hat{N}_0$ was the minimum of the discriminant, $B^2 - A$. Furthermore, we must have $\hat{N}_D \geq \hat{N}_0$, hence the derivative, $2BB' - A'$, of the discriminant must remain positive for all $\hat{N} \in (\hat{N}_D, \infty)$. This is enough to conclude that $\hat{I}_{EI}^{+}$ must be strictly increasing for all $\hat{N} \in [\hat{N}_D, \infty)$ since all terms in its derivative are positive. For the lower arm, $\hat{I}_{EI}^{-}$, we must be a little more careful.

Indeed, as was mentioned, the first term in the derivative is a positive constant. Hence, we are interested mainly in the second term. Since we wish to show that $\hat{I}_{EI}^{-}$ is strictly decreasing, we ask: what is the maximum value of the derivative? The maximum of the derivative is obtained when the second term is minimised.

Now, as $\hat{N}$ is pushed to the extremes, we obtain the two limits

$$\lim_{\hat{N}\searrow\hat{N}_D} \frac{2BB'-A'}{2\sqrt{B^2-A}} = \infty \quad \text{and} \quad \lim_{\hat{N}\to\infty} \frac{2BB'-A'}{2\sqrt{B^2-A}} = -B'.$$

The first limit implies

$$\lim_{\hat{N}\searrow\hat{N}_D} \frac{d\hat{I}_{EI}^{-}}{d\hat{N}}(\hat{N}) = -\infty.$$

Hence, we may choose $\hat{N}_d$ such that

$$\frac{d\hat{I}_{EI}^{-}}{d\hat{N}}(\hat{N}) < 0,$$

for all $\hat{N} \leq \hat{N}_d$. Thus, I_{EI}^{-} is definitely monotonically decreasing up until $\hat{N} = \hat{N}_d$. Next, we look at how the derivative behaves in the interval $(\hat{N}_d, \infty)$.

Since we wish to minimise the second term in the derivative, we need to look for the extreme values of the fraction

$$\frac{2BB'-A'}{2\sqrt{B^2-A}}.$$

These are obtained where the derivative of this term vanishes, so we obtain

$$\frac{(B')^2}{\sqrt{B^2-A}} - \frac{(2BB'-A')^2}{4\sqrt{B^2-A}^3} = 0,$$

which gives us the identity

$$\frac{2BB'-A'}{2\sqrt{B^2-A}} = -B'.$$

Hence, at the extreme points, the fraction

$$\frac{2BB' - A'}{2\sqrt{B^2 - A}}$$

obtains the same value as its limit at infinity. But this leads to a contradiction: suppose the first extreme is a minimum, then there must exist a maximum as well or else the fraction would not converge to its limit value. Evidently, the maximum must lie above the minimum, yet we just calculated that *every* extreme value the fraction obtains is the same, namely $-B'$. A similar argument shows that the fraction can't have a maximum either, since this would imply the existence of a minimum as well. The only way to satisfy this conundrum is to demand that the fraction remain constant at $-B'$ past its extreme value. This is evidently not true, thus we conclude that the fraction is decreasing in $(\hat{N}_d, \infty)$ and I_{EI}^- is strictly decreasing for all $\hat{N} > \hat{N}_D$. □

From the proof of the above lemma, we obtain the following corollaries which will be of use later in the analysis.

Corollary 3. *As $\hat{N}$ approaches infinity we obtain the following limits:*

$$\lim_{\hat{N}\to\infty} \frac{d\hat{I}_{EI}^+}{d\hat{N}} = \frac{-B'}{\beta^T(\mu + \nu_I)} \quad \textit{and} \quad \lim_{\hat{N}\to\infty} \frac{d\hat{I}_{EI}^-}{d\hat{N}} = 0.$$

□

Corollary 4. *The derivatives of $\hat{I}_{EI}^+$ and $\hat{I}_{EI}^-$ approach $+\infty$ and $-\infty$, respectively, as $\hat{N} \to \hat{N}_D$. We refer to this as $\hat{I}_{EI}^\pm$ being infinitely steep at $\hat{N}_D$.* □

Now, we begin the search for endemic equilibria at the special case when $k = 0$.

Lemma 3. *Suppose $k = 0$. Then $\hat{N}_D > 0$ and $\hat{I}_{EI}^\pm(\hat{N}_D) > 0$.*

Proof. Suppose $k = 0$. Now A is constant and positive, thus $\hat{N}_0 = \hat{N}_B$ and $\hat{N}_D > \hat{N}_B$. Clearly, $\hat{N}_B$ is always positive, hence the claim that $\hat{N}_D > 0$ follows. Furthermore, we have $B(\hat{N}_D) < 0$, hence

$$\hat{I}_{EI}^\pm(\hat{N}_D) = \frac{|B(\hat{N}_D)|}{2\beta^T(\mu + \nu_I)},$$

from which the second claim follows. □

Lemma 4. *Suppose $k = 0$. Then $\hat{N}_D \to 0$ and $\hat{I}_{EI}^\pm(\hat{N}_D) \to 0$ as $\beta^H \to \infty$.*

Proof. Note that at $\hat{N}_D$ we must have $|B(\hat{N}_D)| = \sqrt{A}$, hence we obtain

$$\hat{I}_{EI}^{\pm}(\hat{N}_D) = \frac{\sqrt{A}}{2\beta^T(\mu + \nu_I)}.$$

In addition to being constant with respect to $\hat{N}$, A is also constant with respect to β^H. Since β^T is linear (and increasing) with β^H, we conclude

$$\lim_{\beta^H \to \infty} \hat{I}_{EI}^{\pm}(\hat{N}_D) = 0.$$

Recall that $B' = -\mu\beta^T$, hence, as $\beta^H \to \infty$, B becomes arbitrarily steep. This implies that the distance, $d(\hat{N}_B, \hat{N}_D)$, between $\hat{N}_B$ and $\hat{N}_D$ becomes arbitrarily small. On the other hand, it is easily seen from the expression of $\hat{N}_B$ that $\hat{N}_B \to 0$ as $\beta^H \to \infty$. And so we obtain

$$\lim_{\beta^H \to \infty} d(0, \hat{N}_D) = \lim_{\beta^H \to \infty} d(0, \hat{N}_B) + \lim_{\beta^H \to \infty} d(\hat{N}_B, \hat{N}_D) = 0.$$

□

Lemma 5. *Suppose $k = 0$. Then $\hat{I}_{EI}^{-} > 0$ for all $\hat{N} \in (\hat{N}_D, \infty)$.*

Proof. Indeed, we have $A > 0$ and $\hat{N}_0 = \hat{N}_B < \hat{N}_D$, hence $-B > 0$ and $\sqrt{B^2 - A} < -B$ for all $\hat{N} \geq \hat{N}_D$. And so $-B - \sqrt{B^2 - A} > 0$ for all $\hat{N} > \hat{N}_D$ which implies the claim. □

From these considerations we now obtain the result that at least two endemic equilibria can always be found by varying β^H when $k = 0$.

Theorem 4. *Suppose $k = 0$. Then there exists $\beta_0^H \in (0, \infty)$ such that at least two endemic equilibria exist.*

Proof. Choose $\hat{N}_f \in (0, \hat{N}_{\text{free}})$. Now, by Lemma 4, we may choose β_0^H, such that

$$\hat{N}_D < \hat{N}_f \quad \text{and} \quad \hat{I}_{EI}^{\pm}(\hat{N}_D) < \hat{I}_N(\hat{N}_f).$$

Recall that $\hat{N}_{\text{free}}$ depends on the birthrate a, which is an increasing function of β^H, thus $\hat{N}_{\text{free}}$ is increasing with β^H, as is $\hat{I}_N(\hat{N})$ for all $\hat{N} \in (0, \hat{N}_{\text{free}})$, hence we are guaranteed to be able to satisfy the above inequalities since $\hat{I}_N(\hat{N}_f)$ grows with β^H while $\hat{I}_{EI}^{\pm}(\hat{N}_D)$ shrinks.

Now, by Lemma 2, at β_0^H we have

$$\hat{I}_{EI}^{-}(\hat{N}_f) < \hat{I}_{EI}^{\pm}(\hat{N}_D) < \hat{I}_N(\hat{N}_f),$$

thus $\hat{I}_{EI}^{-}(\hat{N}_f)$ is in the interior of $\hat{I}_N$. Lemma 5 guarantees that $\hat{I}_{EI}^{-}$ remains positive for all $\hat{N} \geq \hat{N}_D$ and so, in particular, $\hat{I}_{EI}^{-}$ resides in the *positive* interior of $\hat{I}_N$ and

must eventually escape this interior through the positive part of $\hat{I}_N$. Indeed, the existence of an endemic equilibrium is guaranteed: at $\hat{N}_{\text{free}}$, we have $\hat{I}_{EI}^{-}(\hat{N}_{\text{free}}) > \hat{I}_N(\hat{N}_{\text{free}}) = 0$, thus we have the two inequalities

$$\hat{I}_{EI}^{-}(\hat{N}_f) < \hat{I}_N(\hat{N}_f) \quad \text{and} \quad \hat{I}_{EI}^{-}(\hat{N}_{\text{free}}) > \hat{I}_N(\hat{N}_{\text{free}}).$$

Since $\hat{N}_f < \hat{N}_{\text{free}}$, the isoclines must intersect at some point $\hat{N}_e \in (\hat{N}_f, \hat{N}_{\text{free}})$. By Theorem 2, this implies the existence of one endemic equilibrium.

Furthermore, if $\hat{I}_{EI}^{\pm}(\hat{N}_D)$ does not lie in the positive interior of $\hat{I}_N$, then another endemic equilibrium must necessarily exist for some $\hat{N}_e \in (\hat{N}_D, \hat{N}_f)$. On the other hand, if $\hat{I}_{EI}^{\pm}(\hat{N}_D)$ does lie in the positive interior, then we are still guaranteed another endemic equilibrium; the upper arm, $\hat{I}_{EI}^{+}$, must in this case escape the positive interior at some point too as $\hat{N}$ is increased, which implies the existence of a second equilibrium. This concludes the proof. □

Remark 5. In all of the examples presented in this thesis, there exist at most two endemic equilibria for any of the chosen parameter values. Whether or not the parameters can be fiddled with in such a manner that more than two equilibria exist will not be dwelt upon.

Next, we show that when $k > 0$ we can once again choose β^H in such a way that we are guaranteed the existence of at least one endemic equilibrium. For that, we will require the following lemma.

Lemma 6. *Suppose $k > 0$. Then either $\hat{I}_{EI}^{+}(\hat{N}_A) = 0$ or $\hat{I}_{EI}^{-}(\hat{N}_A) = 0$.*

Proof. Indeed, at $\hat{N}_A$ we have $\sqrt{B^2 - A} = |B|$. Thus we obtain

$$\hat{I}_{EI}^{\pm}(\hat{N}_A) = \frac{-B \pm |B|}{2\beta^T(\mu + \nu_I)}.$$

Depending on the sign of B, either the upper or the lower arm of $\hat{I}_{EI}^{\pm}$ must vanish at this point. □

Theorem 5. *Suppose $k > 0$. Then there exists β_0^H such that at least one endemic equilibrium exists.*

Proof. Once again, recall that $\hat{N}_{\text{free}}$ is increasing with β^H. On the other hand, as is easily seen from its expression, $\hat{N}_A$ approaches 0 as $\beta^H \to \infty$. Indeed, this allows us to pick a β_0^H such that $0 < \hat{N}_A < \hat{N}_{\text{free}}$. By Lemma 6, $\hat{I}_{EI}^{\pm}$ crosses the $\hat{N}$-axis at $\hat{N}_A$, implying that part of $\hat{I}_{EI}^{\pm}$ must reside in the positive interior of $\hat{I}_N$. We now split the proof into two parts.

First, assume that $\hat{I}_{EI}^{+}(\hat{N}_A) = 0$, that is, the upper arm crosses the $\hat{N}$-axis. Now we have

$$0 = \hat{I}_{EI}^{+}(\hat{N}_A) < \hat{I}_N(\hat{N}_A) \quad \text{and} \quad \hat{I}_{EI}^{+}(\hat{N}_{\text{free}}) > \hat{I}_N(\hat{N}_{\text{free}}) = 0.$$

Since $\hat{I}_{EI}^{+}$ is strictly increasing, the isoclines must cross somewhere in the biologically meaningful region giving us an endemic equilibrium.

Now, assume on the contrary that $\hat{I}_{EI}^{-}(\hat{N}_A) = 0$. Since $\hat{I}_{EI}^{-}$ was decreasing and monotone, it obtains positive values for $\hat{N} < \hat{N}_A$. Evidently, $\hat{N}_D < \hat{N}_A$, thus $\hat{I}_{EI}^{\pm}(\hat{N}_D) > 0$. Now, if $\hat{I}_{EI}^{\pm}(\hat{N}_D)$ does not reside within the positive interior, there must exist an endemic equilibrium somewhere in the interval $(\hat{N}_D, \hat{N}_A)$. On the other hand, if $\hat{I}_{EI}^{\pm}(\hat{N}_D)$ does reside within the positive interior, then we shift our focus to $\hat{I}_{EI}^{+}$; it is monotonically increasing, hence we must have

$$\hat{I}_{EI}^{\pm}(\hat{N}_D) < \hat{I}_N(\hat{N}_D) \quad \text{and} \quad \hat{I}_{EI}^{+}(\hat{N}_{\text{free}}) > \hat{I}_N(\hat{N}_{\text{free}}).$$

This implies the existence of an endemic equilibrium. □

Now that we have convinced ourselves of the fact that the system can have endemic equilibria in addition to the trivial and disease-free equilibria, the next question is how these equilibria move about and interact in the phase space as the parameters of the system are varied? In the next section, we present some answers to this question, as we study the bifurcation patterns of the system when the host transmission rate, β^H, is varied.

4.3 Bifurcation analysis

In this section we study the bifurcation patterns of the model. In particular, we focus on finding conditions under which the system exhibits *a backward bifurcation*. Moreover, we show that whenever a backward bifurcation occurs, a saddle-node bifurcation will also occur. Finally, we present a few examples showcasing the rich dynamics of the model. Figure 1 provides a visual aid in understanding the results of this section.

It is well known that in population invasion models the basic reproduction number, R_0, plays an important role in determining the outcome of an invasion event. Indeed, if $R_0 < 1$ for the invading population, it will go extinct, while if $R_0 > 1$, then the invasion will be successful. The point where $R_0 = 1$ is a point of bifurcation. For the time being, we shall simply declare this as fact, but later we show in Theorem 6 that this is indeed the case for our model as well. Mathematically, one talks of a *transcritical* bifurcation in which one equilibrium passes through another, exchanging stabilities in the process; the initially stable equilibrium has become unstable and vice versa. This is known as the *principle of exchange of stabilities* [7]. In our model, the pathogen will be considered the invading population. We will see that this transcritical bifurcation always occurs such that the initially stable disease-free equilibria merges for an instant with an endemic equilibrium, which then slides into

a biologically meaningless region of the phase plane as the bifurcation parameter is varied.

As was mentioned, an exchange of stability happens at the transcritical bifrucation. Mathematically, there is only one type of transcritical bifurcation; two equilibria exchange stabilities as they collide and separate. From a biological point of view, however, there are two. Naively, one might think that the endemic equilibrium involved in the bifurcation always becomes biologically meaningful when the model at hand transitions to a state where $R_0 > 1$ and invasion is possible. When this happens, we talk about a *forward* bifurcation. However, as we will see in our model as well, sometimes it just so happens that the endemic equilibrium involved in the bifurcation exists for $R_0 < 1$ and, in fact, disappears into the biologically meaningless region at $R_0 > 1$. This situation is called a *backward* bifurcation. For a more thorough treatment on this, see [7].

The bifurcation parameter in this analysis is β^H. Recall that the total transmission rate, β^T, was defined as $\beta^T = \beta^H \beta^P$, hence changes in β^H are directly proportional to changes in β^T. And so, as we discuss varying β^H, this will manifest in the equations as variations in β^T.

The reason for varying β^H in the bifurcation analysis is that later we will show that the evolutionarily attracting pathogen transmission rate, β^P, is independent of the value of the host transmission rate. So we fix β^P at the evolutionary attractor, and see how the system behaves when β^H is allowed to evolve. Furthermore, R_0^P is crucial for the bifurcation analysis and monotone in β^H, but not necessarily monotone in β^P. Thus, the bifurcation analysis is relatively simple when β^H is the bifurcation parameter. On the other hand, not much can be said about how the system behaves with respect to changes in β^P, without making some assumptions about the ratio α/β^P.

4.3.1 Conditions for forwards and backwards bifurcations

In this section we look at what happens in the vicinity of $R_0^P = 1$. As mentioned earlier, the bifurcation parameter is the host transmission rate, β^H. For this reason we write β_1^H when β^H is such that that $R_0^P = 1$. Recall that for $k = 0$ we have $R_0^P = 0$, hence throughout this section we implicitly assume that $k > 0$.

Recall that the transcritical bifurcation occurring at $\beta^H = \beta_1^H$ is classified as a forward bifurcation if the endemic equilibrium partaking in the bifurcation exists for $R_0^P > 1$. Translating to β^H, the direction of bifurcation is forward if $\beta^H > \beta_1^H$, since R_0^P is an increasing function of β^H. Conversely, the bifurcation is a backward bifurcation if the endemic equilibrium exists when $\beta^H < \beta_1^H$. Henceforth, we speak of the transcritical bifurcation in terms of β^H rather than R_0^P. So far we have simply supposed that it is known that the transcritical bifurcation occurs at β_1^H, however, Theorem 6 in this section will finally prove this claim.

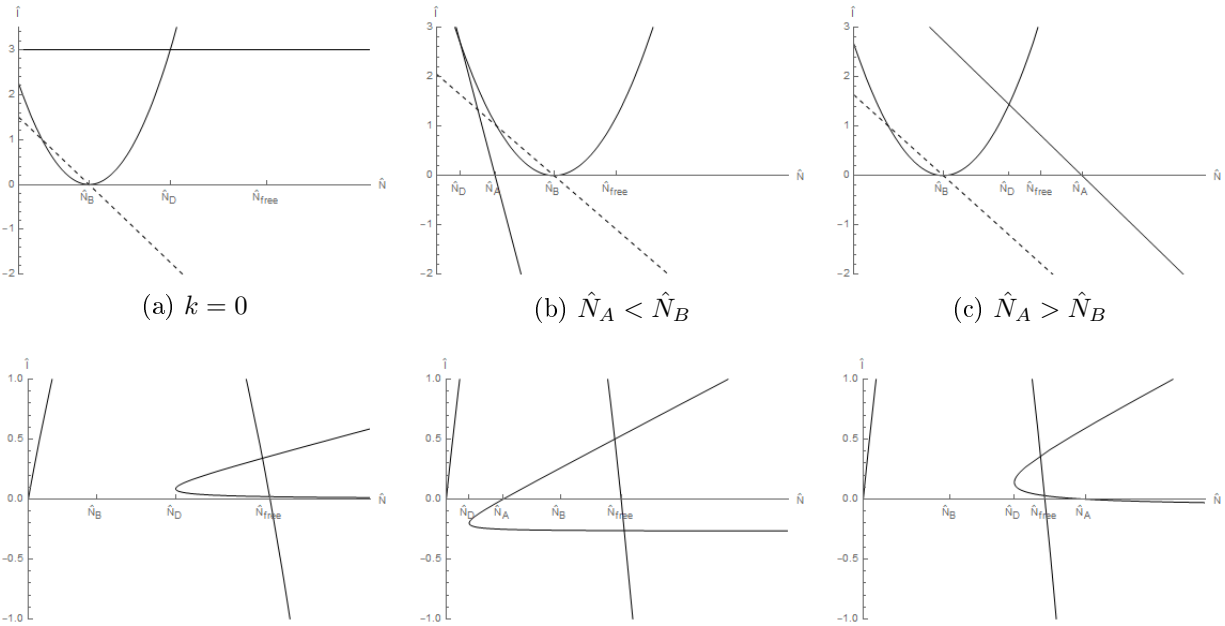

(a) $k = 0$

(b) $\hat{N}_A < \hat{N}_B$

(c) $\hat{N}_A > \hat{N}_B$

(d) At $k = 0$ the transcritical bifurcation does not occur. β^H can always be set so that two equilibria are present. These equilibria merge and disappear through the saddle-node bifurcation.

(e) $R_0^P > 1$. One endemic equilibrium is present. As β^H is decreased, the ordering of $\hat{N}_A$ and $\hat{N}_{\text{free}}$ changes and the equilibrium disappears. The bifurcation is forward in this configuration.

(f) $R_0^P < 1$. Two endemic equilibria are present. As β^H is increased, the ordering of $\hat{N}_A$ and $\hat{N}_{\text{free}}$ changes, in which case only the upper endemic equilibrium remains. The bifurcation is backward in this configuration.

Figure 1: A visual aid for the reader. The three columns represent typical examples of the configurations for each situation. The upper row shows B as the dashed line, A as the straight solid line and B^2 as the parabola. The bottom row shows the corresponding situation in terms of the isoclines $\hat{I}_N$ and $\hat{I}_{EI}^{\pm}$. When β^H is varied, the quantities $\hat{N}_{\text{free}}$, $\hat{N}_A$, $\hat{N}_B$ and $\hat{N}_D$ slide along the $\hat{N}$-axis. When $\hat{N}_A < \hat{N}_{\text{free}}$ we have $R_0^P > 1$ and when $\hat{N}_A > \hat{N}_{\text{free}}$ we have $R_0^P < 1$. The transcritical bifurcation occurs when $\hat{N}_A = \hat{N}_{\text{free}}$. Note that $\hat{I}_{EI}^{\pm}$ crosses the $\hat{N}$-axis at $\hat{N}_A$.

The main results in this section are characterising conditions under which a backward bifurcation occurs at β_1^H and proving that whenever this occurs, or when $k = 0$, a saddle-node bifurcation will occur for some $\beta_{sn}^H < \beta_1^H$ in the biologically meaningful region as well. A saddle-node bifurcation is one in which two initially separate equilibria collide and then disappear entirely, as the bifurcation parameter is varied.

The quantities $\hat{N}_A$ and $\hat{N}_B$ play a significant role in the coming results, hence we repeat their expressions here for easier reference:

$$\hat{N}_A = \frac{\alpha + \mu + \nu_I}{k\beta^T}, \quad \text{whenever} \quad k > 0,$$
$$\hat{N}_B = \frac{\mu(2-k)\alpha + (\mu + \nu_I)(2\mu + k\nu_E)}{\mu\beta^T}.$$

As we shall see in the course of this section, the ordering of $\hat{N}_A$ and $\hat{N}_B$ is of crucial importance in determining which type of transcritical bifurcation that occurs at β_1^H, hence we arrive at our first few lemmas. The first one is of less relevance to the analysis and more of a helpful reference to the reader that has lost track of their roots.

Lemma 7. *Suppose $\hat{N}_A \leq \hat{N}_B$, then the following ordering holds*

$$\hat{N}_D \leq \hat{N}_A \leq \hat{N}_B,$$

where if any of the inequalities are equalities, then both inequalities are equalities. Conversely, suppose $\hat{N}_A > \hat{N}_B$, then the ordering is as follows:

$$\hat{N}_B < \hat{N}_D < \hat{N}_A.$$

Proof. Recall that at $\hat{N}_D$ we have $B^2 - A = 0$. This implies that $A \geq 0$ at $\hat{N}_D$. In particular, A being decreasing, this implies that $\hat{N}_A \geq \hat{N}_D$ regardless of the chosen parameters. Evidently, if $\hat{N}_B = \hat{N}_A$, then we must have $\hat{N}_D = \hat{N}_A = \hat{N}_B$.

Suppose $\hat{N}_A < \hat{N}_B$. Then we have

$$\hat{N}_D \leq \hat{N}_A < \hat{N}_B.$$

But now it is easy to see that the first inequality must be strict as well: suppose $\hat{N}_D = \hat{N}_A$. Then $B(\hat{N}_A)^2 - A(\hat{N}_A) = B(\hat{N}_A)^2 = 0$, which implies that $\hat{N}_A = \hat{N}_B$; a contradiction. Thus, the first claim of the lemma has been proven.

Suppose now that $\hat{N}_A > \hat{N}_B$. Then we have

$$B(\hat{N}_B)^2 - A(\hat{N}_B) = -A(\hat{N}_B) < 0,$$

hence the discriminant, $B^2 - A$, is negative at this point. This implies that $\hat{N}_B < \hat{N}_D$. □

Lemma 8. *Suppose $\beta^H = \beta_1^H$, that is, β^H is such that $R_0^P = 1$. Then $\hat{N}_A = \hat{N}_{free}$.*

Proof. Recall the definition of R_0^P:

$$R_0^P = \frac{k\beta^T \hat{N}_{\text{free}}}{\alpha + \mu + \nu_I}.$$

Indeed, setting this to 1, we obtain

$$\hat{N}_{\text{free}} = \frac{\alpha + \mu + \nu_I}{k\beta^T} = \hat{N}_A.$$

□

Corollary 5. *The following relationship holds*

$$\begin{aligned} R_0^P < 1 \quad &\Leftrightarrow \quad N_A > \hat{N}_{free}, \\ R_0^P > 1 \quad &\Leftrightarrow \quad N_A < \hat{N}_{free}. \end{aligned}$$

□

Lemma 9. *Suppose $\hat{N}_A \leq \hat{N}_B$. Then $\hat{I}_{EI}^+(\hat{N}_A) = 0$ and $\hat{I}_{EI}^- < 0$ for all $\hat{N} > \hat{N}_D$. Conversely, suppose $\hat{N}_A > \hat{N}_B$. Then $\hat{I}_{EI}^-(\hat{N}_A) = 0$ and $\hat{I}_{EI}^+ > 0$ for all $\hat{N} \geq \hat{N}_D$*

Proof. Suppose first that $\hat{N}_A \leq \hat{N}_B$. We have

$$\hat{I}_{EI}^{\pm}(\hat{N}_A) = \frac{-B(\hat{N}_A) \pm |B(\hat{N}_A)|}{2\beta^T(\mu + \nu_I)},$$

since $B(\hat{N}_A) \geq 0$, the claim $\hat{I}_{EI}^+(\hat{N}_A) = 0$ follows. Furthermore, Lemma 2 implies that $\hat{I}_{EI}^- < 0$ for all $\hat{N} > \hat{N}_D$.

Conversely, suppose $\hat{N}_A > \hat{N}_B$. By Lemma 7, $B < 0$ for all $\hat{N} > \hat{N}_D$. By the same considerations as above, we now find that $\hat{I}_{EI}^-(\hat{N}_A) = 0$. Once more, Lemma 7 implies that $\hat{I}_{EI}^{\pm}(\hat{N}_D) > \hat{I}_{EI}^-(\hat{N}_A)$, and so $\hat{I}_{EI}^+ > 0$ for all $\hat{N} \geq \hat{N}_D$. This completes the proof. □

Lemma 10. *The ratio $\hat{N}_A/\hat{N}_B$ is invariant with respect to β^H.*

Proof. A simple calculation proves the claim:

$$\frac{\hat{N}_A}{\hat{N}_B} = \frac{\mu(\alpha + \mu + \nu_I)}{k(\mu(2-k)\alpha + (\mu + \nu_I)(2\mu + k\nu_E))}.$$

□

This result is very useful, since together with Lemma 9, it implies that the arm of $\hat{I}_{EI}^{\pm}$ which crosses the $\hat{N}$-axis does not change as β^H is varied.

Before we present the first theorem of this section, we need to take care of a small technical detail. As has already been alluded to, the system might exhibit a saddle-node bifurcation as well. When discussing the transcritical bifurcation, we need to make sure that the saddle-node bifurcation does not occur at the same point as the transcritical bifurcation. Recall that at the saddle-node bifurcation two equilibria merge before entirely disappearing. In the context of the isoclines, this means that at the point of bifurcation the derivatives of $\hat{I}_{EI}^{\pm}$ and $\hat{I}_N$ must be equal. Next, we show that when $\hat{N}_A \leq \hat{N}_B$ this can never be the case at β_1^H, hence we will not have to worry about this detail in that specific case. In the other case, when $\hat{N}_A > \hat{N}_B$, we shall instead include a condition on the derivatives in the assumptions of our theorems in order to avoid the saddle-node bifurcation occurring at β_1^H. In what follows, we write $\hat{N}_{\text{free}}(\beta_1^H)$ to indicate the disease-free equilibrium at $\beta^H = \beta_1^H$. When the value of β^H is not fixed, we write $\hat{N}_{\text{free}}$ without the argument, in accordance with the notation so far.

Lemma 11. *Suppose $\hat{N}_A \leq \hat{N}_B$ and $\beta^H = \beta_1^H$. Then*

$$\frac{d\hat{I}_{EI}^{+}}{d\hat{N}}(\hat{N}_{free}(\beta_1^H)) > \frac{d\hat{I}_N}{d\hat{N}}(\hat{N}_{free}(\beta_1^H)).$$

Proof. Recall that at β_1^H, we have $\hat{N}_A = \hat{N}_{\text{free}}$. By Lemma 9, it is the upper arm, $\hat{I}_{EI}^{+}$ which intersects $\hat{I}_N$ at $\hat{N}_{\text{free}}$. Moreover, by Lemma 7, for all $\hat{N} > \hat{N}_D$, we have

$$\frac{d\hat{I}_{EI}^{+}}{d\hat{N}} > 0,$$

while at $\hat{N}_{\text{free}}(\beta_1^H) = (a(\beta_1^H) - \mu)/c$ we have

$$\frac{d\hat{I}_N}{d\hat{N}}(\hat{N}_{\text{free}}(\beta_1^H)) = \frac{a(\beta_1^H) - \mu - 2c\hat{N}_{\text{free}}(\beta_1^H)}{\alpha} = -\frac{a(\beta_1^H) - \mu}{\alpha} < 0.$$

Evidently the derivatives can't match in the special case where $\hat{N}_A = \hat{N}_D$, as $\hat{I}_{EI}^{+}$ becomes infinitely steep as $\hat{N}_D$ is approached. □

The next result is due to the implicit function theorem and will form the backbone of our analysis as we determine which type of transcritical bifurcation occurs at β_1^H.

Theorem 6. *Suppose $\beta^H = \beta_1^H$ and*

$$\frac{d\hat{I}_N}{d\hat{N}}(\hat{N}_{free}(\beta_1^H)) \neq \frac{d\hat{I}_{EI}^{+}}{d\hat{N}}(\hat{N}_{free}(\beta_1^H)) \quad or \quad \frac{d\hat{I}_N}{d\hat{N}}(\hat{N}_{free}(\beta_1^H)) \neq \frac{d\hat{I}_{EI}^{-}}{d\hat{N}}(\hat{N}_{free}(\beta_1^H)),$$

depending on which arm of $\hat{I}_{EI}^{\pm}$ *crosses* $\hat{I}_N$ *at* $\hat{N}_{free}(\beta_1^H)$. *Then there exists* $\delta > 0$ *and* $\varepsilon > 0$ *such that* $\hat{I}_{EI}^{\pm} = \hat{I}_N$ *has a unique solution in* $\left(\hat{N}_{free}(\beta_1^H) - \varepsilon, \hat{N}_{free}(\beta_1^H) + \varepsilon\right)$ *for all* $\beta^H \in (\beta_1^H - \delta, \beta_1^H + \delta)$.

Proof. The proof is a simple application of the implicit function theorem.

Define $f(\hat{N}, \beta^H) = \hat{I}_{EI}^{\pm}(\hat{N}, \beta^H) - \hat{I}_N(\hat{N}, \beta^H)$. Now, by our assumption we have

$$\frac{\partial f}{\partial \hat{N}}(\hat{N}_{\text{free}}(\beta_1^H), \beta_1^H) \neq 0,$$

hence the implicit function theorem applies and there exists a neighbourhood $U = (\beta_1^H - \delta, \beta_1^H + \delta)$ for some $\delta > 0$ and a neighbourhood $V = \left(\hat{N}_{\text{free}}(\beta_1^H) - \varepsilon, \hat{N}_{\text{free}}(\beta_1^H) + \varepsilon\right)$ for some $\varepsilon > 0$ and a unique continuous function $g : U \to V$, such that

$$f(g(\beta^H), \beta^H) = 0 \quad \text{for all} \quad \beta^H \in U,$$

and in particular

$$f(g(\beta_1^H), \beta_1^H) = f(\hat{N}_{\text{free}}(\beta_1^H), \beta_1^H).$$

□

Corollary 6. β_1^H *is the point of the transcritical bifurcation.*

Proof. For each $\beta^H \in U$, the values of $g(\beta^H)$ correspond to a unique solution of $\hat{I}_{EI}^{\pm} = \hat{I}_N$, which in turn corresponds to a unique equilibrium of the system. Hence, we conclude that g tracks a unique equilibrium that passes through the disease-free equilibrium at $\beta^H = \beta_1^H$. □

Indeed, Theorem 6 guarantees that as we vary β^H slightly in the vicinity of β_1^H, we can rest assured that an equilibrium passes through the disease-free equilibrium, the two merging exactly at β_1^H. Moreover, determining the type of bifurcation becomes easy: all we need to do is restrict ourselves to a suitably small neighbourhood of $\hat{N}_{\text{free}}$ and find the solution. The implicit function theorem then guarantees that this solution corresponds to the unique bifurcating equilibrium. Recall Theorem 2, which states that a solution, $\hat{N}_e$, of $\hat{I}_{EI}^{\pm} = \hat{I}_N$, corresponds to an endemic equilibrium if and only if $\hat{N}_e \in (0, \hat{N}_{\text{free}})$. In the following theorems, the proofs boil down to checking on which side of $\hat{N}_{\text{free}}$ the solution $\hat{N}_e$ lies as β^H is varied in the vicinity of β_1^H.

Theorem 7. *Suppose* $\hat{N}_A \leq \hat{N}_B$. *Then a forward bifurcation occurs at* $\beta^H = \beta_1^H$.

Proof. By Lemma 9, any endemic equilibria of the system must exist on $\hat{I}_{EI}^{+}$. By Lemma 11, we can apply the implicit function theorem. Hence, let $\delta > 0$ and $\varepsilon > 0$ be at least small enough for the implicit function theorem to apply.

Now, for $\beta^H \in (\beta_1^H - \delta, \beta_1^H)$, we have

$$\hat{N}_{\text{free}} < \hat{N}_A \quad \Leftrightarrow \quad R_0^P < 1.$$

Since $\hat{I}_{EI}^{+}$ obtains positive values only for $\hat{N} > \hat{N}_A$, and $\hat{N}_A > \hat{N}_{\text{free}}$, we know that no endemic equilibria can exist when $R_0^P < 1$, but we know that a unique solution to $\hat{I}_{EI}^{\pm} = \hat{I}_N$ must nonetheless exist somewhere close to $\hat{N}_{\text{free}}(\beta_1^H)$. It's not $\hat{N}_{\text{free}}$ either, so the bifurcating equilibrium must be negative.

On the other hand, for $\beta^H \in (\beta_1^H, \beta_1^H + \delta)$ we have

$$\hat{N}_A < \hat{N}_{\text{free}} \quad \Leftrightarrow \quad R_0^P > 1.$$

From this we also obtain the inequalities

$$\hat{I}_{EI}^{+}(\hat{N}_A) < \hat{I}_N(\hat{N}_A) \quad \text{and} \quad \hat{I}_{EI}^{+}(\hat{N}_{\text{free}}) > \hat{I}_N(\hat{N}_{\text{free}}).$$

Hence, the isoclines have crossed somewhere in the interval $(\hat{N}_A, \hat{N}_{\text{free}})$ implying the existence of an endemic equilibrium.

In summary, we have shown that $R_0^P > 1$ gives rise to an endemic equilibrium, while at $R_0^P < 1$ the equilibrium has transitioned into the biologically meaningless region. Since the conditions of the implicit function theorem are satisfied, this is the unique bifurcating equilibrium. A forward bifurcation has occurred. □

Theorem 7 shows that whenever $\hat{N}_A \leq \hat{N}_B$, we can never have a backward bifurcation. What remains is to check the case where $\hat{N}_A > \hat{N}_B$. Indeed, Lemma 9 tells us that when this is the case, it is the lower arm, $\hat{I}_{EI}^{-}$, that crosses the $\hat{N}$-axis. As usual, at β_1^H, this crossing happens at $\hat{N}_{\text{free}}$, but now we need to be more careful than in the previous case: the derivative of $\hat{I}_{EI}^{-}$ determines the type of transcritical bifurcation. If it happens that

$$\left.\frac{d\hat{I}_{EI}^{-}}{d\hat{N}}\right|_{\hat{N}=\hat{N}_{\text{free}}(\beta_1^H)} < \left.\frac{d\hat{I}_N}{d\hat{N}}\right|_{\hat{N}=\hat{N}_{\text{free}}(\beta_1^H)},$$

then $\hat{I}_{EI}^{\pm}$ lies in the interior of $\hat{I}_N$ only for $\hat{N} > \hat{N}_{\text{free}}$ and backwards bifurcation can not occur. The next theorem will clarify this assertion.

Theorem 8. *Suppose $\hat{N}_A > \hat{N}_B$ and*

$$\left.\frac{d\hat{I}_{EI}^{-}}{d\hat{N}}\right|_{\hat{N}=\hat{N}_{free}(\beta_1^H)} < \left.\frac{d\hat{I}_N}{d\hat{N}}\right|_{\hat{N}=\hat{N}_{free}(\beta_1^H)}$$

at $\beta^H = \beta_1^H$. Then a forward bifurcation occurs.

Proof. Set $\beta^H = \beta_1^H$ and choose $\delta > 0$ and $\varepsilon > 0$ so that the implicit function theorem applies. Recall Lemma 9: since $\hat{N}_A > \hat{N}_B$, it is the lower arm, $\hat{I}_{EI}^-$, that crosses the $\hat{N}$-axis at $\hat{N}_A$. By the condition

$$\left.\frac{d\hat{I}_{EI}^-}{d\hat{N}}\right|_{\hat{N}=\hat{N}_{\text{free}}(\beta_1^H)} < \left.\frac{d\hat{I}_N}{d\hat{N}}\right|_{\hat{N}=\hat{N}_{\text{free}}(\beta_1^H)},$$

it is clear that parts of $\hat{I}_{EI}^-$ lie in the interior of $\hat{I}_N$ for $\hat{N} > \hat{N}_{\text{free}}$.

Now, pick a point $\hat{N}_f \in \left(\hat{N}_{\text{free}}(\beta_1^H), \hat{N}_{\text{free}}(\beta_1^H) + \varepsilon\right)$. Since the chosen ε-neighbourhood excludes the existence of any solutions to $\hat{I}_{EI}^{\pm} = \hat{I}_N$ in this interval, we know that $\hat{I}_{EI}^-(\hat{N}_f) < \hat{I}_N(\hat{N}_f)$ must apply. If $\delta > 0$ is not small enough, by continuity there exists a $\delta_0 > 0$ so small that $\hat{I}_{EI}^- < \hat{I}_N$ remains the case for all $\beta^H \in (\beta_1^H - \delta_0, \beta_1^H)$. But now, since $\beta^H < \beta_1^H$, we have

$$\hat{N}_A > \hat{N}_{\text{free}} \quad \Leftrightarrow \quad R_0^P < 1.$$

Hence $\hat{I}_{EI}^-(\hat{N}_{\text{free}}) > \hat{I}_N(\hat{N}_{\text{free}})$, but this implies that $\hat{I}_{EI}^- = \hat{I}_N$ must have a solution somewhere in the interval $(\hat{N}_{\text{free}}, \hat{N}_f)$. Since the solution is greater than $\hat{N}_{\text{free}}$, the corresponding unique bifurcating equilibrium must be negative.

Conversely, pick $\hat{N}_f \in \left(\hat{N}_{\text{free}}(\beta_1^H) - \varepsilon, \hat{N}_{\text{free}}(\beta_1^H)\right)$ so that
$\hat{I}_{EI}^-(\hat{N}_f) > \hat{I}_N(\hat{N}_f)$. Now, if need be, we may choose $\delta_0 > 0$ so that this inequality is preserved for all $\beta^H \in (\beta_1^H, \beta_1^H + \delta_0)$. But now, we also have

$$\hat{N}_A < \hat{N}_{\text{free}} \quad \Leftrightarrow \quad R_0^P > 1.$$

Hence $\hat{I}_{EI}^-(\hat{N}_A) < \hat{I}_N(\hat{N}_A)$, which implies that a solution must exist in the interval $(\hat{N}_f, \hat{N}_{\text{free}})$. Once again, since we are in the required (ε, δ)-neighbourhood, the implicit function theorem applies and we conclude that the corresponding bifurcating equilibrium is endemic.

In summary, we have shown that $R_0^P > 1$ gives rise to an endemic equilibrium, while at $R_0^P < 1$ the equilibrium has transitioned into the biologically meaningless region. A forward bifurcation has occurred. □

Now, we are beginning to run out of options and it might appear like a backward bifurcation could never occur! However, one more possibility remains, and as the following theorem will show, this is exactly when a backward bifurcation occurs.

Theorem 9. *Suppose* $\hat{N}_A > \hat{N}_B$ *and*

$$\left.\frac{d\hat{I}_{EI}^-}{d\hat{N}}\right|_{\hat{N}=\hat{N}_{free}(\beta_1^H)} > \left.\frac{d\hat{I}_N}{d\hat{N}}\right|_{\hat{N}=\hat{N}_{free}(\beta_1^H)} \tag{19}$$

at $\beta^H = \beta_1^H$. Then a backward bifurcation occurs.

Proof. We proceed as in the proof to the previous theorem. Set $\beta^H = \beta_1^H$ and let $\delta > 0$ and $\varepsilon > 0$ be such that the implicit function theorem applies.

This time the inequality is the other way around, and so we see that part of $\hat{I}_{EI}^-$ resides in the positive interior of $\hat{I}_N$ when $\beta^H = \beta_1^H$. In particular, $\hat{I}_{EI}^-$ exits the positive interior at $\hat{N}_{\text{free}}(\beta_1^H)$.

Since part of $\hat{I}_{EI}^-$ lies in the positive interior at β_1^H, we may pick a point $\hat{N}_f \in \left(\hat{N}_{\text{free}}(\beta_1^H) - \varepsilon, \hat{N}_{\text{free}}(\beta_1^H)\right)$ such that $\hat{I}_{EI}^-(\hat{N}_f) < \hat{I}_N^-(\hat{N}_f)$. Furthermore, we find $\delta_0 > 0$ such that for all $\beta^H \in (\beta_1^H - \delta_0, \beta_1^H)$ the desired property remains. But now we have

$$\hat{N}_A > \hat{N}_{\text{free}} \quad \Leftrightarrow \quad R_0^P < 1,$$

which implies $\hat{I}_{EI}^-(\hat{N}_{\text{free}}) > \hat{I}_N(\hat{N}_{\text{free}})$, and so this implies the existence of a solution in the interval $(\hat{N}_f, \hat{N}_{\text{free}})$; the bifurcating equilibrium is endemic.

Conversely, pick $\hat{N}_f \in \left(\hat{N}_{\text{free}}(\beta_1^H), \hat{N}_{\text{free}}(\beta_1^H) + \varepsilon\right)$. Now $\hat{I}_{EI}^-(\hat{N}_f) > \hat{I}_N(\hat{N}_f)$ and we may preserve this for all $\beta^H \in (\beta_1^H, \beta_1^H + \delta_0)$ provided we choose $\delta_0 > 0$ small enough. But, on the other hand, for all $\beta^H \in (\beta_1^H, \beta_1^H + \delta_0)$, we have

$$\hat{N}_A < \hat{N}_{\text{free}} \quad \Leftrightarrow \quad R_0^P > 1.$$

Hence $\hat{I}_{EI}^-(\hat{N}_{\text{free}}) < \hat{I}_N(\hat{N}_{\text{free}})$ while $\hat{I}_{EI}^-(\hat{N}_f) > \hat{I}_N^-(\hat{N}_f)$. An solution must exist within $(\hat{N}_{\text{free}}, \hat{N}_f)$; the bifurcating equilibrium is negative.

In summary, we have shown that $R_0^P < 1$ gives rise to an endemic equilibrium, while at $R_0^P > 1$ the equilibrium has transitioned into the biologically meaningless region. A backward bifurcation has occurred! □

4.3.2 The saddle-node bifurcation

Recall Theorem 4 which states that, at $k = 0$, we can always choose β^H such that at least two endemic equilibria exist. Furthermore, when $k > 0$, if the assumptions of Theorem 9 hold, then we can also choose $\beta^H < \beta_1^H$ so that at least two endemic equilibria are present. Indeed, one equilibrium lies on the lower arm $\hat{I}_{EI}^-$, as stated by Theorem 9. At this equilibrium the isoclines cross. Moreover, $\hat{I}_{EI}^-$ enters the positive interior of $\hat{I}_N$, as $\hat{N}$ approaches $\hat{N}_D$; a consequence of the derivative condition (19). If $\hat{I}_{EI}^{\pm}(\hat{N}_D)$ does not lie in the positive interior, then the existence of another endemic equilibrium is implied. On the other hand, if $\hat{I}_{EI}^{\pm}(\hat{N}_D)$ remains in the interior, we can start tracing $\hat{I}_{EI}^+$ as $\hat{N}$ is increased. Eventually the upper arm must exit the positive interior, implying the existence of a second endemic equilibrium.

Next we show that a saddle-node bifurcation occurs in the biologically meaningful region if $k = 0$ or the direction of the transcritical bifurcation is backward. We begin by showing that for sufficiently small β^H, the isoclines must separate, that is, they no longer intersect at any point.

Lemma 12. *Suppose $k = 0$ or $k > 0$ and $\hat{N}_A > \hat{N}_B$. Then the isoclines $\hat{I}_N$ and $\hat{I}_{EI}^{\pm}$ must separate as $\beta^H \to 0$.*

Proof. Recall that in both cases $\hat{N}_D > \hat{N}_B$ and $\hat{N}_B \to \infty$ as $\beta^H \to 0$, hence we conclude that $\hat{N}_D \to \infty$ as $\beta^H \to 0$.

Let us first study the case when $k = 0$. Recall Lemma 5, which implies that $\hat{I}_{EI}^{\pm} > 0$ for all $\hat{N} \geq \hat{N}_D$. So we just need to choose β^H small enough that $\hat{N}_{\text{free}} < \hat{N}_D$. This guarantees that the two curves have separated.

Now, suppose instead $k > 0$ and $\hat{N}_A > \hat{N}_B$. Let us take a look at the derivative of $\hat{I}_{EI}^{-}$ at $\hat{N}_A$. We obtain

$$\frac{d\hat{I}_{EI}^{-}}{d\hat{N}}(\hat{N}_A) = \frac{-k\mu(\mu + \nu_E)}{|B(\hat{N}_A)|}.$$

This is constant with respect to β^H. Indeed, the only factor which seemingly depends on β^H is $|B(\hat{N}_A)|$. In this factor, the only term which contains β^H is $-\mu\beta^T\hat{N}_A$. But this we may substitute with

$$\beta^T\hat{N}_A = \frac{\alpha + \mu + \nu_I}{k}.$$

Hence, the derivative above is in fact independent of β^H. Thus, we may choose β_D^H such that $\hat{N}_{\text{free}} < \hat{N}_D$ and we may choose β_d^H such that

$$\frac{d\hat{I}_{EI}^{-}}{d\hat{N}}(\hat{N}_A) > \frac{d\hat{I}_N}{d\hat{N}}(\hat{N}_A).$$

Indeed, we have

$$\lim_{\beta^H \to 0} \frac{d\hat{I}_N}{d\hat{N}}(\hat{N}_A) = \lim_{\beta^H \to 0} \frac{a(\beta^H) - \mu}{\alpha} - \frac{2c(\alpha + \mu + \nu_I)}{\alpha\beta^T} = -\infty,$$

Hence, the lesser of these two transmission rates will guarantee that the two curves have separated.

Here, simply demanding that $\hat{N}_{\text{free}} < \hat{N}_D$ is not enough. Indeed, we might have that $\hat{N}_{\text{free}} < \hat{N}_D$ holds, but $\hat{I}_{EI}^{-}$ is so steep that it intersects $\hat{I}_N$ nonetheless; something that could not happen for $k = 0$ due to the positivity of $\hat{I}_{EI}^{-}$. For this reason we require the condition on the derivatives as well. □

Since the two isoclines can be made to separate provided that β^H is chosen low enough, this implies the existence of a saddle-node bifurcation. Starting from the separated configuration and increasing β^H, there must come a first point of contact between the curves. Immediately after this, as we further increase β^H, this single point of contact splits into two equilibria as $\hat{I}_{EI}^{\pm}$ crosses into the interior of $\hat{I}_N$. In the next theorem, we show that whenever $k = 0$ or $k > 0$ and $\hat{N}_A > \hat{N}_B$ and condition (19) holds, the saddle-node bifurcation occurs at an endemic equilibrium.

Theorem 10. *Suppose $k = 0$ or $k > 0$ and $\hat{N}_A > \hat{N}_B$ and condition (19) holds. Then a saddle-node bifurcation occurs at an endemic equilibrium.*

Proof. The case $k = 0$ is simple. Indeed, $\hat{I}_{EI}^{\pm}$ remains positive for all β^H, thus we can always find a point, β_{sn}^H, such that $\hat{I}_{EI}^{\pm}$ and $\hat{I}_N$ touch at only one point, which is necessarily positive.

For the second case, we need to be a little more careful. Suppose $k > 0$ and $\hat{N}_A > \hat{N}_B$ and the derivative condition (19) holds.

As it was shown, at β_1^H, we had (at least) one endemic equilibrium already present. Now, we may choose δ_1 such that this equilibrium has not disappeared for $\beta^H \in (\beta_1^H - \delta_1, \beta_1^H)$. Furthermore, we may choose δ_2 so that the implicit function theorem applies, in which case, as Theorem 9 shows, another endemic equilibrium exists in the vicinity of $\hat{N}_{\text{free}}$ for all $\beta^H \in (\beta_1^H - \delta_2, \beta_1^H)$. In conclusion, at R_0^P slightly less than 1 we have (at least) two endemic equilibria, which need to merge for the saddle-node bifurcation to occur. Furthermore, no negative equilibria exist.

With $\delta = \min(\delta_1, \delta_2)$, all equilibria still remain on the positive part of $\hat{I}_N$ for all $\beta^H \in (\beta_1^H - \delta, \beta_1^H)$. Furthermore, we must have $\beta_{sn}^H < \beta_1^H - \delta$. Now, suppose the saddle-node bifurcation were to occur in the biologically meaningless region. Then, as β^H approaches β_{sn}^H, all equilibria would need to have transitioned to the negative part of $\hat{I}_N$. Everything being continuous, this implies that at some point an endemic equilibrium would have merged with the disease-free equilibrium on its way to the negative part of $\hat{I}_N$. But this corresponds to $\hat{N}_A = \hat{N}_{\text{free}}$ which is equivalent to $R_0^P = 1$. Now we arrive at a contradiction, since $R_0^P = 1$ if and only if $\beta^H = \beta_1^H$. In conclusion, the saddle-node bifurcation must occur at an endemic equilibrium. □

The assumptions in Theorem 9 can be condensed into one single inequality. First of all, we set $\beta^H = \beta_1^H$. Next, observe that

$$\hat{N}_A > \hat{N}_B \quad \Leftrightarrow \quad B(\hat{N}_A) < 0,$$

which at β_1^H becomes

$$\hat{N}_A > \hat{N}_B \quad \Leftrightarrow \quad B(\hat{N}_{\text{free}}(\beta_1^H)) < 0,$$

Hence, assuming $B(\hat{N}_A) < 0$ guarantees that $\hat{N}_A > \hat{N}_B$ at β_1^H.

Recall the derivative of $\hat{I}_{EI}^{-}$:

$$\frac{d\hat{I}_{EI}^{-}}{d\hat{N}} = \frac{-B'}{2\beta^T(\mu+\nu_I)} - \frac{2BB' - A'}{4\beta^T(\mu+\nu_I)\sqrt{B^2-A}}.$$

Setting $\beta^H = \beta_1^H$ and demanding that $B(\hat{N}_A) < 0$, we obtain

$$\left.\frac{d\hat{I}_{EI}^{-}}{d\hat{N}}\right|_{\hat{N}=\hat{N}_{\text{free}}(\beta_1^H)} = -\frac{k\mu(\mu+\nu_E)}{|B|}.$$

Now, what remains is to satisfy the derivative condition (19), as presented in Theorem 9. Thus, the inequality

$$\left.\frac{d\hat{I}_{EI}^{-}}{d\hat{N}}\right|_{\hat{N}=\hat{N}_{\text{free}}(\beta_1^H)} > \left.\frac{d\hat{I}_N}{d\hat{N}}\right|_{\hat{N}=\hat{N}_{\text{free}}(\beta_1^H)}$$

becomes

$$\begin{aligned} &-\frac{k\mu(\mu+\nu_E)}{|B|} > -\frac{(a_1-\mu)}{\alpha} \\ \Leftrightarrow \quad &\frac{k^2}{(1-k)^2} < \frac{\mu(a_1-\mu)(\alpha+\mu+\nu_I)}{(\mu+\nu_E)[\mu\alpha+(\mu+\nu_I)(a_1-\mu)]}. \end{aligned} \tag{20}$$

Here we denote a_1 to mean $a(\beta_1^H)$.

When this inequality is satisfied, the transcritical bifurcation is backwards. Hence, a saddle-node bifurcation is guaranteed in a biologically meaningful region. Funnily enough, it can be applied to the case where $k = 0$ as well. Although a transcritical bifurcation does not occur at all when $k = 0$, we are nevertheless guaranteed a saddle-node bifurcation as concluded by Theorem 10. This guarantee is confirmed by the above inequality: if we fix $k = 0$, we see that the left hand side of the inequality vanishes, while the right hand side remains positive *for all values* of a. And so, although a_1 does not exist at $k = 0$, this does not matter; the inequality is always satisfied.

On a contrary note, at $k = 1$, one easily sees that the inequality is impossible to satisfy, implying that only forward bifurcation, hence no saddle-node bifurcations, can occur in the SIR-model.

Notice that in setting $R_0^P = 1$ we obtain β_1^H as an implicit function of k. This can be substituted into inequality (20), which can then be solved for k. In this way, we obtain the quantity $k_{\max}$, where evidently $0 < k_{\max} < 1$. For any values $k \geq k_{\max}$, the system can not experience a saddle-node bifurcation in a biologically meaningful region of the phase plane. Furthermore, ν_E only appears in the denominator on the right hand side in inequality (20). This implies that when ν_E is low, $k_{\max}$ is high. Since $k < k_{\max}$ is necessary for endemic equilibria to exist at $R_0^P < 1$, the pathogen

is better able to persist for $R_0^P < 1$ when host individuals are slow to recover from the exposed state.

Later, when we look at conditions under which the host can rid itself of an established pathogen through evolution, we will see that the saddle-node bifurcation is of central importance in this regard. Indeed, we will show that unless $k < k_{\max}$, then the host will never get rid of the pathogen through evolutionary means.

4.4 Examples and bifurcation diagrams

In this section we present some examples of the dynamics of the system of differential equations as presented in (1) and take a look at the rich bifurcation patterns exhibited by the system.

4.4.1 Examples of pathogen invasion at the disease-free equilibrium

Here we look at how the demographic dynamics of the system evolve as a pathogen is introduced to the disease-free population.

Figures 2 to 4 shows how varying β^H and k affect the population dynamics as a disease is introduced to a virgin population. Here we have chosen to plot the fraction of the recovered sub-population against the fraction of the infectious population density, that is, R/N and I/N, respectively.

Plots (a) - (c) in each figure show the early dynamics of the invasion event up to about 192 years after the invasion event. Plots (g) - (i) (when they exist) show the late dynamics, about 1730 years after the invasion event. Plots (d) - (f) (when they exist) give insights to when the dynamics following an epidemic begin to even out and stabilise on the endemic equilibrium, if they ever do so.

The initial condition has been set to

$$(N(0), E(0), I(0), R(0)) = \left(\hat{N}_{\text{free}}, 0, 10^{-4}, 0\right).$$

Note that we have replaced $S(t)$ with $N(t)$ in this example.

The time-scale used for this example is one week per unit of time and the parameters have been chosen to reflect what could be expected in a human society.

The death rate has been set so that life expectancy in the absence of a pathogen is 50 years, hence we have

$$\mu \approx \frac{1}{2600}.$$

The exponential birth rate, a, is a logistic function such that at $\beta^H = 1$ the exponential birth rate is roughly one birth every two years:

$$a(\beta^H) \approx \frac{\frac{1}{104}}{1 + e^{-15\beta^H}}.$$

Notice the high multiplier in the exponent of the exponential; indeed, the assumption is that the exponential birth rate rises rapidly at low transmission rates but quickly saturates. The parameter c has simply been set so that $\hat{N}_{\text{free}} = 3$ when $\beta^H = 1$. In other words,

$$c = \frac{a(1) - \mu}{3}.$$

The recovery rates ν_E and ν_I have both been set so that the expected time to recovery is 3 weeks. And so we have

$$\nu_E = \nu_I \approx \frac{1}{3}.$$

The pathogen transmission rate has been set to $\beta^P = 1$ and the virulence to $\alpha(1) \approx \frac{1}{297}$. This value implies that roughly one percent of those who exit the infectious state do so by succumbing to the disease. In other words, we have set $\alpha(1)$ such that

$$\frac{\alpha(1)}{\alpha(1) + \nu_I} \approx \frac{1}{100}.$$

Note the exceedingly low fraction of infectious individuals in the cases that the dynamics converge on an endemic equilibrium (plots (g) and (h) of Figure 2, for example). Indeed, from the R-isocline we must have

$$\hat{N} > \hat{R} = \frac{\nu_I}{\mu}\hat{I} \approx 867\hat{I}.$$

Hence the low density of infectious individuals.

Note that in the real world populations are not infinite, hence the law of large numbers ceases to be a good approximation as the density of infectious individuals becomes very small. Indeed, when only a handful of people are sick, stochastic processes dominate the dynamics. That said, the animal that originally hosted a zoonotic disease can function as a reservoir for the pathogen while the human population remains resistant [19]. Once the susceptible sub-population has been replenished, the pathogen may once again invade and cause a second epidemic. For instance, bats are known to harbour a variety of viruses that have caused zoonotic epidemics in the past [20]. In particular, the currently ongoing COVID-19 pandemic is due to zoonosis originating in bats.

Remark 6. Due to the exceedingly low densities of the infectious individuals, the numerics tended to behave somewhat erratically at times. Namely, sub-population densities which approached 0 (E and I in particular) sometimes crossed over into the negative region, most likely due to the discrete time steps used in the numerical approximation. This is of course impossible mathematically, as stated by Corollary 2. To fix this, whenever a sub-population density crossed over to negative values, its value was reset at a very low density of 10^{-6}. Unfortunately, this fix is not

perfect, and does affect the population dynamics. Indeed, the artificial resetting of the population densities causes the periodicities and severities of the epidemics to behave somewhat erratically due to the discontinuities in the dynamics. Hence, the reader should take these results with a grain of salt.

As can be seen, for each combination of β^H and k in Figures 2 to 4, the early dynamics of an invasion event are characterised by a chain of epidemics following the initial invasion. Furthermore, the initial epidemic is always noticeably more widespread, but shorter in its duration. Evidently, this is due to the host population being virgin, and so the pathogen is able to become much more widespread as it grows quickly. Consequently, this also spells an early demise for the pathogen as it quickly depletes the supply of susceptible individuals. In the subsequent epidemics, we see that part of the population is still in the recovered sub-population, hence pathogen growth is slower and not as widespread as before.

In plot (a) of Figure 2 the initial epidemic lasts for about 400 weeks, more than seven and a half years! Here $\beta^H = 0.4$ and $k = 0.3$.

As β^H and k are increased, the duration of the initial epidemic decreases significantly, but in return, the severity also increases dramatically. Although not visible in the plots, the proportion of infectious individuals peaks at roughly 2.3% in plot (b) of Figure 2 and at roughly 6.8% in plot (c). In Figures 3 and 4, the lowest peak is just above 14% infectious individuals in Figure 3 (a) and the highest peak is at roughly 37% in Figure 4 (c). In all plots excluding Figure 2 (a), the initial epidemic lasts less than 200 weeks and in plot (c) of Figure 4, where $\beta^H = 0.48$ and $k = 0.85$, the initial epidemic lasts only about 45 weeks.

Turning out attention to the periods between epidemics, we notice that the period between the initial and second epidemic is always longer than the periods between the rest of the epidemics. This is a consequence of the initial epidemic being so widespread; the susceptible sub-population takes longer to replenish to a level that can support another epidemic. In Figure 2 the period between the initial and second epidemics is roughly 4000 weeks, or 77 years, while in Figure 4 this has shortened to just 29 or so years.

Although increasing β^H and k both help to solidify the presence of the pathogen, as is evident from the fact that R_0^P is increasing in both of these parameters, their effect on the long term dynamics are rather opposite. Indeed, increasing k quickly results in the disappearance of limit cycles, while increasing β^H promotes the appearance of limit cycles and prolongs the dampening of the cycles in the cases that the dynamics converge to an endemic equilibrium. Although not shown in the Figure 2, at $k = 0.3$ the introduction of a pathogen to the virgin host population results in cyclically occurring epidemics for all $\beta^H \geq 0.46$. The correlation between low k and the occurrence of limit cycles is something that can be seen in many examples throughout this thesis. The first such example presenting itself in the next section,

where we look at the bifurcation diagrams of the system.

From all three Figures discussed, we may conclude a few things. First, someone experiencing any of the situations presented in Figures 2 to 4, would probably be tempted to conclude that the disease has been eradicated once the initial epidemic is over. Indeed, the pathogen lays dormant after the first epidemic for a significant amount of time; up to 77 years in Figure 2 and still about 28 years, half the expected lifetime, in Figure 4. In reality the exceedingly low fraction of infectious individuals between the epidemics might very well result in the eradication of the pathogen. However, as these plots show, it is of utmost importance to truly make sure that no cases remain before declaring a pathogen eradicated; as the susceptible sub-population is replenished a dormant pathogen will eventually give rise to a new epidemic, no matter how rare it initially was.

Secondly, the cyclically occurring epidemics immediately bring to mind one phenomenon: seasonally occurring epidemics. However, as is seen in these examples, the cycles presented by this model are on a totally different time-scale. Indeed, these cycles have periodicities of several years, in contrast to the seasonally occurring influenza epidemics, for example. However, this demographic example disregards the existence of multiple strains of a pathogen. As is commonly understood, seasonal epidemics are not caused by a single influenza strain, but a plethora of strains that whose respective prevalences alternate as immunity towards a specific strain is slowly lost in the host population [8].

Finally, it seems rather difficult to determine the later dynamics of the population solely based on the early dynamics. For example, in Figure 2 the early dynamics at $\beta^H = 0.44$ and $\beta^H = 0.48$ (plots (b) and (c)) are very similar, yet the final result is that $\beta^H = 0.44$ results in an stable endemic equilibrium (plot (h)), while $\beta^H = 0.48$ results in cyclically occurring epidemics (plot (i)). Perhaps one indication of where the dynamics are heading in the early dynamics, is that the severity of the epidemics is decreasing for $\beta^H = 0.44$ while the severity is rather constant or even slightly increasing for $\beta^H = 0.48$. In any case, the observed early dynamics are a bad predictor of the long term dynamics. Hence, one is better off relying on measuring the parameters. Limit cycles hint at the existence of a Hopf bifurcation, and so one can measure the parameters and fit these to the bifurcation patterns of the model to get an estimate of the long term dynamics.

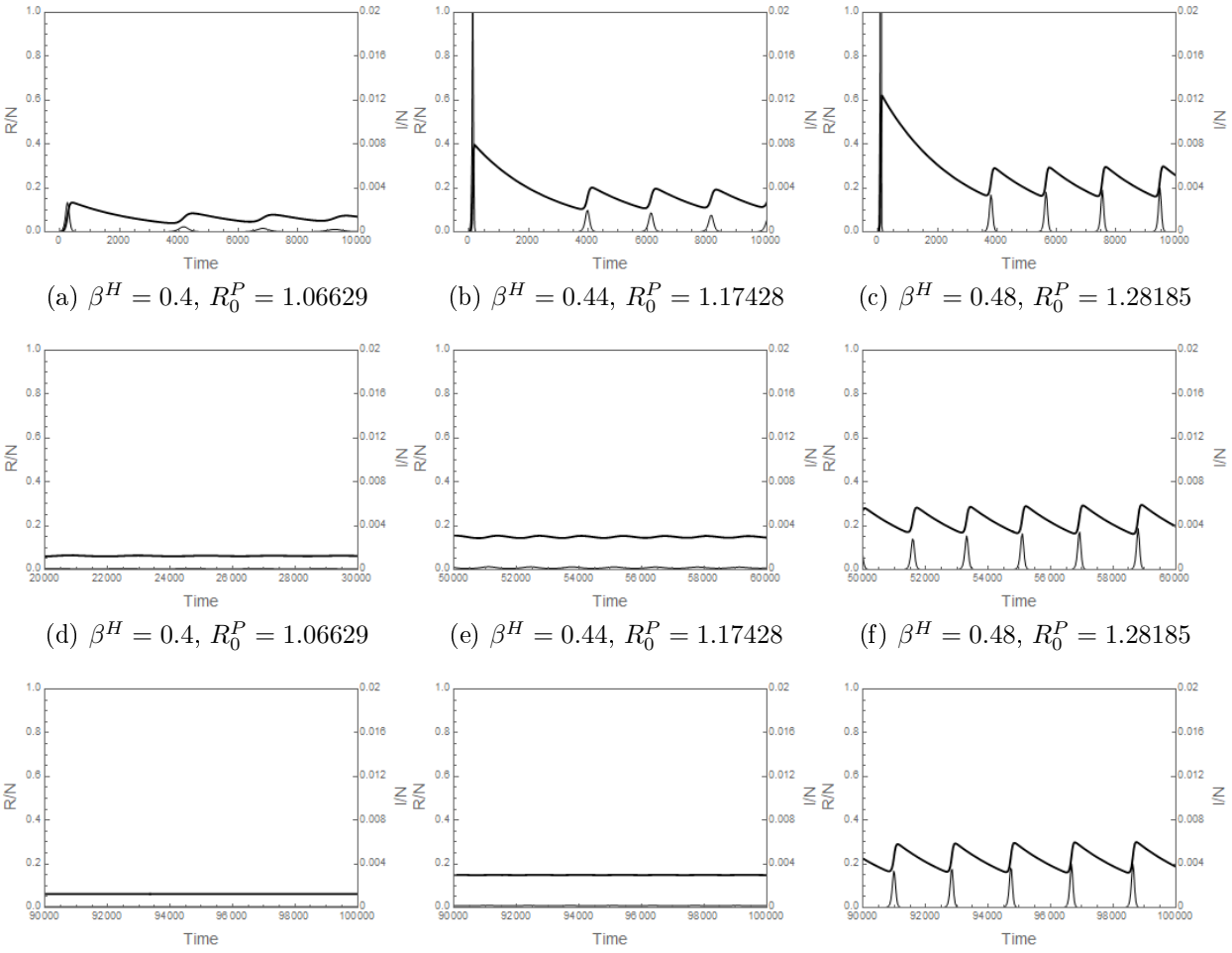

(a) $\beta^H = 0.4$, $R_0^P = 1.06629$ (b) $\beta^H = 0.44$, $R_0^P = 1.17428$ (c) $\beta^H = 0.48$, $R_0^P = 1.28185$

(d) $\beta^H = 0.4$, $R_0^P = 1.06629$ (e) $\beta^H = 0.44$, $R_0^P = 1.17428$ (f) $\beta^H = 0.48$, $R_0^P = 1.28185$

(g) $\beta^H = 0.4$, $R_0^P = 1.06629$ (h) $\beta^H = 0.44$, $R_0^P = 1.17428$ (i) $\beta^H = 0.48$, $R_0^P = 1.28185$

$$\nu_E = \nu_I = 0.333, \quad \mu = 0.00038, \quad c = (a(1) - \mu)/3, \quad \alpha = 0.00337,$$
$$k = 0.3, \quad k_{\max} = 0.033, \quad a = 0.0096/(1 + e^{-15\beta^H}).$$

Figure 2: Examples of the ensuing population dynamics following the invasion of a pathogen in a virgin host population. The thick line shows the fraction of the recovered sub-population while the thin line shows the fraction of the infectious sub-population. The left vertical axis in each plot indicates the fraction of the recovered sub-population while the right vertical axis indicates the fraction of the infectious sub-population. The recovered sub-population is shown as the thick solid line, while the infectious sub-population is shown as the thin solid line in each plot. Note the difference in magnitude in the vertical axes; indeed, the infectious sub-population is never very large at all while the recovered sub-population consistently reaches significant fractions. The first row show the early dynamics, with time extending from 0 to 10 000. The last row shows the later dynamics, with time extending from 90 000 to 100 000. Here time is measured as 1 week per unit. Hence, the early dynamics extend to about 192 years after the initial invasion and the late dynamics range from roughly 1731 to 1923 years after the initial invasion. Note the extremely low value for $k_{\max}$.

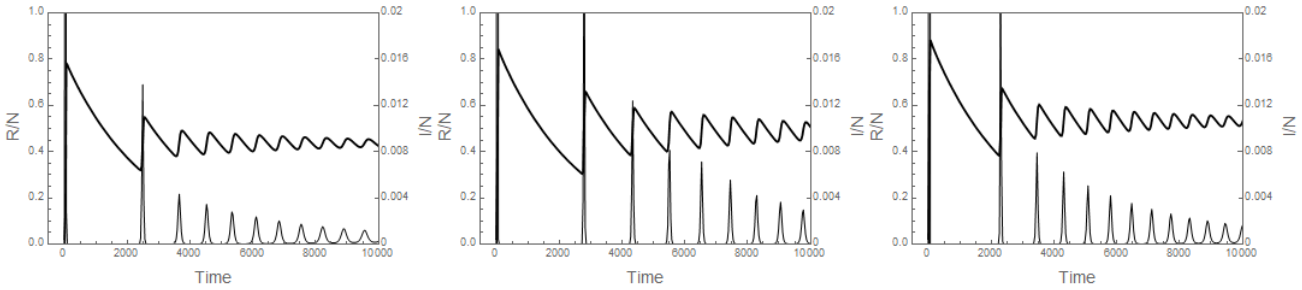

(a) $\beta^H = 0.4$, $R_0^P = 1.77715$ (b) $\beta^H = 0.44$, $R_0^P = 1.95714$ (c) $\beta^H = 0.48$, $R_0^P = 2.13642$

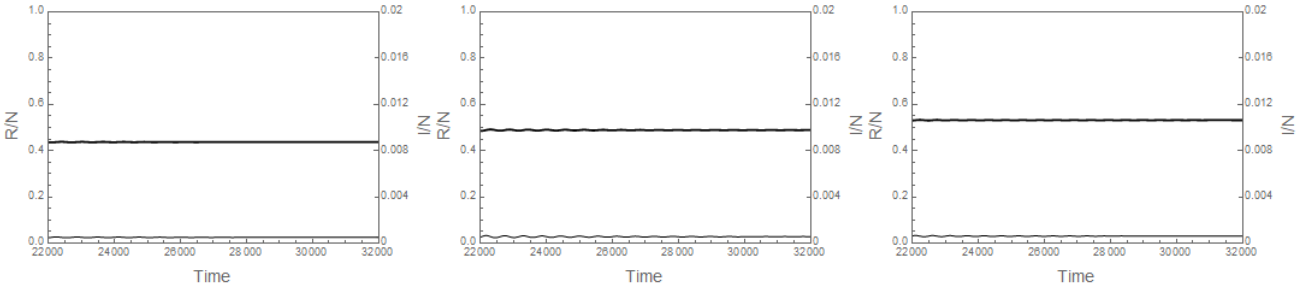

(d) $\beta^H = 0.4$, $R_0^P = 1.77715$ (e) $\beta^H = 0.44$, $R_0^P = 1.95714$ (f) $\beta^H = 0.48$, $R_0^P = 2.13642$

$$\nu_E = \nu_I = 0.333, \quad \mu = 0.00038, \quad c = (a(1) - \mu)/3, \quad \alpha = 0.00337,$$
$$k = 0.5, \quad k_{\max} = 0.033, \quad a = 0.0096/(1 + e^{-15\beta^H}).$$

Figure 3: Similar to Figure 2, but this time $k = 0.5$. As can be seen, in each plot the early dynamics are initially cyclic, but eventually converge to a stable endemic equilibrium.

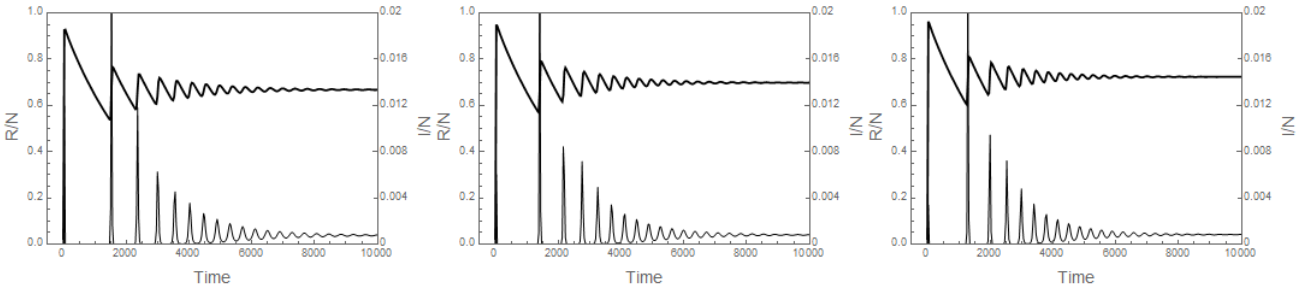

(a) $\beta^H = 0.4$, $R_0^P = 3.02116$ (b) $\beta^H = 0.44$, $R_0^P = 3.32714$ (c) $\beta^H = 0.48$, $R_0^P = 3.63192$

$$\nu_E = \nu_I = 0.333, \quad \mu = 0.00038, \quad c = (a(1) - \mu)/3, \quad \alpha = 0.00337,$$
$$k = 0.85, \quad k_{\max} = 0.033, \quad a = 0.0096/(1 + e^{-15\beta^H}).$$

Figure 4: Similar to Figure 2, but here k has been bumped up to $k = 0.85$. Consequently, the cycles have much shorter periods and convergence is quick. Furthermore, there is barely any difference in the dynamics as β^H is varied.

4.4.2 Bifurcation diagrams

In this section we take a look at the different kinds of bifurcation patterns that the system can exhibit. These are depicted in Figure 5, where we showcase forward and backward transcritical bifurcations, saddle-node bifurcations and Hopf bifurcations.

Plots (a) and (b) of Figure 5 give an overview of the system as β^H and k are varied. Here the shaded region indicates the region of coexistence, that is, the pathogen can persist in the host population in this region. The dashed line indicates the transcritical bifurcation, the thin solid line indicates a saddle-node bifurcation and the thick solid line indicates a Hopf bifurcation. Stable limit cycles can appear in the region bounded by the thick and thin solid lines.

The cross-sections of plots (a) and (b) indicated by the horizontal lines and labelled c. to f. are showcased in more detail in plots (c) to (f), respectively. In these plots k has been fixed, and β^H is instead plotted against the equilibrium total population density, $\hat{N}$. All unstable equilibria are denoted by the dashed curves, while stable equilibria or stable limit cycles are indicated by solid curves. The thick solid lines indicate stable equilibria, while the thin solid lines indicate stable limit cycles.

The straight line (dashed or solid) indicates the disease-free total population density, $\hat{N}_{\text{free}}$. At β_1^H, one endemic equilibrium passes through the disease-free equilibrium, as demanded by the transcritical bifurcation. Indeed, the endemic equilibria are tracked by the curved offshoot of $\hat{N}_{\text{free}}$. In particular, we see that in plot (c) the transcritical bifurcation is backwards; two endemic equilibria are present for $\beta^H < \beta_1^H$. Moreover, in plot (c), the two endemic equilibria that exist at $\beta^H < \beta_1^H$ are unstable. This is due to the stable limit cycle that exists at $\beta^H > \beta_1^H$. Indeed, as β^H approaches β_1^H from above, the limit cycle passes too close to the disease-free equilibrium: once $\beta^H < \beta_1^H$ the disease-free equilibrium becomes locally attracting, and the limit cycle disappears as the orbit converges to $\hat{N}_{\text{free}}$.

In contrast to this, we see in plot (f) that no stable limit cycles exist, and so one endemic equilibrium remains stable up until the saddle-node bifurcation, where it collides and disappears together with the unstable endemic equilibrium that participated in the transcritical bifurcation.

Plot (d) exhibits an interesting case in which a limit cycle appears, but then collapses back into a stable equilibrium right as the endemic equilibrium is about pass through the disease-free equilibrium at β_1^H. Plot (e) is similar to (d), only this time no limit cycles appear, and so this is a classic example of a forward bifurcation.

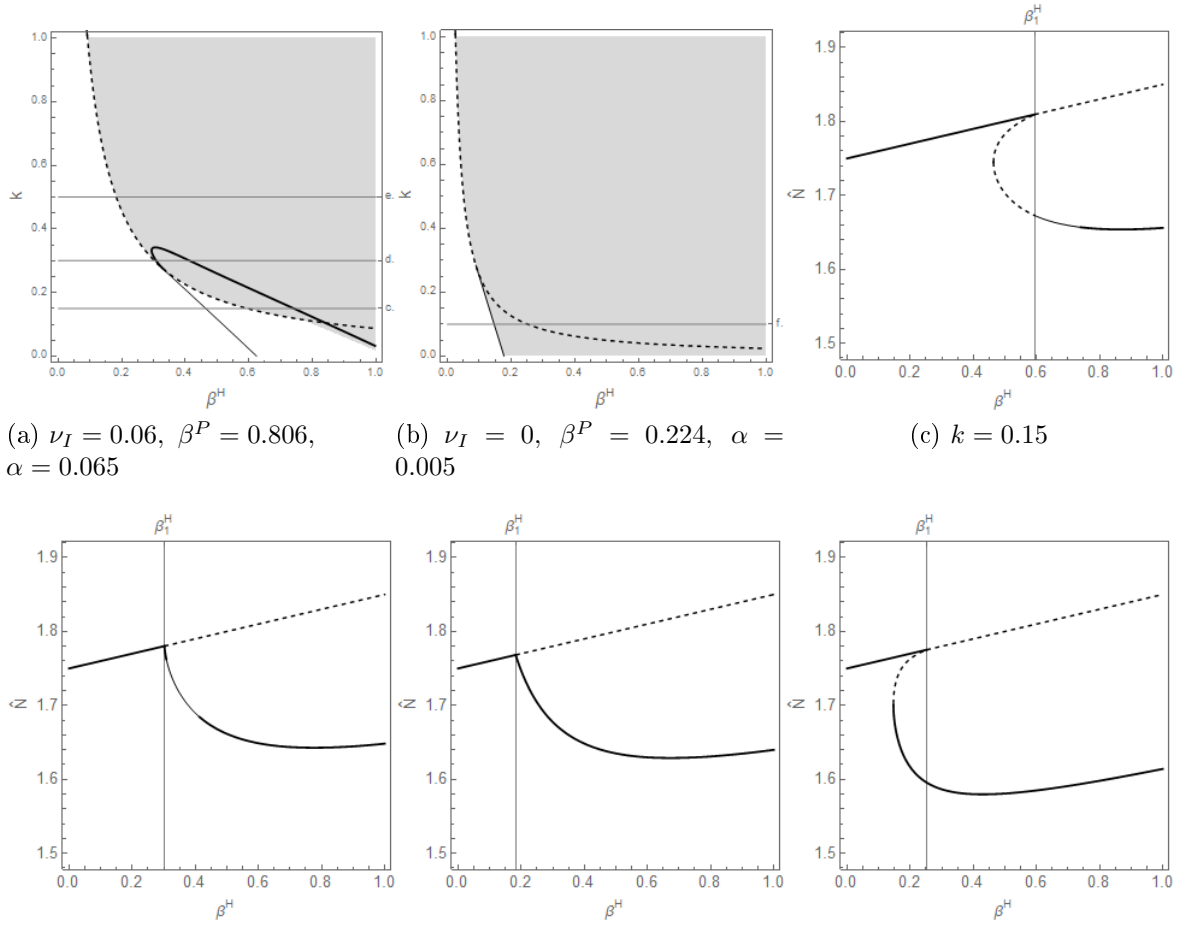

(a) $\nu_I = 0.06$, $\beta^P = 0.806$, $\alpha = 0.065$

(b) $\nu_I = 0$, $\beta^P = 0.224$, $\alpha = 0.005$

(c) $k = 0.15$

(d) $k = 0.3$

(e) $k = 0.5$

(f) $k = 0.1$

$$\nu_E = 0.05, \quad \mu = 0.005, \quad c = 0.02, \quad \alpha = 0.1(\beta^P)^2, \quad a = 0.04 + 0.002\beta^H.$$

Figure 5: Plots (a) and (b) show the region of coexistence in gray with the various bifurcations indicated by the lines as β^H and k are varied. Plots (c) - (f) show typical bifurcation diagrams as k is fixed to specific values. The thick solid lines indicate stable equilibria, the thin solid lines stable limit cycles and the dashed lines indicate the lack of any stable attractor in the vicinity of the corresponding equilibrium. Where the plots (c) - (f) fit in plots (a) and (b) is indicated by the horizontal lines in plots (a) and (b).

5 Mutant invasion analysis

Previously we spoke of invasion in the context of a pathogen invading a virgin host population. In the following sections we study the conditions under which a rare mutant appearing in the host and pathogen populations, respectively, can invade and eventually replace the existing resident population. That is, we do not speak of the pathogen invading the host, rather we speak of a mutant pathogen invading a resident pathogen meta-population and, similarly, a mutant host invading a resident host population. By a pathogen meta-population, we mean a population of pathogen populations. Indeed, each individual infected host carries within it a pathogen population; the meta-population then refers to this population of populations that is tracked by the number of infected hosts.

The model parameters subject to mutations will be the transmission rates, namely β^H for the host and β^P for the pathogen. These parameters will be referred to as *strategies*, and will often be indexed by r and m depending on whether or not they are the *resident* or *mutant* strategies, respectively. Moreover, we also refer to the different pathogen strategies as *strains*.

Recall our evolutionary assumptions **AD1 - AD3** from section 2.2. Mutations will be considered a rare occurrence, hence whenever a mutant appears in a resident population, we assume that the resident will have established itself at its demographic attractor. Moreover, we will suppose that only one mutation occurs at any one time and a new mutation will not occur before previous mutant has either established itself at a demographic attractor or disappeared.

When a population consists of only one strategy we speak of a monomorphic population, when two strategies are present we speak of a dimorphic population. For the time being we shall accept that an invasive strategy will replace the resident strategy, thus becoming the new resident. However, this is something that will be treated and discussed at the end of each section on mutant host and pathogen invasion analysis, respectively.

5.1 Invasion fitness and selection gradient

When a mutation occurs in a resident population, initially the mutant sub-population will be extremely rare. For this reason we disregard interactions between mutant individuals in our models describing the initial growth of a rare mutant in a resident population; two mutants are simply too unlikely to meet in the vast ocean of residents. Mathematically speaking, we linearise the systems of differential equations describing the mutant dynamics around the mutant-free equilibrium. The gist of the invasion analysis is then to check whether or not this equilibrium is unstable against invasion from the mutant. That is, we make a small perturbation by adding a tiny mutant population to the mutant-free equilibrium and study under which conditions

this perturbation grows; a situation totally analogous to pathogen invasion of the disease-free equilibrium.

In this section we will occasionally pass from talking about our specific model to a more general context. In these cases, we replace the resident and mutant strategies, β_r^i and β_m^i, with the variables x and y, respectively, to indicate that the results hold for *any* evolutionary models, rather than just our model.

For the evolution of the pathogen we introduce a separate model, which describes the dynamics of an initially rare mutant. We then look at the eigenvalues of the Jacobian matrix of this system at the mutant-free equilibrium. From these eigenvalues we derive the *fitness function*, $s^P_{\beta_r^P}(\beta_m^P)$, of the pathogen, which describes the long term exponential growth rate of an initially rare mutant strategy, β_m^P, in an established resident population with strategy β_r^P. In particular, whenever $s^P_{\beta_r^P}(\beta_m^P) > 0$ the mutant will be invasive, while on the other hand, if $s^P_{\beta_r^P}(\beta_m^P) < 0$, the mutant can not invade [3].

On the other hand, when investigating the evolutionary dynamics of the host, looking at the Jacobian matrix of the system describing the spread of a rare mutant host strategy in an established resident host population is less fruitful; the expressions become too complicated. Fortunately, in this case we can derive an expression for the fitness of a mutant host by studying R_0^H. However, this time we have two host populations, namely the resident and the mutant, and so we shift our interpretation so that $R_0^H(\beta_r^H, \beta_m^H)$ gives the basic reproduction number of a mutant host population with strategy β_m^H in the environment of the equilibrated resident host population with strategy β_r^H. As a consequence, when $\beta_m^H = \beta_r^H$, that is, the mutant is the same as the resident, we have

$$R_0^H(\beta_r^H, \beta_r^H) = \hat{R}_0^H = 1,$$

as demanded by (13) in section 4.1.2. When the mutant strategy is not the same as the resident strategy, we have that $R_0^H(\beta_r^H, \beta_m^H) - 1$ is sign-equivalent to the fitness function, $s^H_{\beta_r^H}(\beta_m^H)$, as is shown in [2]. Thus, if $R_0^H(\beta_r^H, \beta_m^H) > 1$, then the mutant strategy can spread in the resident population, while if $R_0^H(\beta_r^H, \beta_m^H) < 1$, it can not.

In a general context, when assuming, as we will, that evolution proceeds through very small mutation steps, one can use the linear approximation

$$s_x(y) = s_x(x) + D(x)(y - x), \tag{21}$$

where $D(x)$ is the *selection gradient*, defined by

$$D(x) = \left.\frac{\partial s_x(y)}{\partial y}\right|_{y=x},$$

to describe the fitness of a mutant strategy. Note that since the resident is assumed to be at its demographic attractor, it will not experience any long term exponential growth, hence $s_x(x) = 0$. This is known as the *principle of selective neutrality of the resident*, or in other words, the resident is selectively neutral with respect to itself. Thus, the sign of $D(x)$ determines which mutations can invade and which can not. When the selection gradient vanishes, that is, we have $D(x) = 0$ we call the corresponding strategy a *singular strategy* and indicate it by a star, for example x^*, or in our particular model, β^{H*} and β^{P*}. These singular strategies are either evolutionarily attracting or repelling and here interesting phenomena can occur. When the singular strategy is such that $s_{x^*}(y) < 0$ for all y in some neighbourhood of x^* no mutant strategies y can invade and replace the resident x^*. Hence, we call this strategy a locally evolutionarily stable strategy (ESS). For more on this, see [3].

In the case of the host, in which we replace the fitness function with R_0^H, assuming once more that mutations steps are very small, one can relate R_0 to s by taking the logarithm. Indeed, for small mutation steps d, we have

$$\log R_0(x, x + d) = T_f(x, x + d)s_x(x + d) + O(\|d\|^2), \tag{22}$$

where $T_f(x, y)$ is the mutant's average age of giving birth in the resident environment, for more on this see [4]. The take away here is that the derivative $\partial_y R_0$ is sign-equivalent to the derivative $\partial_y s$, when evaluated at $y = x$. Indeed, we have

$$\partial_y \log R_0(x, y) = \frac{\partial_y R_0(x, y)}{R_0(x, y)},$$

and

$$\partial_y \left(T_f(x, y)s_x(y)\right) = s_x(y)\partial_y T_f(x, y) + T_f(x, y)\partial_y s_x(y).$$

And so, at $y = x$ we obtain

$$\partial_y R_0(x, x) = T_f(x, x)\partial_y s_x(x).$$

Evidently, the average age of giving birth, $T_f(x, x)$, must be positive, hence the two derivatives are sign-equivalent. And so, the derivative of R_0 evaluated at $y = x$ is sign equivalent to the selection gradient obtained from the fitness function, s. From here on, instead of dealing with the derivative of the invasion fitness, we will instead work with the derivative of R_0^H evaluated at $\beta_m^H = \beta_r^H$, and treat it as the selection gradient. That is, we write

$$D^H(\beta_r^H) = \partial_{\beta_m^H} R_0^H \Big|_{\beta_m^H = \beta_r^H}.$$

Finally, note that by (22) above, we have

$$R_0^H(\beta_r^H, \beta_r^H) = 1 \quad \Leftrightarrow \quad s^H_{\beta_r^H}(\beta_r^H) = 0,$$

as expected.

5.2 Mutant host invasion analysis

In this section we study under which conditions a mutant host can invade a resident host population. We make the explicit assumption that the host is at an endemic equilibrium. In the disease-free case, evolution of the host is straightforward and characterised by an effort to evolve as high β^H as possible. Indeed, in the absence of a pathogen, there is no cost in increasing β^H. Hence, a mutant with a higher transmission rate has a higher exponential birth rate, and so it will outcompete and replace the resident. See section 8.1 in the Appendix for the details. This evolution towards higher β^H in the absence of the pathogen provides an explanation for why the pathogen can invade in the first place; R_0^P increases with β^H, and so eventually the host will evolve $R_0^P > 1$ allowing the pathogen to invade.

5.2.1 Invasion at endemic equilibria

We will study the evolution of the host through R_0^H. Recall that upon an infectious contact between two host individuals, it is the *receiving* part in the interaction that determines the value of β^H. In this way, when looking at $R_0^H(\beta_r^H, \beta_m^H)$, we find that β_r^H only plays a role in determining the resident demographic attractor, while β_m^H determines the value of all the β^T terms which can be explicitly seen in the expression of R_0^H, as given in (12). To clarify, we write (12) here again, this time indexing the related terms depending on whether their values are determined by the mutant or the resident strategies. As all of the sub-population densities are determined by the resident, we denote them by the index res. We obtain

$$R_0^H(\beta_r^H, \beta_m^H) = \frac{(a_m - c\hat{N}_{res})}{\mu(\alpha + \mu + \nu_I)} \frac{P}{T}, \tag{23}$$

where

$$P = \mu(\alpha + \mu + \nu_I)\left((2-k)\beta_m^T \hat{I}_{res} + \mu + \nu_E\right) + \beta_m^T \hat{I}_{res}\left(\beta_m^T \hat{I}_{res} + k(\mu + \nu_E)\right)(\mu + \nu_I),$$
$$T = (\beta_m^T \hat{I}_{res} + \mu)(\beta_m^T \hat{I}_{res} + \mu + \nu_E) - (1-k)\beta_m^T \hat{I}_{res}\nu_E.$$

The expression (23) is very cumbersome to work with, so we resort to using the selection gradient, D^H, instead to study the invadability of mutant strategies. Recall the linear approximation of the invasion fitness, (21), by which a mutant strategy, β_m^H, can invade if and only if

$$D^H(\beta_r^H)(\beta_m^H - \beta_r^H) > 0.$$

Since the selection gradient is evaluated for $\beta_m^H = \beta_r^H$, we may leave out the indexing. With this in mind, we obtain

$$D^H(\beta^H) = \frac{a'}{\mu(\alpha + \mu + \nu_I)} \frac{P}{T} + \frac{a - c\hat{N}}{\mu(\alpha + \mu + \nu_I)} \frac{1}{T}\left(P' - \frac{PT'}{T}\right). \tag{24}$$

Where the derivatives of P and T with respect to β_m^H (evaluated at $\beta_m^H = \beta_r^H$) are

$$P' = \beta^P \hat{I} \left[(\mu + \nu_I) \left(2\beta^T \hat{I} + k(\mu + \nu_E) \right) + \mu(\alpha + \mu + \nu_I)(2 - k) \right],$$
$$T' = \beta^P \hat{I} \left(2(\beta^T \hat{I} + \mu) + k\nu_E \right).$$

Now, with help from the isocline identities, we may simplify P and T. We obtain

$$P = \frac{\mu(\alpha + \mu + \nu_I)(1 - k)\beta^T \hat{I}\hat{N}}{\hat{E}},$$
$$T = \frac{(1 - k)\beta^T \hat{I}(a - c\hat{N})\hat{N}}{\hat{E}},$$

and furthermore

$$\begin{aligned} TP' - PT' &= -\beta^P \hat{I}\alpha\mu(\beta^T \hat{I} + \mu + \nu_E) \left[(2 - k)\beta^T \hat{I} + k(\mu + \nu_E) \right] \\ &= \frac{-\beta^P \alpha\mu(1 - k)^2 (\beta^T)^2 \hat{S}\hat{I}^3 (2\hat{E} + k\hat{S})}{\hat{E}^2}. \end{aligned}$$

Now, by substituting these identities into (24), we obtain

$$\begin{aligned} D^H(\beta^H) &= \frac{a'}{a - c\hat{N}} + \frac{a - c\hat{N}}{\mu(\alpha + \mu + \nu_I)} \left(\frac{TP' - PT'}{T^2} \right) \\ &= \frac{1}{a - c\hat{N}} \left(a' - \frac{\beta^P \alpha(2\hat{E} + k\hat{S})\hat{S}\hat{I}}{(\alpha + \mu + \nu_I)\hat{N}^2} \right). \end{aligned} \tag{25}$$

Recall Corollary 2, which states that the endemic equilibrium lies within the biologically meaningful region, hence $a - c\hat{N}$ is always positive. Indeed, in the absence of a disease, we have $a - c\hat{N} = a - c\hat{N}_{\text{free}} = \mu$, while on the other hand, at an endemic equilibrium we must have $\hat{N} < \hat{N}_{\text{free}}$, and so in this case $a - c\hat{N} > a - c\hat{N}_{\text{free}}$. Thus, the sign of $D^H(\beta^H)$ is determined by the difference inside the parenthesis, and the singular strategies, β^{H*}, where the selection gradient vanishes, are those for which we have

$$a'(\beta^{H*}) = \frac{\beta^P \alpha(\hat{E} + \hat{E}_0)\hat{S}\hat{I}}{(\alpha + \mu + \nu_I)\hat{N}^2}. \tag{26}$$

Recall that $\hat{E}_0 = \hat{E} + k\hat{S}$ is the immediately infectious sub-population density. Evidently, D^H is a beast to work with analytically. Nevertheless, the right hand side of (26) provides us with a concrete threshold value, the calculation of which is not a problem in numerical examples. When the coupling, a', between a and β^H is above the threshold value, then $D^H > 0$ and the host will be inclined to evolve higher

transmission rates. Conversely, when the coupling is lower than the threshold, then $D^H < 0$ and the host is inclined to evolve lower transmission rates.

Most quantities appearing on the right hand side of (26) are fairly easily observable. However, differentiating between susceptible and exposed individuals can be somewhat difficult. That said, at equilibrium we may use the isocline identities to our benefit. In particular, isocline identity (4) gives us

$$\hat{E} = \frac{(1-k)\hat{I}(\alpha+\mu+\nu_I)}{\beta^T\hat{I}+k(\mu+\nu_E)}.$$

What remains then is to find a good estimate for k. This could be done through extensive testing, where k is the ratio of symptomatic individuals to total number of pathogen carriers.

As discussed in [5], we can nevertheless show analytically that when backwards bifurcation does *not* occur, that is, $k \geq k_{\max}$, then at β_1^H, the selection gradient of the host will always be positive. In particular, this implies that the host strategy can never pass through the transcritical bifurcation by means of evolution alone if $k \geq k_{\max}$.

Indeed, at β_1^H, we have $\hat{I} = 0$ and $\hat{N} = \hat{N}_{\text{free}}$, in which case, D^H simplifies to

$$D^H(\beta_1^H) = \frac{a'}{a - c\hat{N}_{\text{free}}} = \frac{a'}{\mu}, \tag{27}$$

which, by our assumptions, is positive. And so, we obtain the following theorem.

Theorem 11. *Suppose $k \geq k_{max}$. Then*

$$D^H(\beta_1^H) > 0.$$

□

At a forward transcritical bifurcation the positive selection gradient at β_1^H is due to the fact that the vanishing density of $\hat{I}$ reduces the negative impact of the pathogen on the host. Conversely when the transcritical bifurcation is backwards, $\hat{I}$ can remain high at β_1^H in which case evolving lower β^H can remain beneficial for the host past β_1^H.

Remark 7. With Theorem 11 in mind, let us return to consider $k_{\max}$. Recall that $k_{\max}$ was solved from inequality (20):

$$\frac{k^2}{(1-k)^2} < \frac{\mu(a_1-\mu)(\alpha+\mu+\nu_I)}{(\mu+\nu_E)[\mu\alpha+(\mu+\nu_I)(a_1-\mu)]}$$

Now we see that the denominator on the right hand side of this inequality contains the term $\nu_E\nu_I a_1$, that is a term completely independent of μ. On the other hand,

every term in the numerator is multiplied by μ. Supposing μ is significantly smaller than the recovery rates, ν_E and ν_I, or the exponential birth rate at β_1^H, a_1, then $k_{\max}$ will be very small in return. The effect of ν_E on $k_{\max}$ is particularly pronounced, as it is totally absent in the numerator. Indeed, in the example of section 4.4.1 we have $k_{\max} = 0.033$. In this case the region where the host could possibly eradicate the pathogen through evolution is vanishingly small, and lies outside the region of coexistence altogether for all $\beta^H \in [0, 1]$.

Note that the above analysis assumes the host is at an equilibrium. However, as we remarked at the end of section 4.3, the system exhibits limit cycles as well, in which case the above results do not hold. Next we present how the selection gradient is calculated when the host has instead reached a stable limit cycle.

5.2.2 Invasion at limit cycles

As was mentioned in the section on the bifurcation analysis, the system exhibits Hopf bifurcations. In the case that the Hopf bifurcation is *supercritical*, that is, a stable limit cycle occurs in a neighbourhood of the related equilibrium point, we need to employ a different method for calculating the selection gradient, D^H. This method involves solving the system and finding the limit cycle numerically. In this section we give a description of the algorithm used to calculate the selection gradient for a population at a limit cycle. This algorithm is based on the method described in [1].

Suppose we have found a limit cycle, that is, the algorithm described in the bifurcation analysis has returned a pair, (F_n, Π), where F_n is a point on the limit cycle, and Π is the period of the limit cycle. We now wish to calculate whether or not a rare mutant host can grow in this environment as the host tracks one revolution along the limit cycle. To do this, we need the linearised mutant dynamics, which are given by

$$\begin{aligned}
\frac{dS_m}{dt} &= (a_m - cN_{res})N_m + \nu_E E_m - (\beta_m^T I_{res} + \mu)S_m, \\
\frac{dE_m}{dt} &= (1-k)\beta_m^T I_{res} S_m - (\beta_m^T I_{res} + \mu + \nu_E)E_m, \\
\frac{dI_m}{dt} &= \beta_m^T (kS_m + E_m)I_{res} - (\alpha + \mu + \nu_I)I_m, \\
\frac{dR_m}{dt} &= \nu_I I_m - \mu R_m.
\end{aligned} \tag{28}$$

From these equations, we may calculate how each mutant sub-population evolves as the resident completes one revolution on the limit cycle. Indeed, we calculate the

quantities

$$
\begin{aligned}
M_S &= (S_m(\Pi), E_m(\Pi), I_m(\Pi), R_m(\Pi)), \quad (S_m(0), E_m(0), I_m(0), R_m(0)) = (1,0,0,0),\\
M_E &= (S_m(\Pi), E_m(\Pi), I_m(\Pi), R_m(\Pi)), \quad (S_m(0), E_m(0), I_m(0), R_m(0)) = (0,1,0,0),\\
M_I &= (S_m(\Pi), E_m(\Pi), I_m(\Pi), R_m(\Pi)), \quad (S_m(0), E_m(0), I_m(0), R_m(0)) = (0,0,1,0),\\
M_R &= (S_m(\Pi), E_m(\Pi), I_m(\Pi), R_m(\Pi)), \quad (S_m(0), E_m(0), I_m(0), R_m(0)) = (0,0,0,1).
\end{aligned}
$$

From these quantities, we may now construct the *monodromy matrix*,

$$M = [M_S, M_E, M_I, M_R],$$

where the columns of the matrix are given by the vectors M_i. Iterations of the monodromy matrix describe dynamics of the mutant under successive revolutions along the limit cycle. Hence, the eigenvalues of M tell us whether or not the mutant population is growing in the resident population. Note that M is a non-negative matrix, and so, by the Perron-Frobenius theorem, the leading eigenvalue λ_M is real and non-negative. This leading eigenvalue of the matrix is analogous to R_0^H; if $\lambda_M > 1$, then the mutant will spread. In accordance with identity (22), relating R_0 to the invasion fitness, the invasion fitness of a mutant host is given by

$$s_{\beta_r^H}(\beta_m^H) = \frac{\log \lambda_M(\beta_r^H, \beta_m^H)}{\Pi}.$$

Here we have substituted the average age of giving birth, T_f, with Π, since that is the elapsed time between iterations of M.

Finally, to calculate the selection gradient, we simply approximate the derivative, using the formula

$$D^H = \frac{\frac{\log \lambda_M(\beta_r^H, \beta_r^H + 0.0001)}{\Pi} - \frac{\log \lambda_M(\beta_r^H, \beta_r^H)}{\Pi}}{0.0001}.$$

Note that, in theory, $\log \lambda_M(\beta_r^H, \beta_r^H) = 0$ since the resident is selectively neutral with respect to itself. Indeed, at $\beta_m^H = \beta_r^H$, (28) becomes the system (1). In this case the monodromy matrix is the identity matrix, hence $\lambda_M = 1$. However, with numerical methods, one rarely gets *exactly* 0 (especially when the effective limit cycle is only a numerical approximation), and so the term is included in the calculation in an effort to minimise errors.

5.2.3 Invasion implies substitution

So far we have characterised conditions for when a mutant host can invade the resident host population. But what happens after this invasion event? Does the mutant drive the resident to extinction and replace it as the new resident or do the

two different strategies persist in a peaceful coexistence? These questions can be posed and answered in two different situations: far away from singular strategies where the selection gradient is non-zero, and at the singular strategies where the gradient vanishes.

In the former case, much work has been done to generalise the so called "invasion implies substitution"-theorem to a large class of unstructured and structured models. In particular, [11] shows that for our particular model, invasive mutants will replace the resident population whenever $D^H(\beta_r^H) \neq 0$, provided that the mutation steps are sufficiently small. For a more detailed description of how [11] relates to our particular model, see section 8.3 in the Appendix. One should note that these results only apply when the resident is at an equilibrium. What happens at limit cycles is unclear, but let us suppose for the sake of argument that in these cases the resident is also replaced by invasive mutants.

The replacement of the resident with each successful invasion event means that as we look at the long term evolution of the host in section 5, we can rest assured that the host will traverse the evolutionary landscape towards its evolutionary attractor as a single monomorphic population, that is, only one strategy will be present in the population at any one time.

5.3 Mutant pathogen invasion analysis

In this section we study the invadability of mutant pathogen strategies. Similarly to the host, the evolving parameter here will be the *pathogen transmission rate*, β^P. We begin by presenting different models describing the dynamics of a rare mutant pathogen in a resident population.

As was discussed in the introduction to section 5, we will determine invadability of the mutant by looking at the stability of the mutant-free equilibrium. This involves looking at the Jacobian matrix of the mutant pathogen dynamics and finding the leading eigenvalue. The dynamics in the invasion analysis will be at most two dimensional, hence we present this following theorem to simplify the analysis later on.

Theorem 12. *Consider the following 2-dimensional system of ordinary differential equations:*

$$\begin{aligned} \dot{x} &= f(x, y), \\ \dot{y} &= g(x, y), \end{aligned}$$

where f and g are both $C^1(\mathbb{R}^2, \mathbb{R})$. Furthermore, suppose there exists an equilibrium $(\hat{x}, \hat{y})$ such that the trace of the Jacobian matrix, J, at this equilibrium is negative, that is,

$$\operatorname{tr}(J(\hat{x}, \hat{y})) < 0.$$

Then the stability of the equilibrium, $(\hat{x}, \hat{y})$, is determined by the determinant of the Jacobian matrix.

Proof. The Jacobian matrix is given by

$$J = \begin{bmatrix} \partial_x f(x,y) & \partial_y f(x,y) \\ \partial_x g(x,y) & \partial_y g(x,y) \end{bmatrix}.$$

The eigenvalues, λ, are obtained by solving the *characteristic equation* $\det(J - \lambda \mathbb{I}) = 0$, where $\mathbb{I}$ is the identity matrix. We obtain

$$\lambda_{\pm} = \frac{\operatorname{tr}(J) \pm \sqrt{(\operatorname{tr}(J))^2 - 4\det(J)}}{2}. \tag{29}$$

Now, suppose the trace is negative at $(\hat{x}, \hat{y})$. Then it is clear that $\operatorname{Re}(\lambda_-) < 0$, while

$$\operatorname{Re}(\lambda_+) < 0 \quad \Leftrightarrow \quad \det(J) > 0.$$

□

In the following analysis, will see that when the mutant's strategy is the same as the resident's, that is $\beta_m^P = \beta_r^P$, then the trace of the Jacobian matrix, $\operatorname{tr}(J)$, is always negative. We then assume that mutation steps are sufficiently small, so that, by continuity, $\operatorname{tr}(J)$ remains negative for the mutant strategy as well. This way we can apply Theorem 12, in which case invadability boils down to looking at the determinant. Since we are looking for mutations that *can* invade the resident population, we are particularly interested in cases where $\det(J) < 0$.

5.3.1 Mutant pathogen dynamics

We will assume that a mutant pathogen can only arise within a host that already carries the resident pathogen. Once a mutation occurs, the affected host will carry two different strains of the pathogen. Namely, the resident strain r and the mutant strain m. Hosts carrying both strains will be referred to as *mixed strain* carriers, and denoted E_{mix} and I_{mix}. Furthermore, their corresponding parameters will carry the subscript mr, take β_{mr}^P and α_{mr}, for example. In a similar fashion, hosts that are infected by a pure mutant strain will be denoted by E_{mut} and I_{mut} and their relevant rates will carry the subscript m. Finally, resident strain carriers will be denoted E_{res} and I_{res}.

We shall also require that $\beta_i^P \leq \beta_{mr}^P \leq \beta_j^P$, where i and j represent the pure mutant and resident strains. In particular, if $\beta_m^P = \beta_r^P$, then this implies that $\beta_{mr}^P = \beta_r^P$.

To discuss the mechanisms of infection between individuals carrying different strains, we introduce some notation. When an exposed individual carrying a pathogen strain

i is in a successful contact (i.e. one that results in an infection) with an infectious individual carrying a pathogen strain j we will write $E_i \otimes I_j$. The outcome of this contact will be denoted by an arrow, and the resulting infectious individual I_l will signify that the exposed individual E_i underwent the transition $E_i \to I_l$. In short, we write

$$E_i \otimes I_j \to I_l.$$

Moreover, if the outcome of a contact is uncertain, that is, the resulting infectious individual might carry a strain l_1 with probability p and a strain l_2 with probability $q = 1 - p$, then we write

$$E_i \otimes I_j \to pI_{l_1} \oplus qI_{l_2}$$

Similarly, a susceptible individual might become immediately infectious or transition into the exposed category. Hence

$$S \otimes I_i \to (1-k)E_j \oplus kI_j.$$

Since all contacts mentioned in this section are assumed to be successful, we will forget the difference and simply talk about the successful contacts as *interactions* between individuals.

When modelling the interactions between different strain carriers, the main problem is the question of how to accurately model interactions involving mixed strains. Without an underlying model describing the within-host dynamics, one must resort to making broad assumptions regarding these interactions. Initially one is tempted to keep these assumptions minimal, and so a naive approach would be to declare that whenever both strains are involved in an interaction, the outcome is always a mixed strain. Hence we obtain the rule

$$\begin{aligned} &E_i \otimes I_j \to I_{mix}, \quad \text{if } i = mix \text{ or } j = mix \text{ or } i \neq j, \\ &E_i \otimes I_i \to I_i, \quad \text{otherwise}, \\ &S \otimes I_j \to (1-k)E_j \oplus kI_j. \end{aligned} \tag{30}$$

As we will see, this rule leads to an overrepresentation of the mixed strain.

Now, since a mutation event gives rise to a mixed strain carrier, and interactions involving mixed strain carriers always result in mixed strain carriers, one easily sees that the above rule gives no means for a pure mutant strain to arise, and so the mutant will entirely spread through the individuals carrying a mixed strain and we may ignore the pure strains. Thus, we obtain the following linearised dynamics

$$\begin{aligned} \frac{dE_{mix}}{dt} &= \beta_{mr}^T(1-k)\hat{S}I_{mix} - (\beta_r^T\hat{I}_{res} + \nu_E + \mu)E_{mix}, \\ \frac{dI_{mix}}{dt} &= \beta_{mr}^T k\hat{S}I_{mix} + \beta_r^T E_{mix}\hat{I}_{res} + \beta_{mr}^T\hat{E}_{res}I_{mix} - (\alpha_{mr} + \mu + \nu_I)I_{mix}. \end{aligned}$$

At $\beta_m^P = \beta_r^P$ the Jacobian matrix of this system is

$$J = \begin{bmatrix} -(\beta^T \hat{I}_{res} + \nu_E + \mu) & \beta^T(1-k)\hat{S} \\ \beta^T \hat{I}_{res} & \beta^T k\hat{S} + \beta^T \hat{E}_{res} - (\alpha + \mu + \nu_I) \end{bmatrix}.$$

Notice that, by the isocline identity (7), the coefficient J_{22} is 0. Furthermore, the trace of J is negative, hence stability is determined by the determinant. For $k < 1$ we obtain

$$\det(J) = -(\beta^T)^2(1-k)\hat{S}\hat{I}_{res} < 0, \tag{31}$$

and so the resident can invade itself, thus the principle of selective neutrality is not satisfied; this is not a good model for the mutant pathogen dynamics.

Furthermore, without having a means of purifying the resulting mixed strain meta-population, some rather difficult questions of interpretation arise: should the mixed strain be considered a single strategy rather than two strategies? And what if the mutant is still invasive in the new mixed strain resident, does further mixing occur?

In what follows, we will present four different models, all based on a slight variation to the naive approach of ruleset (30). In addition, to resolve the problem of mixed strain residents, we introduce the probabilities ε_r and ε_m, which describe the probability per successful contact that an interaction involving *both* strains will result in a pure strain; resident or mutant, respectively. The underlying idea here being that occasionally, whenever both strains are present, an interaction will tip the balance in favour of one strain such that the other strain goes extinct through some stochastic process.

The sum of these probabilities, $\varepsilon := \varepsilon_r + \varepsilon_m$, is assumed to be so low that upon an invasion event, the mixed strain will spread among the hosts, thus establishing itself as a new temporary resident and, upon having established itself, the remaining pure strain sub-population, $I_r + I_m$, will be so rare that any interactions within this sub-population can be neglected. This allows us to perform a *time-scale separation*, that is, we can model the invasion event in two parts obtaining the *initial phase dynamics*, in which the mutant strain only exists and spreads as a mixed strain, and the *late phase dynamics*, in which the mixed strain has become the new resident and we look at the initial growth of a pure mutant strain that has appeared in a resident mixed strain population through the very slow stochastic process determined by ε. In practice, to obtain the initial phase dynamics, we set $\varepsilon = 0$, thus retaining only the variables that evolve in so called *fast time*. The slow dynamics are then obtained by replacing the fast variables with their so called quasiequilibria, obtained from the fast dynamics, and scaling time to be $\tau = \varepsilon t$. The late phase dynamics are *not* the slow dynamics, but rather the fast dynamics that come after the slow dynamics have had time to affect the system. Hence, the initial and late phase dynamics are on the same time-scale, but separated temporally by the very slow ε-process.

As we will see, all of the following models will satisfy the principle of selective neutrality and, furthermore, they will all lead to the same evolutionary dynamics of the pathogen when the resident is at an equilibrium. At the end of this section we take a brief look at invasion at limit cycles.

The case of a weak established pathogen. We begin by presenting a model in which the rules of infection are very simple. The underlying assumption here is that the established pathogen colony in an exposed individual has no effect at all on the outcome of an interaction. One could imagine that the established pathogen is putting the host under increased stress, but it is not really thriving itself either due to the immune system of the host combating the infection. Hence, when a secondary infection comes along, it is the pathogen load of this secondary infection which takes off, while the established pathogen becomes obsolete in comparison. We obtain the ruleset:

$$
\begin{aligned}
&E_i \otimes I_{mix} \to (1-\varepsilon) I_{mix} \oplus \varepsilon_r I_{res} \oplus \varepsilon_m I_{mut},\\
&E_i \otimes I_j \to I_j, \quad \text{if } j \neq mix,\\
&S \otimes I_{mix} \to (1-k)\left[(1-\varepsilon) E_{mix} \oplus \varepsilon_r E_{res} \oplus \varepsilon_m E_{mut}\right] \oplus k\left[(1-\varepsilon) I_{mix} \oplus \varepsilon_r I_{res} \oplus \varepsilon_m I_{mut}\right],\\
&S \otimes I_j \to (1-k) E_j \oplus k I_j, \quad \text{if } j \neq mix.
\end{aligned}
$$

Keep in mind that interactions involving both strains here do not always carry the chance of a pure strain to arise, since we *explicitly* assumed that the established colony does not play a role in determining the outcome of an interaction. Indeed, only when both strains are present in the *infecting* individual is there a chance for the ε-process to occur.

To simplify notation, we will henceforth write I^{ε}_{mix} instead of $(1-\varepsilon) I_{mix} \oplus \varepsilon_r I_{res} \oplus \varepsilon_m I_{mut}$ and E^{ε}_{mix} for the analogous situation. Hence, the above ruleset becomes

$$
\begin{aligned}
&E_i \otimes I_{mix} \to I^{\varepsilon}_{mix},\\
&E_i \otimes I_j \to I_j, \quad \text{if } j \neq mix,\\
&S \otimes I_{mix} \to (1-k) E^{\varepsilon}_{mix} \oplus k I^{\varepsilon}_{mix},\\
&S \otimes I_j \to (1-k) E_j \oplus k I_j, \quad \text{if } j \neq mix.
\end{aligned}
\tag{32}
$$

From these rules we deduce the following linearised mutant pathogen dynamics:

$$
\begin{aligned}
\frac{dE_{mut}}{dt} &= (1-k)\beta^T_m \hat{S} I_{mut} + \varepsilon_m (1-k)\beta^T_{mr} \hat{S} I_{mix} - (\beta^T_r \hat{I}_{res} + \nu_E + \mu) E_{mut},\\
\frac{dE_{mix}}{dt} &= (1-\varepsilon)(1-k)\beta^T_{mr} \hat{S} I_{mix} - (\beta^T_r \hat{I}_{res} + \nu_E + \mu) E_{mix},\\
\frac{dI_{mut}}{dt} &= k\beta^T_m \hat{S} I_{mut} + \varepsilon_m \left(k\beta^T_{mr} \hat{S} I_{mix} + \beta^T_{mr} \hat{E}_{res} I_{mix}\right) + \beta^T_m \hat{E}_{res} I_{mut} - (\alpha_m + \mu + \nu_I) I_{mut},\\
\frac{dI_{mix}}{dt} &= (1-\varepsilon)\left(k\beta^T_{mr} \hat{S} I_{mix} + \beta^T_{mr} \hat{E}_{res} I_{mix}\right) - (\alpha_{mr} + \mu + \nu_I) I_{mix}.
\end{aligned}
$$

Now, by our assumptions, the mutation event results in an initial mixed strain carrier. From this point on, the only way to produce pure mutant strain carriers is through the very slow process of random chance, governed by ε_m. Performing the time-scale separation, that is, setting $\varepsilon = 0$, we obtain the initial phase dynamics, which describes the beginning of an invasion.

The initial phase dynamics of ruleset (32) are given by

$$\begin{aligned} \frac{dE_{mix}}{dt} &= (1-k)\beta^T_{mr}\hat{S}I_{mix} - (\beta^T_r\hat{I}_{res} + \nu_E + \mu)E_{mix}, \\ \frac{dI_{mix}}{dt} &= \left(\beta^T_{mr}(k\hat{S} + \hat{E}_{res}) - (\alpha_{mr} + \mu + \nu_I)\right) I_{mix}. \end{aligned} \tag{33}$$

Notice that, while the mixed strain sub-population is rare, E_{mix} does not contribute to the dynamics of I_{mix}, and so we do not need to actually consider its equation; mixed strain exposed individuals are considered lost to the mutant. Hence, invadability of the mixed strain is determined by the sign of the parenthesis in $\dot{I}_{mix}$: the mixed strain sub-population will grow if

$$\beta^T_{mr}(k\hat{S} + \hat{E}_{res}) - (\alpha_{mr} + \mu + \nu_I) > 0,$$

or, in terms of the immediately infectable individuals,

$$\hat{E}_{0res} > \hat{E}_{0mix}.$$

Moreover, from this it is easy to see that at $\beta^P_m = \beta^P_r$ we have $\dot{I}_{mix} = 0$ and so the resident is selectively neutral.

Given that the mutant is able to invade and spread in the initial phase, we enter the late phase dynamics. Here, the mixed strain sub-population will be considered a temporary resident, the mutant as initially rare, having originated through the very slow ε-process, and the original resident will be left out of the dynamics entirely. Indeed, if a mixed strain was able to spread in the original resident meta-population, then any mixed strain that now reverts back to the original resident strain will be selectively inferior and will fail to thrive in the new environment. Once again, notice that pure mutant strain exposed individuals, E_{mut}, do not contribute to the population of pure mutant infectious individuals, hence the corresponding differential equation can be discarded. Thus, for the late phase dynamics we obtain the following linearised dynamics

$$\frac{dI_{mut}}{dt} = \left(\beta^T_m(k\hat{S} + \hat{E}_{mix}) - (\alpha_m + \mu + \nu_I)\right) I_{mut}. \tag{34}$$

Keep in mind that here $\hat{S}$ refers to the new equilibrium, corresponding to β^P_{mr}, and thus does not have the same value as in the initial phase dynamics. However, since susceptible individuals don't carry strains, and it is not relevant to keep track of which specific $\hat{S}$ we are talking about, we leave the subscript out.

Once again, the sign of the parenthesis determines invadability and we conclude that purification of the mixed strain occurs if

$$\hat{E}_{0mix} > \hat{E}_{0mut}.$$

The above invasion model is rather simplistic in the assumption that the established pathogen *never* influences the outcome of an interaction. For this reason, we now present a slight relaxation to this principle. However, as we shall see, we obtain an identical invasion model as in the very simplistic model.

So, suppose the established colony in an exposed individual is still weakened by the continued interference from the host's immune system. But now, assume that if the established colony is a *pure* strain, then the established strain will be prevalent enough within the host to have an effect on the outcome of an interaction. We obtain the ruleset

$$\begin{aligned}
&E_i \otimes I_{mix} \to I^{\varepsilon}_{mix},\\
&E_i \otimes I_j \to I^{\varepsilon}_{mix}, \quad \text{if } i \neq mix \text{ and } i \neq j,\\
&E_i \otimes I_j \to I_j, \quad \text{otherwise,}\\
&S \otimes I_{mix} \to (1-k)E^{\varepsilon}_{mix} \oplus kI^{\varepsilon}_{mix},\\
&S \otimes I_j \to (1-k)E_j \oplus kI_j, \quad \text{if } j \neq mix.
\end{aligned} \tag{35}$$

Performing the time-scale separation we obtain the initial phase dynamics:

$$\begin{aligned}
\frac{dE_{mix}}{dt} &= (1-k)\beta^T_{mr}\hat{S}I_{mix} - (\beta^T_r\hat{I}_{res} + \mu + \nu_E)E_{mix},\\
\frac{dI_{mix}}{dt} &= \left(\beta^T_{mr}(k\hat{S} + \hat{E}_{res}) - (\alpha_{mr} + \mu + \nu_I)\right) I_{mix}.
\end{aligned}$$

But this is exactly the same as (33)! In a similar fashion, the late phase dynamics are exactly the same as in (34). Indeed, the differences between rulesets (32) and (35) occur only at interactions $E_i \otimes I_j$, where one participant is a resident strain and the other is a pure mutant strain. However, throughout the invasion process a resident and a pure mutant are never expected to meet. Initially, when the resident is present, the mixed strain is expected to invade and replace the resident strain before pure mutant strain individuals get a chance to appear. On the other hand, once the mixed strain has replaced the resident strain, the resident strain will be selectively inferior in the new environment and so, as the ε-process gives rise to pure strain individuals, the resident strain individuals will disappear very quickly after appearing.

The case of a strong established pathogen. In contrast to the previous part, suppose the outcome of an interaction is completely determined by the established colony. In this case one might imagine that the pathogen strain colonising the

exposed individual is very well established and so occupies most, if not all, of the habitable sites within the host. Hence, as the exposed individual enters an interaction, the additional pathogen load fails to colonise an already crowded space, rather working as a springboard for the established colony as the immune system is put under too much stress. With these considerations in mind we obtain the following ruleset:

$$\begin{aligned} &E_{mix} \otimes I_j \to I^{\varepsilon}_{mix}, \\ &E_i \otimes I_j \to I_i, \quad \text{if } i \neq mix, \\ &S \otimes I_{mix} \to (1-k)E^{\varepsilon}_{mix} \oplus kI^{\varepsilon}_{mix}, \\ &S \otimes I_j \to (1-k)E_j \oplus kI_j, \quad \text{if } j \neq mix. \end{aligned} \tag{36}$$

Performing the time-scale separation, we first obtain the following initial phase dynamics:

$$\begin{aligned} \frac{dE_{mix}}{dt} &= \beta^T_{mr}(1-k)\hat{S}I_{mix} - (\beta^T_r \hat{I}_{res} + \nu_E + \mu)E_{mix}, \\ \frac{dI_{mix}}{dt} &= \beta^T_{mr}k\hat{S}I_{mix} + \beta^T_r \hat{I}_{res}E_{mix} - (\alpha_{mr} + \mu + \nu_I)I_{mix}. \end{aligned} \tag{37}$$

Notice that this time, E_{mix} does contribute to the mixed strain infectious individuals, hence we can't reduce the system to a single equation as in the previous situation.

These dynamics yield the Jacobian matrix

$$J = \begin{bmatrix} -(\beta^T_r \hat{I}_{res} + \nu_E + \mu) & \beta^T_{mr}(1-k)\hat{S} \\ \beta^T_r \hat{I}_{res} & \beta^T_{mr}k\hat{S} - (\alpha_{mr} + \mu + \nu_I) \end{bmatrix}.$$

At $\beta^P_m = \beta^P_r$, the trace of the Jacobian matrix is clearly negative as $J_{22} = -\beta^T_r \hat{E}_{res}$. Hence, assuming that mutations occur in a small enough neighbourhood around the resident strategy, we can assume that the trace is negative for all invading mutants. And so, by Theorem 31, invadability is determined by the determinant:

$$\begin{aligned} \det(J) &= -(\beta^T_r \hat{I}_{res} + \nu_E + \mu)\left(\beta^T_{mr}k\hat{S} - (\alpha_{mr} + \mu + \nu_I)\right) - \beta^T_{mr}\beta^T_r(1-k)\hat{S}\hat{I}_{res} \\ &= -(\beta^T_r \hat{I}_{res} + \nu_E + \mu)\left(\beta^T_{mr}(k\hat{S} + \hat{E}_{res}) - (\alpha_{mr} + \mu + \nu_I)\right), \end{aligned}$$

which is negative if

$$\beta^T_{mr}(k\hat{S} + \hat{E}_{res}) - (\alpha_{mr} + \mu + \nu_I) > 0.$$

Hence, the mixed strain is able to invade if

$$\hat{E}_{0res} > \hat{E}_{0mix}.$$

From this we move on to the late phase dynamics, which are as follows:

$$\frac{dE_{mut}}{dt} = \beta_m^T(1-k)\hat{S}I_{mut} - (\beta_{mr}^T\hat{I}_{mix} + \nu_E + \mu)E_{mut},$$
$$\frac{dI_{mut}}{dt} = \beta_m^T k\hat{S}I_{mut} + \beta_{mr}^T\hat{I}_{mix}\hat{E}_{mut} - (\alpha_m + \mu + \nu_I)I_{mut}.$$

Evidently, discounting the changed indexing, these dynamics are identical to (37). Hence we have purification if

$$\hat{E}_{0mix} > \hat{E}_{0mut}.$$

Much like in the previous case, with a weak established pathogen, this initial invasion model is rather simplistic. So, let us see what happens when the established pathogen is not taken to be quite so strong as to completely negate the effects of the secondary pathogen load. Indeed, suppose that if the additional load in an interaction is a pure strain, then it will affect the outcome of the interaction, and the established strain only fully determines the outcome in cases where the additional load is a mixed strain. We obtain the ruleset

$$\begin{aligned}
&E_{mix} \otimes I_j \to I_{mix}^{\varepsilon},\\
&E_i \otimes I_j \to I_{mix}^{\varepsilon}, \quad \text{if } j \neq mix \text{ and } i \neq j,\\
&E_i \otimes I_j \to I_i, \quad \text{otherwise,}\\
&S \otimes I_{mix} \to (1-k)E_{mix}^{\varepsilon} \oplus kI_{mix}^{\varepsilon},\\
&S \otimes I_j \to (1-k)E_j \oplus kI_j, \quad \text{if } j \neq mix.
\end{aligned} \tag{38}$$

Once again, the difference to the more simplistic ruleset occurs in interactions $E_i \otimes I_j$, where one participant is a resident strain and the other is a pure mutant strain. Hence, they are never expected to meet and so the initial and late phase dynamics are once again identical to the more simplistic formulation.

In conclusion, perhaps surprisingly, the two quite opposite invasion model formulations, in which the established pathogen colony is weak in one and strong in the other, lead to the same criteria of invadability for a mutant pathogen. Namely, the mutant pathogen is able to invade and spread as a mixed strain in the resident meta-population only if

$$\hat{E}_{0res} > \hat{E}_{0mix},$$

and furthermore, purification of the mixed strain occurs if

$$\hat{E}_{0mix} > \hat{E}_{0mut}.$$

Combining these two inequalities we find that a mutant invasion-purification chain occurs if

$$\hat{E}_{0res} > \hat{E}_{0mix} > \hat{E}_{0mut}. \tag{39}$$

5.3.2 Pathogen invasion at limit cycles

Suppose the demographic attractor of the resident population is a limit cycle. How do we determine the invadability of a mutant pathogen strain in this case? Let us consider the case where the established pathogen colony is weak and proceed as we did in the previous section on host invasion analysis.

So, suppose the established pathogen is weak, then in the initial phase dynamics we only have one equation to worry about:

$$\frac{dI_{mix}}{dt} = \left(\beta_{mr}^T(kS + E_{res}) - (\alpha_{mr} + \mu + \nu_I)\right) I_{mix}.$$

Dividing on both sides by I_{mix}, we obtain the following equivalent formulation:

$$\frac{d\log(I_{mix})}{dt} = \beta_{mr}^T(kS + E_{res}) - (\alpha_{mr} + \mu + \nu_I).$$

Now, as we did with the mutant host, we wish to track the mutant population density as we let the resident population complete one revolution on the limit cycle. Hence, we integrate over time from 0 to Π, where Π is the period of the limit cycle. We obtain

$$\log(I_{mix}(\Pi)) - \log(I_{mix}(0)) = \beta_{mr}^T k \int_0^\Pi S(t)dt + \beta_{mr}^T \int_0^\Pi E_{res}(t)dt - \Pi(\alpha_{mr} + \mu + \nu_I).$$

This does not seem very helpful at first, however we may perform a little trick: choose $\beta_m^P = \beta_r^P$. Now we have $I_{mix} = I_{res}$, which is on a limit cycle with period Π, hence the left hand side vanishes and we obtain the following identity:

$$k\langle S\rangle + \langle E_{res}\rangle = \frac{\alpha_r + \mu + \nu_I}{\beta_r^T} = \hat{E}_{0res}, \tag{40}$$

where $\langle\cdot\rangle$ indicates the *time average* of the respective population density, that is, we denote

$$\langle S\rangle = \frac{1}{\Pi}\int_0^\Pi S(t)dt \quad \text{and} \quad \langle E\rangle = \frac{1}{\Pi}\int_0^\Pi E(t)dt.$$

Thus, going back to the situation where $\beta_m^P \neq \beta_r^P$, and this time using identity (40) to our advantage, we conclude that in one revolution along the limit cycle, the mixed strain grows and invades, that is $I_{mix}(\Pi) > I_{mix}(0)$, if and only if

$$\beta_{mr}^T\left(k\langle S\rangle + \langle E_{res}\rangle\right) - (\alpha_{mr} + \mu + \nu_I) > 0,$$

or in other words, if and only if

$$\hat{E}_{0res} > \hat{E}_{0mix}.$$

For the late phase dynamics, the situation is exactly the same except that we change the indices accordingly. Thus, the invasion-purification chain occurs if

$$\hat{E}_{0res} > \hat{E}_{0mix} > \hat{E}_{0mut},$$

exactly like in the case where the resident was at an equilibrium.

In the case that the established pathogen colony is strong things are not so simple. Indeed both the initial and late phase dynamics are described by a two dimensional system. Hence we can't perform the same trick as in the previous case; we're forced to construct the monodromy matrix just like we did for the host invasion analysis. Unfortunately, here we run out of analytical tools and are forced to continue with numerical methods.

In the end we can only choose one pathogen invasion model to work with as we study the evolutionary dynamics of the system (1). Thus, we choose to work with the case of the weak established colony and remark that when the resident population is at an equilibrium, then the case of a weak established pathogen *coincides* in its qualitative behaviour with the case of the strong established pathogen.

5.3.3 Invasion implies substitution

Here we show that when the resident strain β_r^P is such that $\hat{E}_{0res}$ is monotone, then the invasion of a mutant strain will lead to the extinction of the resident. When $R_0^P(\beta_r^P) > 1$, then we will see that the mutant strain becomes the new resident, otherwise it might happen that both the resident and mutant strains become extinct.

Suppose the resident is in a region where $\hat{E}_0$ is monotone, that is, when an invasive mutant appears we have

$$\hat{E}_{0res} > \hat{E}_{0mix} > \hat{E}_{0mut}.$$

Can the two pathogen strains coexist within the same host?

As noted at the very end of the previous section, we've chosen to work with the model of the weak established pathogen. Hence, in the initial phase dynamics the immediately infectable sub-population density is given by

$$E_{mix} + E_{res} + kS.$$

Moreover, at limit cycles the time averages of these quantities are the same as the equilibrium quantities, as shown in section 5.3.2. For this reason, it is enough to consider what happens at equilibria.

Theorem 13. *Suppose* $R_0^P(\beta_r^P) > 1$ *and that an invasive mutant appears, such that*

$$\hat{E}_{0res} > \hat{E}_{0mix} > \hat{E}_{0mut}.$$

Then coexistence of the mutant and resident pathogen strains is impossible, and the mutant strain will eventually replace the resident strain.

Proof. We prove the theorem by studying the initial phase dynamics. The proof is exactly the same for the late phase dynamics, one only has to change the indices accordingly.

Contrary to the claim of the theorem, suppose the dimorphic meta-population of the mixed and resident strain pathogens has equilibrated. Then we must have

$$\hat{R}_0^P(\beta_r^P) = 1 \quad \text{and} \quad \hat{R}_0^P(\beta_{mr}^P) = 1.$$

But now, we see that this can't be true. Indeed we have

$$\tilde{R}_0^P(\beta_r^P) = \frac{E_{mix} + E_{res} + kS}{\hat{E}_{0res}} < \frac{E_{mix} + E_{res} + kS}{\hat{E}_{0mix}} = \tilde{R}_0^P(\beta_{mr}^P).$$

And so, if the resident has equilibrated, then the mixed strain is still growing. Conversely, if the mixed strain has equilibrated, then the resident must be decreasing. Because $R_0^P(\beta_r^P) > 1$ we know that $R_0^P(\beta_{mr}^P) > 1$ as well. Hence, in conclusion, both pathogen strains can not coexist indefinitely and since the mixed strain is invasive and protected from extinction in the absence of the resident strain, we know that the resident strain must disappear from the meta-population. □

Interestingly, if we forgo the assumption that $R_0^P(\beta_r^P) > 1$ in the above theorem, that is, we assume instead $R_0^P(\beta_r^P) < 1$, then nothing guarantees that the mutant strain will persist in the host. It may happen that both strains decline to the verge of extinction. We know that the resident will necessarily be pushed to extinction, but if it happens that $R_0^P(\beta_{mr}^P) < 1$, then the mixed strain is not protected from extinction and it can disappear as well! Examples of this happening are shown and discussed below, in section 6.1.3.

Now that we are convinced that an invasive mutant pathogen strain will replace the resident pathogen whenever

$$\hat{E}_{0res} > \hat{E}_{0mix} > \hat{E}_{0mut}$$

holds, we may look at how evolution of the pathogen proceeds in a more grander context. In particular, we also discuss what happens when $\hat{E}_0$ is *not* monotone.

6 Evolutionary dynamics

In the following sections we study how the pathogen and host strategies change in evolutionary time.

6.1 Evolutionary dynamics of the pathogen

We begin this section by showing that pathogen evolution defines an optimisation model in the regions where $\hat{E}_0$ is monotone. After this we study the qualitative features of pathogen evolution and look at some concrete examples. In particular, we place an emphasis on the occurrence of the phenomenon of evolutionary suicide; when does the long term evolution of the pathogen result in the extinction of the pathogen?

6.1.1 Characteristics of pathogen evolution

In this section we look at the characterising features of pathogen evolution. In particular, we show that pathogen evolution proceeds according to an optimisation model when the resident is far away from a singular strategy.

An evolutionary model is an optimisation model, if, for the resident strategy x and mutant strategy y, there exists a function, W, such that the difference

$$\tilde{s}_x(y) := W(y) - W(x), \tag{41}$$

is sign-equivalent to the fitness function, $s_x(y)$. We call the difference $\tilde{s}_x(y)$ the *fitness advantage* of a strategy y against a resident strategy x. The strategy, x^*, which locally maximises W is the locally optimal strategy. This strategy is also a locally evolutionarily stable strategy (ESS), since

$$\tilde{s}_{x^*}(y) < 0 \quad \Leftrightarrow \quad s_{x^*}(y) < 0$$

for all other nearby strategies y, hence the locally optimal strategy can not be invaded. Moreover, $\tilde{s}_y(x^*) > 0$ for all nearby strategies $y \neq x^*$, hence the locally optimal strategy can also invade any other nearby strategies [6]. Evidently, the optimal strategy is also a singular strategy, as the selection gradient must change sign at this strategy. More generally, any strategies corresponding to an extreme value of W are singular strategies by the sign-equivalence of the fitness advantage, $\tilde{s}$, and the fitness function, s.

Recall that mutant pathogen invadability was characterised by the inequality (39) in all the different models of mutant pathogen invasion presented in section 5.3. To reiterate, assuming small mutation steps, the invasion-purification chain will occur if

$$\hat{E}_{0res} > \hat{E}_{0mix} > \hat{E}_{0mut}.$$

Henceforth, we will consider $\hat{E}_0$ as a function of β^P and differentiate between strains by having the subscript on β^P rahter than $\hat{E}_0$. And so, the invasion-purification chain is equivalently characterised by

$$\hat{E}_0(\beta^P_r) > \hat{E}_0(\beta^P_{mr}) > \hat{E}_0(\beta^P_m). \tag{42}$$

Indeed, we can now define a fitness advantage

$$\tilde{s}_{\beta_r^P}(\beta_m^P) = \hat{E}_0(\beta_r^P) - \hat{E}_0(\beta_m^P). \tag{43}$$

The fitness advantage defined like this works well as long as the resident is sufficiently far away from any extreme values of $\hat{E}_0$. Indeed, assuming mutant strategies can only occur in some small neighbourhood with radius $\delta > 0$ around the resident strategy β_r^P, then $\hat{E}_0$ is monotone as long as any singular strategies, β^{P*}, lie outside of the δ-neighbourhood. In this monotone region, the inequality $\hat{E}_0(\beta_r^P) > \hat{E}_0(\beta_m^P)$ implies (42), and so any invasion event will result in the invasion-purification chain and evolution will progress as a succession of monomorphic pathogen meta-populations toward lower values of $\hat{E}_0$. Furthermore, the optimal strategy, β^{P*}, is the strategy which locally minimises $\hat{E}_0$. Indeed, it is an ESS and will henceforth be referred to as such and denoted β_{ESS}^P.

Recall that $\beta^P \in [0, 1]$. By this, there can be two kinds of local minima of $\hat{E}_0$, namely an interior minimum, that is, a minimum such that $\beta_{ESS}^P < 1$, and a boundary minimum obtained at $\beta_{ESS}^P = 1$.

In the δ-neighbourhood of an interior ESS the optimisation model breaks down. Given that a resident strategy lies close enough to the interior ESS, an invasive mutant might overshoot the interior ESS. For example, we might end up with the ordering $\beta_r^P < \beta_{ESS}^P < \beta_m^P$, and consequently we can end up with the following situation:

$$\hat{E}_0(\beta_m^P) > \hat{E}_0(\beta_{mr}^P) > \hat{E}_0(\beta_{ESS}^P).$$

In this case the pure mutant will not be invasive in the late phase dynamics where the mixed strain has become the resident and so purification will not happen; the mixed strain will persist as the new resident indefinitely. Without including the within host dynamics of the pathogen, it is difficult to draw any conclusions on how evolution proceeds in this region. However, with δ being small, evolution will proceed in a straight forward manner to a very small neighbourhood of the interior ESS. Furthermore, with each successive invasion event, the transmission rate of the mixed strain must always move closer to the interior ESS.

At the boundary ESS, $\beta_{ESS}^P = 1$, the evolution of the pathogen follows the optimisation model until the ESS. Indeed, in this case $\hat{E}_0$ is necessarily monotone at $\beta^P = 1$, because $\beta^P > 1$ is not considered.

Remark 8. Allowing for some speculation, the rather unrestricted evolutionary behaviour near the ESS might underlie the existence of multiple similar strains of a single pathogen. Indeed, as long as the mixed strain moves closer to the ESS with each successive mutation, the number and distribution of pure strains is unrestricted. Consequently, many of the pure strains are also protected by the mixed strain; removal of one pure strain might cause the mixed strain to move further from the

ESS, hence the disappearance of these pure strains from the mixed strain is not evolutionarily viable.

The tendency to diversify might be at the root of a process known as *antigenic variation*, where the phenotype of a virus changes in response to the acquired immunity of the host [8]. When the pathogen evolution leads to a natural tendency to diversify around the ESS, the pathogen is much more resistant to the host becoming immune as a diverse population can more effectively produce an effective mutation in response to immunity. In contrast, at the boundary ESS, further mutations are always evolutionarily inferior, hence the pathogen is much less diverse and as such more susceptible to being eradicated through the acquired immunity of the host.

This could help bridge the gap between the long periods of a cyclically occurring epidemic, as seen in the demographic example of section 4.4.1, and the seasonally occurring influenza epidemics that we see in the real world, which are attributed to the phenotype of the virus alternating between epidemics. However, without including the within host dynamics of the pathogen, we stress that this is nothing but speculation and a better formulated model of evolution might very well do away with this unrestricted evolution, in particular when the acquired immunity of the host is taken to be strain specific, rather than pathogen specific as it is in our model.

In conclusion, the pathogen will evolve as a single monomorphic population either to the boundary ESS or until it reaches a small neighbourhood of its interior ESS. What happens after the δ-neighbourhood of the interior ESS has been reached is beyond the scope of this thesis, but in any case we can be sure that whatever the composition of the pure strains in this region, the effective transmission rate, which is given by the mixed strain must converge to the interior ESS. The host is oblivious to whether or not the pathogen is a pure or mixed strain and so, in section 6.2, as we set the pathogen to its interior ESS and look at the evolutionary dynamics of the host, we do not need to worry about the unrestricted evolutionary behaviour of the pathogen near the interior ESS.

We conclude this section by presenting the following result on the possibility of evolutionary suicide on the part of the pathogen:

Theorem 14. *Suppose there exists $\beta_0^P \in (0,1]$ such that $R_0^P(\beta_0^P) > 1$. Then a pathogen with the initial strategy β_0^P can not commit evolutionary suicide.*

Proof. Notice that we can write R_0^P as follows:

$$R_0^P(\beta^P) = \frac{\beta^T k \hat{N}_{\text{free}}}{\alpha + \mu + \nu_I} = \frac{k\hat{N}_{\text{free}}}{\hat{E}_0(\beta^P)}.$$

Hence, pathogen evolution will proceed in the direction which maximises R_0^P and so, any pathogen strategy that lies in a region where $R_0^P > 1$ will remain in such a region as it evolves towards its ESS.

Recall that, by Corollary 2, an endemic attractor must always exist for $R_0^P > 1$; the disease-free and trivial equilibria are both unstable (Appendix, 8.2). Hence, the pathogen will persist in the host population for all β^P such that $R_0^P(\beta^P) > 1$. This proves the claim. □

A consequence of Theorem 14 is that, in the biological context, some drastic change must occur for pathogen evolution to result in evolutionary suicide. Indeed, a pathogen can only invade a virgin host population when $R_0^P > 1$ for the pathogen transmission rate. However, if evolutionary suicide is to happen, then we must have $R_0^P(\beta_{ESS}^P) < 1$. From these considerations we immediately obtain the following corollary to Theorem 14:

Corollary 7. *A necessary condition for pathogen suicide is $k < k_{max}$ at β_{ESS}^P.* □

Before delving straight into the examples of pathogen evolution showcased in Figures 6 - 8, let us gain a better understanding of the evolutionarily stable strategies, β_{ESS}^P, and how the virulence, α, affects the existence and nature of these.

6.1.2 The extreme values of $\hat{E}_0$

In this short section we study the long term features of pathogen evolution. In particular, we place an emphasis on the singular strategies, and how the virulence, α, affects the nature and location of these strategies.

Recall that α is an increasing function of β^P and that we had defined

$$\beta^P = q^P,$$

where q^P was the probability of the pathogen establishing itself in the receiving host. In particular, this means that β^P is bounded to the closed interval $[0, 1]$, and so $\hat{E}_0$ will always have a minimum with respect to β^P. As we already mentioned, we refer to the local minima of $\hat{E}_0$ that are achieved for some $\beta^P < 1$ as interior minima, to differentiate from a possible minimum achieved at $\beta^P = 1$, which we refer to as the boundary minimum.

As $\beta^P \to 0$ we have

$$\lim_{\beta^P \to 0} \hat{E}_0 = \lim_{\beta^P \to 0} \frac{\alpha + \mu + \nu_I}{\beta^H \beta^P} = \infty.$$

Hence, the pathogen will never evolve to $\beta^P = 0$ and so, if an interior minimum does not exist, then the pathogen will always evolve towards the boundary ESS. Moreover, if an interior *maximum* exists, then this implies that at least one interior minimum must exist as well. More generally, if a local maximum exists, then a local minimum must exist, but in this case we can't be sure that the local minimum is within the unit interval.

At the interior extrema, the derivative of $\hat{E}_0$ must vanish, and so we have

$$\begin{aligned} \frac{\partial \hat{E}_0}{\partial \beta^P} &= \frac{\alpha'}{\beta^T} - \frac{\beta^H(\alpha+\mu+\nu_I)}{(\beta^T)^2} = \frac{1}{\beta^T}\left(\alpha' - \frac{\alpha+\mu+\nu_I}{\beta^P}\right) = 0 \\ \Leftrightarrow \quad & \alpha' - \frac{\alpha+\mu+\nu_I}{\beta^P} = 0. \end{aligned} \tag{44}$$

As can be seen, the interior extrema are independent of the host strategy. Hence, pathogen evolution is entirely independent of any particular value of the host strategy. We collect our findings in the following theorem:

Theorem 15. *The locations of all evolutionarily stable strategies of the pathogen are independent of the host strategy β^H and the parameter k.*

Proof. For the interior ESSs, (44) proves the claim. On the other hand, suppose $\beta^P = 1$ is an ESS such that

$$\frac{\partial \hat{E}_0}{\partial \beta^P}(1) < 0.$$

Now suppose varying k or β^H results in the sign of this derivative changing. By continuity, there must then exist a point, k_0 or β_0^H, where

$$\frac{\partial \hat{E}_0}{\partial \beta^P}(1) = 0.$$

But now, $\hat{E}_0$ is locally minimised at $\beta^P = 1$. This is a contradiction, because the locations of the local extrema of $\hat{E}_0$ are invariant with respect to changes in k or β^H. □

At the local extrema of $\hat{E}_0$ the second derivative determines the nature of these values. Indeed, calculating the second derivative yields

$$\begin{aligned} \frac{\partial^2 \hat{E}_0}{\partial (\beta^P)^2} &= \frac{\alpha''}{\beta^T} - \frac{\beta^H \alpha'}{(\beta^T)^2} - \left(\frac{\beta^H \partial_P \hat{E}_0}{\beta^T} - \frac{(\beta^H)^2 \hat{E}_0}{(\beta^T)^2}\right) \\ &= \frac{\alpha''}{\beta^T} - \frac{\beta^H}{\beta^T}\left(\partial_P \hat{E}_0 + \frac{\partial_P \hat{E}_0}{\beta^T}\right). \end{aligned}$$

Here we've used the shorthand notation

$$\partial_P \hat{E}_0 := \frac{\partial \hat{E}_0}{\partial \beta^P}.$$

In particular, at the extreme values this becomes

$$\left.\frac{\partial^2 \hat{E}_0}{\partial (\beta^P)^2}\right|_{\beta^P = \beta^{P*}} = \frac{\alpha''}{\beta^T}.$$

Hence, if $\alpha'' \geq 0$ for all β^P, then no local maxima can exist and evolution will go towards a unique ESS; either the interior minimum of $\hat{E}_0$ or the boundary minimum. Moreover, if $\alpha'' \leq 0$ for all β^P, then no local minima can exist, and in this case evolution will tend towards the boundary ESS. In the next section, we present examples of pathogen evolution, where α has been chosen such that $\alpha'' > 0$ in one example, $\alpha'' < 0$ in another and in a third the sign of α'' varies.

6.1.3 Examples of pathogen evolution

In this section we present a few examples of pathogen evolution. In each example we have attempted to showcase three situations in particular: one in which there exist regions where $R_0^P > 1$ (plot (b) in Figures 6 to 8), one in which stable endemic equilibria exist despite $R_0^P < 1$ everywhere (plot (c) in each Figure 6 and 8), and one in which an ESS has lost stability such that pathogen evolution leads to evolutionary suicide (plot (d) in each figure). In each figure, plot (a) shows the chosen trade-off between the virulence α and the pathogen transmission rate β^P.

In Figure 6 we've chosen the trade-off between the virulence and pathogen host transmission rate to be quadratic. In plot (b), part of $\hat{E}_0$ lies in a region where $R_0^P > 1$, as indicated by the shaded region. Thus, a pathogen with β^P ranging in the interval $[0.2, 0.6]$ can invade a virgin host population.

Supposing a pathogen has invaded, plot (c) and (d) show what happens as k is decreased. Indeed, in both plot (c) and (d) the region where $R_0^P > 1$ has completely disappeared. Nevertheless, in plot (c) the pathogen can still persist in the host for a variety of transmission rates, including the ESS. In plot (d), however, the pathogen is not so lucky: while it can still persist for some values of β^P, we see that the ESS has become unstable. Hence, a pathogen that has not yet been eradicated at this point, is doomed to commit evolutionary suicide.

Conversely, plot (e) and (f) show how the evolutionary dynamics change as β^H is decreased. In plot (e) the pathogen can still persist at, and close to, the ESS, while in plot (f) it can no longer persist for any values of β^P. In this figure, and in Figures 7 and 8, it seems as though evolutionary suicide occurs only when k is sufficiently low. When β^H is decreased but k is kept at its original value, the examples suggest that the interior ESS's are always the last to lose stability. The dependence of evolutionary suicide on the value of k is of course expected in light of Corollary 7.

Remark 9. It should be noted that in these examples at most two endemic equilibria exist for any chosen parameter values. In particular, the two endemic equilibria exist only when a backward bifurcation has occurred. Recall the *principle of exchange of stability* at the transcritical bifurcation [7]. Hence, when two endemic equilibria exist, one is necessarily always unstable because it has inherited the instability of

the disease-free equilibrium through the backward transcritical bifurcation. Thus, in the plot we only track the other endemic equilibrium, which has the potential of being either locally attracting or hosting a stable limit cycle. This allows us to conclude the type of bifurcation that occurs as β^P is varied, since if the endemic equilibrium that is being tracked persists for $R_0^P < 1$, then we know that a backward bifurcation has occurred.

By the above remark, we may conclude for Figure 6 that in plot (b), the direction of the transcritical bifurcation is forward as β^P enters the shaded region from below and backward when it exits the shaded region. Indeed, the endemic equilibrium persists for a while in $R_0^P < 1$ when $\beta^P > 0.6$.

In Figure 7 the chosen trade-off between β^P and α has been chosen to be logistic. This way we have two ESSs, namely the interior minimum, as indicated by the vertical notch, and $\beta^P = 1$. As k and β^H are each decreased (plots (c) and (e), respectively), we see that the region of $R_0^P > 1$ splits in two. In this case, the unlucky pathogen invades in a region where evolution leads to the interior ESS, while the somewhat more lucky pathogen invades such that evolution leads towards $\beta^P = 1$. Indeed, we see that as k and β^H are each further lowered (plots (d) and (f), respectively), the interior minimum loses stability before $\beta^P = 1$ does. Note that this is not a universal property of the model: one can engineer the system such that the order of stability loss is reversed, in contrast to our example. Once again, plot (d) shows an example of evolutionary suicide, where a pathogen may persist in the host even though $R_0^P < 1$, but as it evolves towards the interior minimum it commits evolutionary suicide. No examples of evolutionary suicide were found as β^H was varied.

In all plots except (b) of Figure 7 the transcritical bifurcations are backwards, as can be seen from the endemic equilibrium persisting in the region where $R_0^P < 1$.

In Figure 8 we have chosen α so that no interior minimum exists. This time the ESS is $\beta^P = 1$ and it is globally attracting. Here we see that the transcritical bifurcations visible in plots (b) and (e) are both backwards. Once again, plot (d) provides a clear example of evolutionary suicide; the stable endemic equilibrium destabilises as the pathogen approaches its ESS. The destabilisation happens through a Hopf bifurcation. Since $R_0^P < 1$, the disease-free equilibrium is locally attracting. By continuity, for β^P very close to the Hopf bifurcation, the limit cycles are stable and attracting. However, as we further increase β^P the limit cycles very quickly destabilise as the orbits wander too close, and eventually converge, to the locally attracting disease-free equilibrium.

Interestingly, one would expect that as the pathogen minimises $\hat{E}_0$ through evolution, hence maximising R_0^P, it would only become more entrenched. Recall Theorem 13, where we included the assumption that $R_0^P(\beta_r^P) > 1$ prior to the invasion of a

mutant pathogen. Here we see an example of what can happen when this assumption is excluded; when k is too low a mutant invasion event can backfire, resulting in the pathogen committing evolutionary suicide. Recall that k is the fraction of susceptibles that become infectious upon a single successful contact with an infectious individual. Furthermore, a mutant pathogen always appears in an endemic population, that is, the sub-population density of the immediately infectious individuals, $\hat{E}_0$, is always ready-made for the mutant. For this reason, the evolution of the pathogen is in a sense blind to the threat of minimising $\hat{E}_0$ too much. A rare mutant pathogen experiences a bountiful environment upheld by the resident, but as the resident is outcompeted, the mutant finds itself in an unsustainable situation; although R_0^P is now greater, k is simply too low to sustain the pathogen meta-population. Too many infections are lost to the sub-population of exposed individuals. This also explains why suicide does not occur when β^H is decreased. Varying β^H has no effect on the fraction of susceptibles becoming immediately infectious, hence in this case going for maximum R_0^P is always beneficial. As a result, the ESS is last to lose stability as β^H is decreased.

Common to all three examples is that the pathogen is quite sensitive to changes in k, while it is comparatively more resistant to changes in β^H. For example, in Figure 6 the pathogen can readily invade a virgin host population when $\beta^H = 0.65$ and $k = 0.2$, but decreasing k by just 0.05 to $k = 0.15$ causes the ESS to lose stability and any pathogen that had not yet evolved to the ESS to commit evolutionary suicide. On the other hand, it takes a decrease of 0.11 in β^H for the pathogen to be driven to extinction under the same circumstances.

In a biological context this can be thought of as changes in the environment which result in a stronger resistance to the disease (lower k) being more effective at eradicating the pathogen than changes in host behaviour, such as lowering the contact rate between individuals. However, this reasoning feels somewhat awkward, and a better approach would be to look at it from the converse point of view.

Suppose the host is initially in an environment where the pathogen can not invade. Then any change in the environment that could be interpreted as resulting in an increase in k, such as a famine, extreme temperatures or war can very easily push the host into a situation where the pathogen can invade. Now, if the change in k persists, then the host will have to make a comparatively big change in its own strategy, β^H, to return to the initial situation and get rid of the pathogen.

Us humans are able to carry out the necessary changes in β^H through deliberate action, but for animals these changes can, for the most part, only happen through the slow process of evolution. Furthermore, since the pathogen can persist even though it can not invade, once the imagined disaster is over and k has returned to its original value, the pathogen might still happily persist. Thus, a sudden chance event, perhaps lasting for no more than a few years, can take thousands if not tens

of thousands of years of host evolution to reverse. In the next section we look at examples of how host evolution proceeds when the pathogen is present and has converged evolutionarily to its ESS.

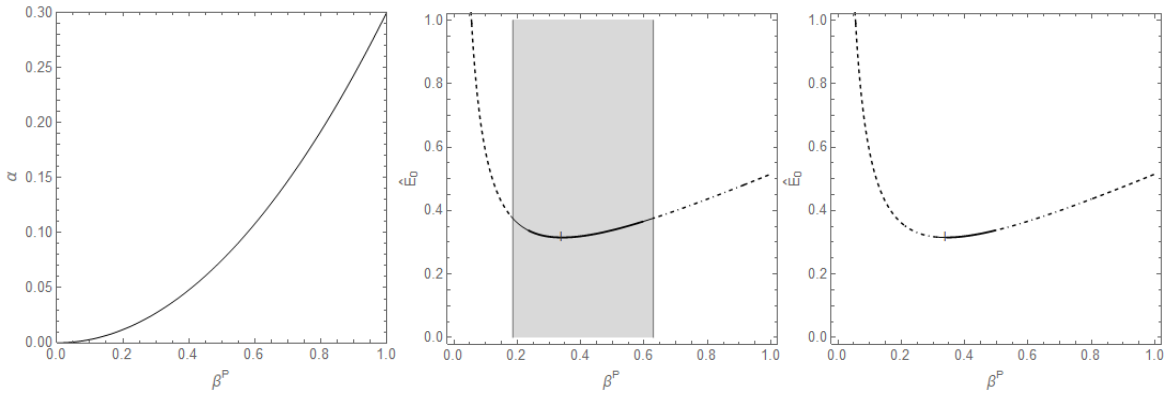

(a) $\alpha = 0.3(\beta^P)^2$ (b) $\beta^H = 0.65, \quad k = 0.2$ (c) $\beta^H = 0.65, \quad k = 0.16$

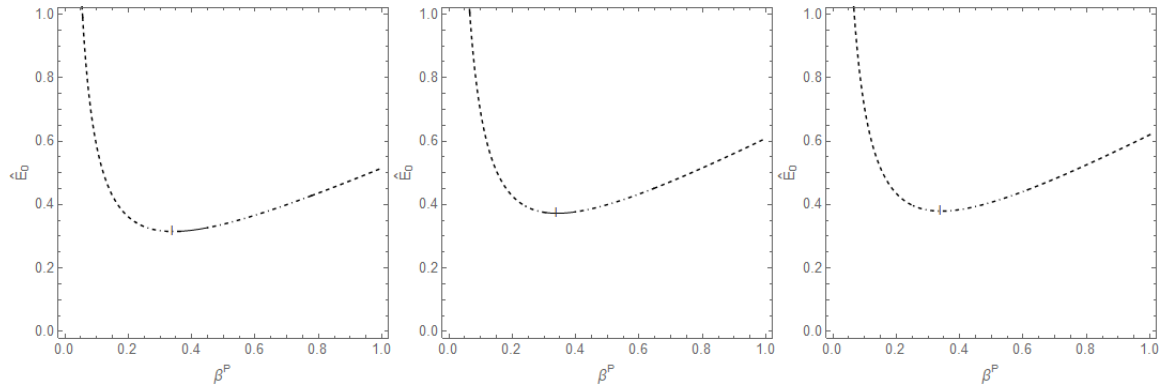

(d) $\beta^H = 0.65, \quad k = 0.15$ (e) $\beta^H = 0.55, \quad k = 0.2$ (f) $\beta^H = 0.54, \quad k = 0.2$

$$\nu_E = 0.05, \quad \nu_I = 0.03, \quad \mu = 0.005, \quad c = 0.02, \quad a = 0.04 + 0.004\beta^H.$$

Figure 6: An example of pathogen evolution with α chosen such that $\alpha'' > 0$. Here a unique minimum exists, and so evolution is straightforward after a pathogen has invaded a virgin population. The shaded region indicates $R_0^P > 1$. The solid lines indicate that a pathogen can persist within the host population; thin lines for limit cycles and thick lines for stable equilibria. The dot-dashed line indicates that an endemic equilibrium exists, but the pathogen can not persist. The simple dashed line indicates that no endemic equilibria exist. The notch indicates the minimum of $\hat{E}_0$, hence it shows the precise location of the interior (in this case global) minimum.

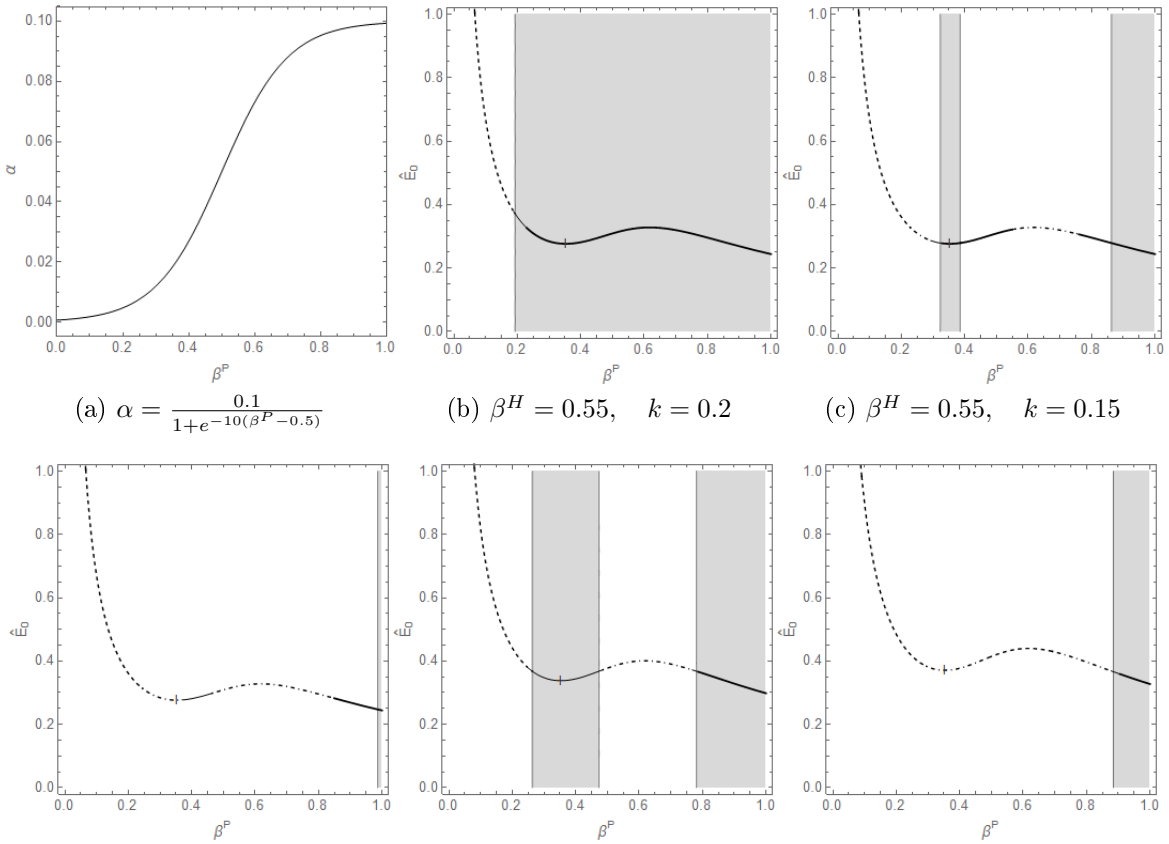

(a) $\alpha = \frac{0.1}{1+e^{-10(\beta^P-0.5)}}$ (b) $\beta^H = 0.55, \quad k = 0.2$ (c) $\beta^H = 0.55, \quad k = 0.15$

(d) $\beta^H = 0.55, \quad k = 0.1$ (e) $\beta^H = 0.45, \quad k = 0.2$ (f) $\beta^H = 0.41, \quad k = 0.2$

$$\nu_E = 0.05, \quad \nu_I = 0.03, \quad \mu = 0.005, \quad c = 0.02, \quad a = 0.04 + 0.004\beta^H.$$

Figure 7: An example of pathogen evolution with α chosen to be a logistic function. The shaded region indicates $R_0^P > 1$. The solid lines indicate that a pathogen can persist within the host population; thin lines for limit cycles and thick lines for stable equilibria. The dot-dashed line indicates that an endemic equilibrium exists, but the pathogen can not persist. The simple dashed line indicates that no endemic equilibria exist.

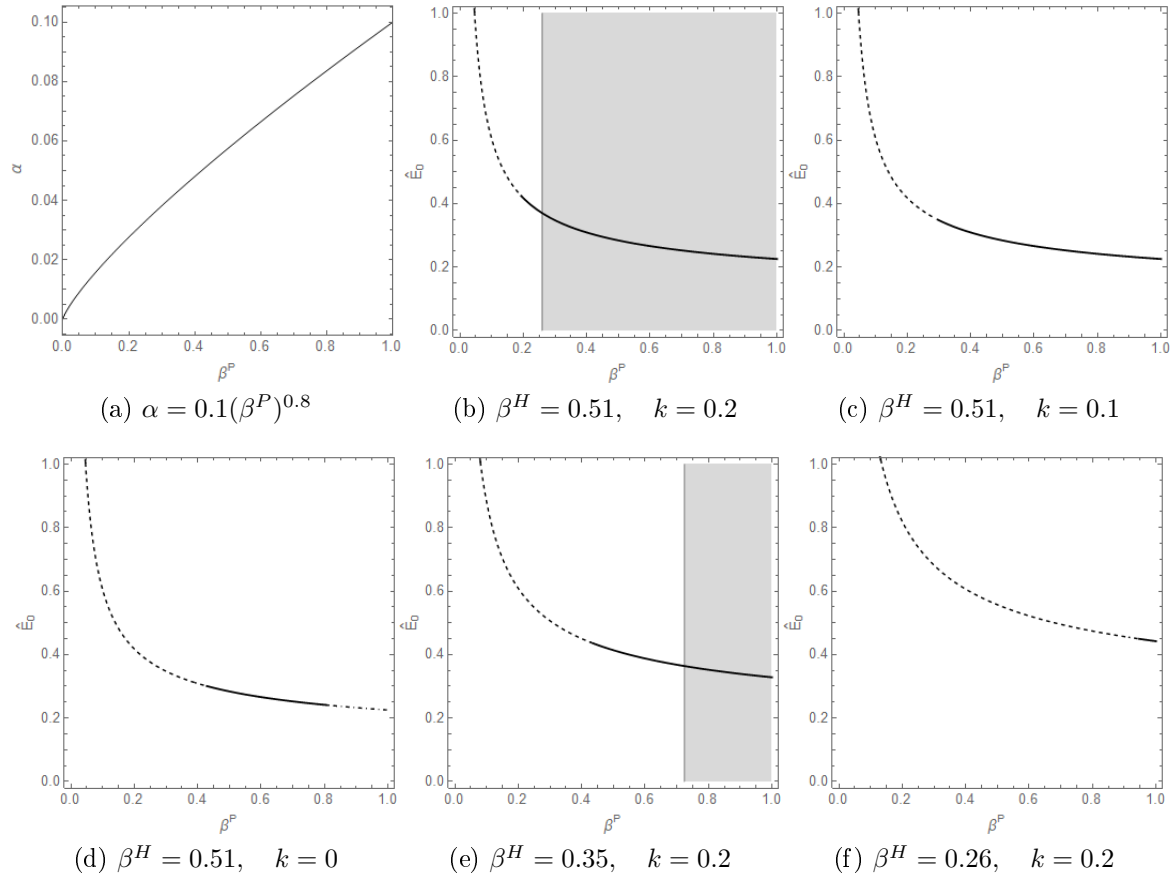

(a) $\alpha = 0.1(\beta^P)^{0.8}$ (b) $\beta^H = 0.51, \quad k = 0.2$ (c) $\beta^H = 0.51, \quad k = 0.1$

(d) $\beta^H = 0.51, \quad k = 0$ (e) $\beta^H = 0.35, \quad k = 0.2$ (f) $\beta^H = 0.26, \quad k = 0.2$

$$\nu_E = 0.05, \quad \nu_I = 0.01, \quad \mu = 0.005, \quad c = 0.02, \quad a = 0.04 + 0.004\beta^H.$$

Figure 8: An example of pathogen evolution with α chosen such that $\alpha'' < 0$. This time no interior minima exist, and so the pathogen is inclined to globally evolve toward $\beta^P = 1$. The shaded region indicates $R_0^P > 1$. The solid lines indicate that a pathogen can persist within the host population; thin lines for limit cycles and thick lines for stable equilibria. The dot-dashed line indicates that an endemic equilibrium exists, but the pathogen can not persist. The simple dashed line indicates that no endemic equilibria exist.

6.2 Evolutionary dynamics of the Host

In this section we look at the evolutionary dynamics of the host. In particular, we are interested in the conditions needed for the host to rid itself of the pathogen through evolving lower β^H. We begin by looking at the global evolutionary dynamics of the host as the pathogen lies at its ESS. After this we look at how robust evolution of the host at the saddle-node bifurcation is to changes in k.

6.2.1 A discussion on the virulence and exponential birth rate

A common practice in all of the preceding examples has been the variation of two parameters and looking at how the dynamics of the system change in response. Indeed, this section is no exception, and so we prepare the coming examples of host evolution with brief discussions on the virulence and exponential birth rate.

The virulence. Assuming that pathogen evolution is a fast process in comparison to host evolution (cf. evolution of vertebrates to evolution of bacteria), we may ask what are the evolutionary dynamics of the host as the pathogen remains at its ESS. For this reason, a natural choice of one parameter to vary would be somehow related to the virulence; how does the host evolve as the pathogen becomes increasingly deadly? As we will see, with our choice of trade-off between the pathogen transmission rate, β^P, and the virulence, α, this is not such a straightforward question.

Recall that the singular strategy, β^{P*}, corresponding to an interior minimum of $\hat{E}_0$ is an ESS and, in particular, independent of β^H. Moreover, the locations of any of the extreme values of $\hat{E}_0$ do not change in response to varying β^H. Consequently, the derivative of $\hat{E}_0$ does not change sign at any point, implying that $\beta^P = 1$ also remains evolutionarily attracting for every β^H, given that it is attracting for some β^H.

Supposing α is of the form $v_\alpha(\beta^P)^{w_\alpha}$, where $w_\alpha > 1$, then $\hat{E}_0$ has a unique global minimum. If this minimum lies within the unit interval, then the ESS is obtained from (44), otherwise the ESS is $\beta^P_{ESS} = 1$, hence we obtain

$$\beta^P_{ESS} = \min\left(\left(\frac{\mu + \nu_I}{v_\alpha(w_\alpha - 1)}\right)^{\frac{1}{w_\alpha}},\ 1\right),$$

and furthermore

$$\begin{aligned}
&\alpha(\beta^P_{ESS}) = \frac{\mu + \nu_I}{w_\alpha - 1}, \quad \text{when} \quad \beta^P_{ESS} < 1,\\
&\alpha(1) = v_\alpha, \quad \text{otherwise.}
\end{aligned}$$

From this we see the effect of varying different quantities. If we choose to vary v_α, then $\alpha(\beta^P_{ESS})$ remains constant, given that $\beta^P_{ESS} < 1$. This is great if one wishes to

look at how host evolution reacts to changes in β^P_{ESS} without affecting the virulence. On the other hand, when $\beta^P_{ESS} = 1$, then varying v_α is an excellent choice if one wishes to vary α and nothing else.

Varying w_α seems like an interesting choice, yet perhaps somewhat complex. From the expression of $\alpha(\beta^P_{ESS})$ we immediately notice the prospect of $\alpha \to \infty$ as $w_\alpha \to 1$. In our biological context, however, it is worth pointing out that since $\beta^P \in [0, 1]$, α can not in fact escape to infinity. Indeed, the minimum of $\hat{E}_0$ lies outside of the unit interval if

$$1 < w_\alpha \leq 1 + \frac{\mu + \nu_I}{v_\alpha},$$

in which case varying w_α has no effect on either the ESS or the virulence as long as the above inequality is satisfied. If the rate of recovery is significantly bigger than the maximum virulence, $\alpha(1)$, then this inequality can be expected to hold. For example, in Figures 2 to 4, the recovery rate was set so that the expected time to recovery was 3 weeks and the risk of succumbing to the disease rather than recovering was 1%. Hence we obtain the fraction

$$\frac{\nu_I}{\alpha(1)} = \frac{\nu_I}{v_\alpha} = 99.$$

Indeed, demanding that

$$w_\alpha > 1 + \frac{\mu + \nu_I}{v_\alpha} > 100$$

in an effort to bring the global minimum of $\hat{E}_0$ within the unit interval would be absolutely ludicrous in this case. Hence, we settled for choosing $\beta^P_{ESS} = 1$ in the examples showcased in Figures 2 to 4.

Remark 10. Recall Remark 8, in which we speculated that the unrestricted evolution occurring in a neighbourhood of the interior minimum of $\hat{E}_0$ could help bridge the gap between the long periods of the limit cycles of our model and the seasonally occurring epidemics seen in the real world. As we know, the seasonally occurring influenza epidemics are not particularly deadly, and so the above reasoning seems to provide a counterpoint to this speculation. Indeed, supposing $\partial_{\beta^P}\hat{E}_0(1) < 0$, then $\beta^P_{ESS} = 1$ does not have this property of unrestricted evolution; the pathogen will remain monomorphic throughout its evolution. However, the feasibility of evolving $\beta^P = 1$ in the real world is questionable. It would imply that the infecting host would give off the pathogen to the receiving host at *every* contact. Furthermore, the maximum virulence, $\alpha(1)$, is a very theoretical concept; who knows what potential virulence a pathogen might have if it were to evolve maximum β^P?

Varying μ and ν_I have the same quite straightforward effect on β^P_{ESS} and the virulence. The virulence, in particular, is linear in both parameters. A recovered host is as good as a dead host from the point of view of the pathogen, and so this

similar relationship between the two parameters is expected. On the other hand, from the point of view of the host there is a very big difference between a recovered host and a dead host, and so the effects of varying these two parameters are not at all similar in the grand coevolutionary context.

In summary, varying v_α is a good choice if one supposes the risk of succumbing to the is fairly low. On the other hand, varying w_α is a complex and interesting choice when $\beta^P_{ESS} < 1$. Finally, varying ν_I affects the virulence in a very straightforward manner, while the effect on the host is less straightforward. Moreover, if $\beta^P_{ESS} = 1$, then varying ν_I is an excellent way to indirectly change the deadliness of the pathogen without directly changing the value of the virulence.

In the first example of this section, we've chosen the virulence to be of the form $\alpha = 0.1(\beta^P)^2$, in particular, we have fixed $v_\alpha = 0.1$ and $w_\alpha = 2$. Hence, $\hat{E}_0$ has a unique minimum in the interval $(0, 1)$ in all plots of Figure 9. That said, we've chosen to vary ν_I. Less for its effect on the virulence, and more so due to its effect on the bifurcation patterns of the system. In particular, it is interesting to compare recoverable diseases to the case where recovery is impossible. Later on, in the example showcased in Figure 12, we fix $\nu_I = 0$ and instead vary v_α as we study host evolution robustness at the saddle-node bifurcation.

The exponential birth rate. So far in the examples of this thesis we have seen two kinds of trade-offs between the exponential birth rate, a, and the host transmission rate, β^H, being used. Indeed, these trade-offs take the shape of a logistic trade-off (although part of the logistic function lies outside the realm of biological interpretation), which we used in Figures 2 to 4, and an affine trade-off, as seen in the bifurcation diagrams.

Recall that we had defined the host transmission rate as the product of the contact rate, r, and the probability that the host is unable to prevent infection, q^H. Yet, a is a function of the product of these, namely β^H. Now, as we consider the evolution of the host, we need to decide in which of these factors, q^H or r, the evolution happens. Indeed, it is reasonable to expect that a reacts very differently in response to changes in either of these factors of the transmission rate.

In Figures 2 to 4 we reasoned that at low contact rates the exponential growth rate is low, but rapidly increases as the contact rates increase. However, as the contact rate is further increased, the trade-off quickly saturates. In other words, the coupling, a', is high for low β^H, and then quickly converges to 0 as β^H increases. Take for example mammals, whose reproduction involves a period of pregnancy followed by, in many cases, an extended period of child-care during which the female will not mate again. Further increasing the contact rate will not have any effect on this natural bound on the birth rate. On the other hand, females need to be in contact with males to mate and have offspring in the first place; for this reason we assume that the exponential birth rate rapidly decreases as the contact rate approaches

0. With this reasoning, we obtain the logistic trade-off used in the aforementioned figures.

On the other hand, how a reacts in response to changes in q^H is somewhat of a mystery. However, this time there is no reason to expect the trade-off to saturate as $q^H \to 1$. High q^H means that the host is putting less effort into combating the pathogen, and so more resources are left over for growth, hence we still expect a to be increasing with q^H.

In the examples showcased in Figures 9 and 12 we've chosen to use an affine increasing trade-off between a and β^H, hence keeping the coupling, a', constant and positive. Recall that the singular strategies of the host, β^{H*}, satisfy the equation

$$D^H(\beta^{H*}) = 0 \quad \Leftrightarrow \quad a'(\beta^{H*}) = \frac{\beta^P \alpha(2\hat{E} + k\hat{S})\hat{S}\hat{I}}{(\alpha + \mu + \nu_I)\hat{N}^2},$$

Where D^H is the selection gradient of the host. Keeping the trade-off simple makes exploring the parameter space significantly easier. Moreover, this means that the results of Figure 9 are best interpreted in terms of evolution through q^H, rather than r. To contrast this, Figure 11 shows how the results of Figure 9 can change when the interpretation, and consequently the trade-off, is switched to consider evolution in the contact rate.

6.2.2 Host evolution at the pathogen ESS

Figure 9 depicts the long term evolution of the host as the recovery rate, ν_I, and the trade-off between a and β^H are varied. Here a has been chosen to be of the form

$$a(\beta^H) = 0.04 + b_a \beta^H,$$

where we vary the coupling, b_a, in the different plots of Figure 9.

The shaded region seen in the plots of Figure 9 is the region of coexistence, that is, the region where the pathogen can persist in the host population. This region has been coloured in two shades of grey to indicate the sign of the selection gradient, D^H, of the host at each point, (β^H, k), of the plot. Dark grey indicates $D^H < 0$ and light grey indicated $D^H > 0$. The boundary of these two regions indicate the singular strategies, β^{H*}. If we fix k and focus on a cross section of the plot, then β^{H*} is evolutionarily attracting if

$$D^H(\beta^{H*} - \delta) > 0 \quad \text{and} \quad D^H(\beta^{H*} + \delta) < 0$$

for arbitrarily small $\delta > 0$. Conversely, β^{H*} is evolutionarily repelling if the above inequalities are reversed.

Similarly to plots (a) and (b) of the bifurcation diagrams (Figure 5), the dashed line indicates the transcritical bifurcation, $R_0^P > 1$ to the right of the dashed line

and $R_0^P < 1$ to the left. To provide some perspective into how R_0^P changes, the dot-dashed line indicates where $R_0^P = 2$. The thick solid line indicates a Hopf bifurcation and the thin solid line indicates a saddle-node bifurcation. The region bounded by the thick and thin lines hosts the limit cycles of the system.

A horizontal line can be seen cutting through each plot. This line marks the value of $k_{\max}$, and so the host can not eradicate the pathogen through evolution above this line. Recall Theorem 11, which states that $D^H(\beta_1^H) > 0$, given that $k \geq k_{\max}$. At first glance it might look as though the host evolves lower β^H through the transcritical bifurcation even for $k \geq k_{\max}$ in many of the plots, but the mathematical impossibility of this implies that the evolutionary attractor just lies very close to the transcritical bifurcation. Particularly, in plots (a) to (c) of Figure 9 the evolutionary attractor is indistinguishable from the transcritical bifurcation.

When there is no hope of recovery, that is, $\nu_I = 0$, we see that for $k < k_{\max}$ the host invariably drives the pathogen to extinction, given that the pathogen invades before β^H is too high, otherwise the host happily submits to the pathogen and evolves toward maximum β^H. As the recovery rate, ν_I, is increased, the Hopf bifurcation appears and grows with ν_I, and the situation becomes more complex. Plots (g) and (h) clearly show the existence of limit cycles that are evolutionarily attracting. In plots (d)-(f) it can be difficult to see what happens at $k < k_{\max}$, and so the reader is referred to Figure 10, which shows enlarged plots of these cases. Indeed, in plot (d) (refer to Fig. 10(a)) the pathogen is driven to extinction, while in plot (e) (refer to Fig. 10(b)) an evolutionarily attracting limit cycle begins to appear. And finally, we see in plot (f) (refer to Fig. 10(c)) that an evolutionarily attracting endemic demographic attractor exists now for all values of k, and so the pathogen can no longer be driven to extinction.

A striking result of Figure 9 is that the coupling, b_a, must be very low for the host to evolve lower β^H. For example, in plot (i) we have $b_a = 0.004$. In other words, for every unit of β^H the exponential birth rate increases only by 0.004, less than the background death rate. Yet, we see that the region of negative selection gradient has begun to shrink, and so the host is inclined to evolve higher β^H despite the presence of the pathogen. Furthermore, here $\alpha(\beta_{ESS}^P) = 0.065$, more than the recovery rate, which is $\nu_I = 0.06$. Thus the pathogen is extremely deadly too! However, it should be noted that the recovery rates, ν_E and ν_I, are only about one order of magnitude higher than the background death rate. This could explain the heavy inclination to submit to the pathogen and evolve high β^H by the host; there is not much to be gained in avoiding the pathogen through low β^H when the expected lifetime is not very long to begin with. From these considerations we surmise that if the benefit from avoiding the pathogen altogether is great, then this allows for a negative selection gradient even when the coupling, b_a, is strong. However, it should

be noted that a long expected lifetime alone does not necessarily imply that the benefit of avoiding the pathogen is high. Indeed, this has to be balanced against the probability of recovering from the pathogen, namely

$$\frac{\nu_I}{\alpha + \mu + \nu_I}.$$

For example, with the parameter values used in the examples showcased in Figures 2 to 4, we see that the probability of surviving an infection is about 0.989. Hence, the benefit of avoiding the pathogen altogether is lessened by the fact that one is nearly certainly going to survive an infection.

Another striking feature of the plots is that the evolutionary attractor lies very close to the transcritical bifurcation, that is, the evolutionarily attracting singular strategy, β^{H*} is very close to β_1^H. What this means is that as the host reaches this evolutionary attractor, the pathogen is not only extremely vulnerable to random fluctuations in β^H but also to fluctuations in k. Suppose the host is a herbivore that benefits from warm winters, then one can expect k to decrease in response to a warm winter; easier access to food implies a stronger immune system. A pathogen that has persisted in its host throughout the millennia will probably not have managed to do so on the very edge of the region of coexistence. To counter this, one might argue, for example, that the fast pathogen evolution allows it to keep up with variations in β^H and k. However, recall Theorem 15: the pathogen ESS at an interior minimum of $\hat{E}_0$ is independent of these variations!

Turning our attention to evolution of the contact rate, r, we see in Figure 11 how the evolutionary dynamics change. In plot (a) and (b) of Figure 11 we use the affine trade-off, while in plot (c) and (d) we have switched to the logistic trade-off. Plot (e) provides a visual comparison between the two trade-offs.

Here we see that, for the most part, the evolutionary attractor lies far away from the transcritical bifurcation. This is due to the coupling between a and β^H being strong at low values of β^H, giving rise to a positive selection gradient. On the other hand, the selection gradient is now ubiquitously negative for high β^H as a result of the saturation of the trade-off. In comparison to the affine trade-off, the pathogen is no longer so vulnerable to fluctuations in β^H or k. However, note that in plot (c), evolution of the host will lead to the eradication of the pathogen at low k; something that can not happen with the affine trade-off, as seen in plot (a).

Remark 11. While it might seem like the ability to eradicate the pathogen through evolution is an advantage for the host, suggesting that the low values of $k_{\max}$ that accompany hosts with comparably long life spans (recall Remark 7) are to the disadvantage of the host, we must remember that the evolutionary eradication of the pathogen is enabled by the pathogen's ability to persist at parameter values where $R_0^P < 1$. Hence, when $k_{\max}$ is negligible, the pathogen is doomed as soon as $R_0^P < 1$.

In particular, the low $k_{\max}$ is welcome for us humans who have the ability to take deliberate action against a pathogen; as long as we lower β^H so that $R_0^P < 1$, we don't need to worry about the pathogen persisting indefinitely despite our best efforts to eradicate it.

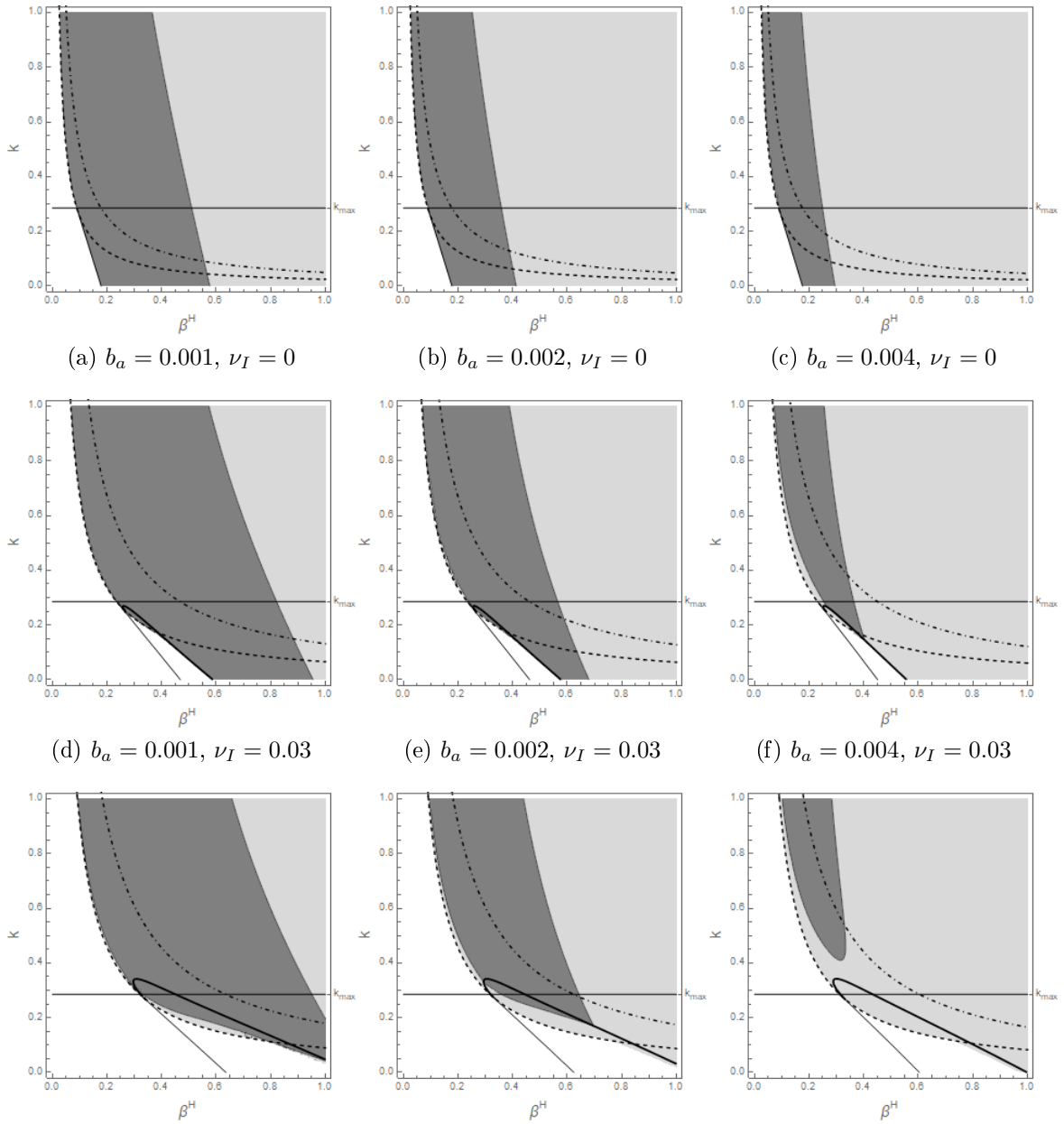

(a) $b_a = 0.001$, $\nu_I = 0$ (b) $b_a = 0.002$, $\nu_I = 0$ (c) $b_a = 0.004$, $\nu_I = 0$

(d) $b_a = 0.001$, $\nu_I = 0.03$ (e) $b_a = 0.002$, $\nu_I = 0.03$ (f) $b_a = 0.004$, $\nu_I = 0.03$

(g) $b_a = 0.001$, $\nu_I = 0.06$ (h) $b_a = 0.002$, $\nu_I = 0.06$ (i) $b_a = 0.004$, $\nu_I = 0.06$

$$\nu_E = 0.05, \qquad \mu = 0.005, \quad c = 0.02, \quad \alpha = 0.1(\beta^P)^2, \quad a = 0.04 + b_a\beta^H.$$

Figure 9: A collection of plots showcasing host evolution as the pathogen is at its evolutionary attractor for different values of b_a and ν_I. The dashed line indicates $R_0^P = 1$, the dot-dashed line indicates $R_0^P = 2$. The thick solid line indicates a Hopf bifurcation and the thin solid line indicates a saddle-node bifurcation. The endemic demographic attractors that are situated within the region bounded by the thick and thin solid lines are stable limit cycles. For each row, respectively, the values of the pair $(\beta^P_{ESS}, \alpha_{ESS})$ are (approximately): $(0.224, 0.005)$; $(0.592, 0.035)$; $(0.806, 0.065)$.

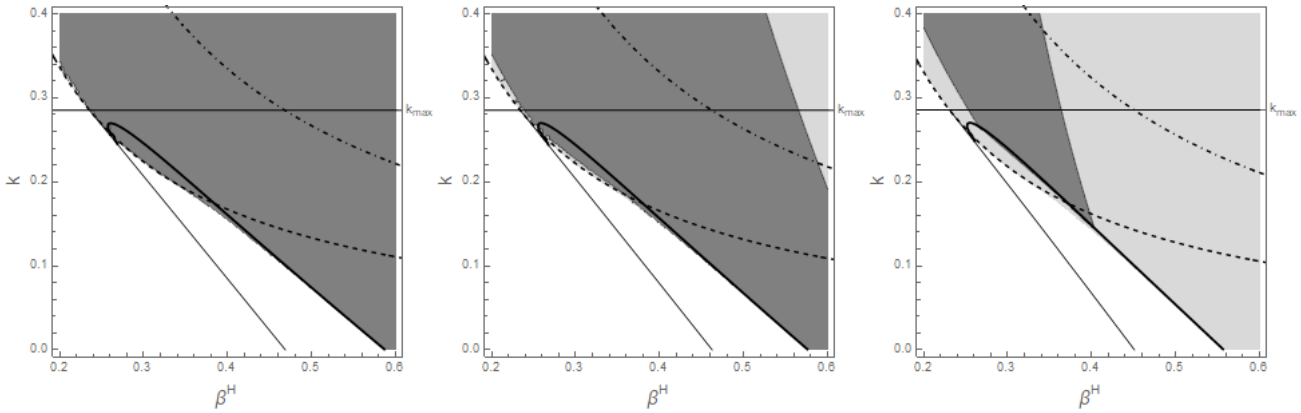

(a) $b_a = 0.001$, $\nu_I = 0.03$ (b) $b_a = 0.002$, $\nu_I = 0.03$ (c) $b_a = 0.004$, $\nu_I = 0.03$

$$\nu_E = 0.05, \qquad \mu = 0.005, \quad c = 0.02, \quad \alpha = 0.1(\beta^P)^2, \quad a = 0.04 + b_a\beta^H.$$

Figure 10: Increased resolution plots corresponding to the second row of Figure 9. Plot (a) corresponds to plot (d) of Figure 9, plot (b) to (e) and plot (c) to (f).

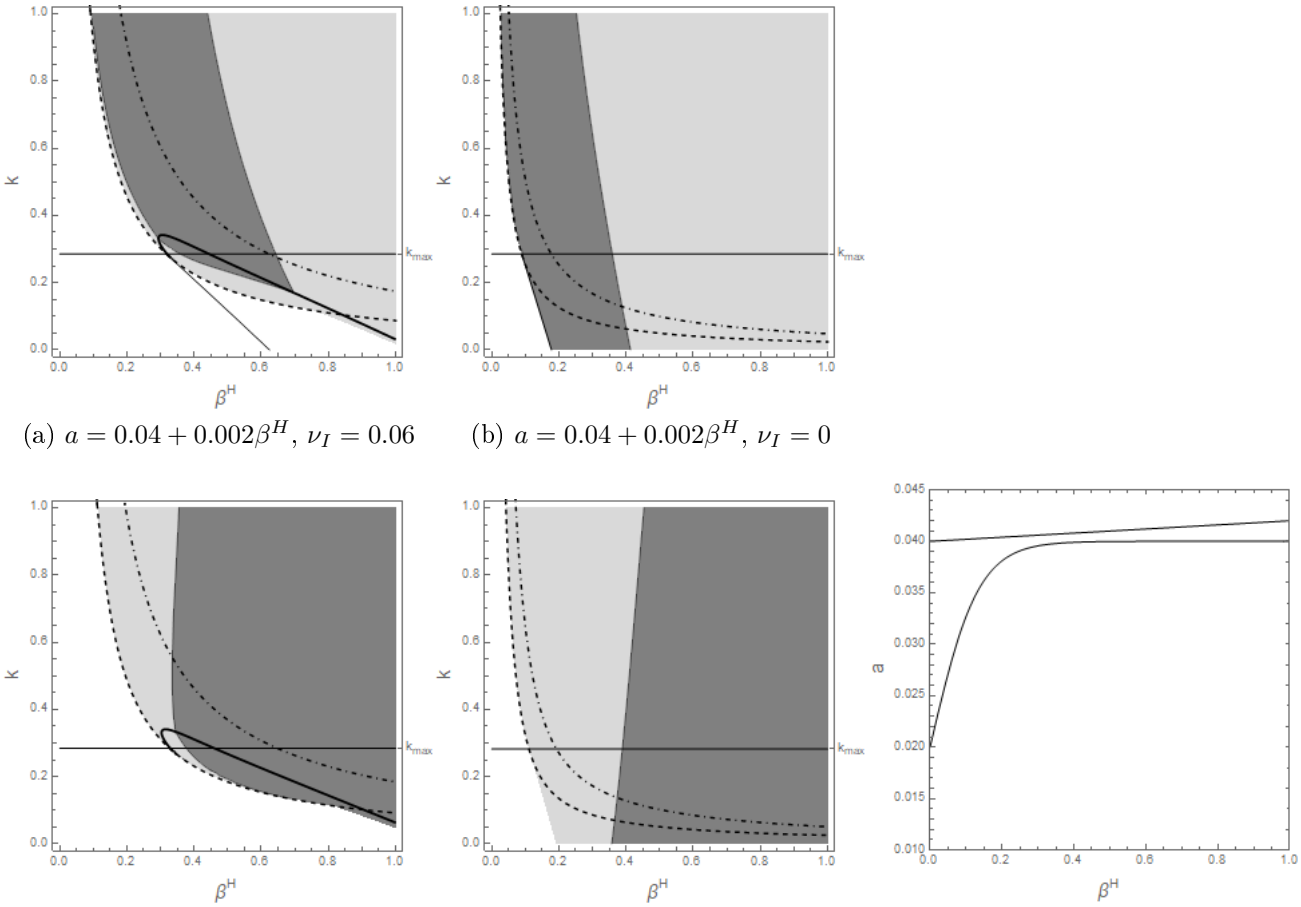

(a) $a = 0.04 + 0.002\beta^H$, $\nu_I = 0.06$ (b) $a = 0.04 + 0.002\beta^H$, $\nu_I = 0$

(c) $a = \frac{0.04}{1+e^{-15\beta^H}}$, $\nu_I = 0.06$ (d) $a = \frac{0.04}{1+e^{-15\beta^H}}$, $\nu_I = 0$ (e) A comparison of the trade-offs

$$\nu_E = 0.05, \qquad \mu = 0.005, \quad c = 0.02, \quad \alpha = 0.1(\beta^P)^2$$

Figure 11: A comparison between affine trade-off between a and β^H and a perhaps more realistic trade-off. The more complex expression for a in plots (c) and (d) caused a breakdown in the numerics when calculating the saddle-node bifurcation, hence the thin line seen in the upper row is unfortunately not present in the lower row.

6.2.3 Host evolution robustness at the saddle-node bifurcation

In this section we study conditions under which the host can evolve through the saddle-node bifurcation, hence eradicating the pathogen. The main question being: how robust is host evolution at the saddle-node to changes in k. Recall that the host can only rid itself of the pathogen when $k < k_{\max}$. Here we restrict ourselves to the cases where the saddle-node bifurcation is reached without a Hopf-bifurcation occurring.

Let us first look at an extreme case of our population model. The reason being that this extreme case can not undergo Hopf bifurcations. If we set $\alpha = \nu_I = 0$, we obtain a two-dimensional cartoon version of the original model; $\hat{N}$ remains constant at $\hat{N}_{\text{free}}$, while $\nu_I = 0$ implies that no individuals can ever enter the recovered state R. Indeed, the dynamics become

$$\begin{aligned} \frac{dE}{dt} &= (1-k)\beta^T(\hat{N}_{\text{free}} - E - I)I - (\beta^T I + \nu_E + \mu)E, \\ \frac{dI}{dt} &= k\beta^T(\hat{N}_{\text{free}} - E - I)I + \beta^T EI - \mu I. \end{aligned} \tag{45}$$

The Jacobian matrix of this system is

$$J = \begin{bmatrix} -\left((2-k)\beta^T I + \mu + \nu_E\right) & (1-k)\beta^T(\hat{N}_{\text{free}} - E - I) - (1-k)\beta^T I - \beta^T E \\ (1-k)\beta^T I & k\beta^T(\hat{N}_{\text{free}} - E - I) - k\beta^T I - \mu \end{bmatrix}.$$

And at an endemic equilibrium we have

$$k\beta^T(\hat{N}_{\text{free}} - \hat{E} - \hat{I}) = \mu - \beta^T \hat{E}.$$

Substituting this into J, we see that

$$\operatorname{tr}(J) = -2\beta^T \hat{I} - \nu_E - \mu - \beta^T \hat{E} < 0.$$

Hence, whenever the eigenvalues are complex, their real parts can never be non-negative (this is easily deduced from (29) in the proof of Theorem 12). Recall that a Hopf bifurcation occurred when a complex conjugate pair of eigenvalues was purely imaginary. Because the above Jacobian matrix can never have purely imaginary eigenvalues at an endemic equilibrium, no Hopf bifurcations can occur.

This is a nice and simple model, but without virulence the host will never be inclined to evolve lower β^H; being increasingly susceptible to the pathogen comes at no cost. However, everything being continuous, we can perturb this system while preserving much of the qualitative behaviour. In particular, we wish to keep the appearance of Hopf bifurcations to a minimum.

Figure 12 depicts host evolution at the saddle-node bifurcation. Here an effort was made to keep a and α similar to the first row in Figure 9. Indeed, they are of the form $a = 0.04 + b_a\beta^H$ and $\alpha = v_\alpha(\beta^P)^2$, where b_a and v_α are varied in the plots of Figure 12. Note that the pathogen is not assumed to be at its ESS this time, hence the choice of varying v_α. In this section we are only considering β^H in a fairly small neighbourhood around the saddle-node bifurcation value, β^H_{sn}, hence a can be taken to be a *linear approximation* of whatever the actual trade-off is. In this sense, we do not need to worry about the interpretation behind the trade-off as we did previously.

For each point (β^P, k) of the plots (a)-(i) in Figure 12, β^H has been solved such that the system is at the saddle-node bifurcation, β^H_{sn}. The thick solid line on the edge of the shaded region indicates $k_{\max}$. Indeed, for $k > k_{\max}$ there can be no biologically meaningful saddle-node bifurcation hence the shaded region does not extend above this line. Once again, the light gray region indicates a positive selection gradient, D^H, while the dark gray indicates a negative gradient. The unshaded area appearing in the lower right corner of the plots is an area where the saddle-node bifurcation is reached after a Hopf bifurcation has occurred, hence that part has been left out of the analysis. The pathogen ESS has been marked on the horizontal axis. The nearly vertical dashed line seen in each plot will be explained shortly.

Examining the shape of the region of negative gradient, we see that host evolution is indeed very robust against changes in k. In particular, for low b_a one needs to bump k almost all the way up to $k_{\max}$ for an initially negative selection gradient to change sign.

But does this result hold in a biological context? It is unlikely that a sudden change in k would result in a corresponding sudden change in β^H. Rather, suppose we are initially at the saddle-node bifurcation when $k = 0$, denote this value of the transmission rate as β^H_{sn0}. Now, suppose a sudden environmental change is such that k is increased, but β^H remains unchanged at $\beta^H = \beta^H_{sn0}$. This is why the nearly vertical dashed line is plotted; it indicates where β^H_{sn0} is a singular value, that is where $D^H(\beta^H_{sn0}) = 0$. To the right of the dashed line, we have $D^H(\beta^H_{sn0}) < 0$ and to the left we have $D^H(\beta^H_{sn0}) > 0$. Indeed, as we vary k in this context, we see that the direction of evolution remains largely unchanged here as well.

Notice that the pathogen ESS only exists in the region of negative gradient when the coupling, b_a, is low. Hence, for the system to ever reach the saddle-node bifurcation in the first place, the coupling must be very weak. Although, when this happens the pathogen is practically doomed; small variations in k will not save it from extinction.

On the other hand, looking at things from the perspective of the pathogen, recall that for our particular choice of trade-off between the virulence, α, and pathogen

transmission rate, β^P, we have

$$\beta^P_{ESS} = \left(\frac{\mu}{v_\alpha}\right)^{\frac{1}{2}} \quad \text{and} \quad \alpha(\beta^P_{ESS}) = \mu.$$

Hence, v_α has no effect on the virulence, while lowering it increases β^P_{ESS}. This means that a pathogen whose transmission rate is strongly coupled to the virulence is more likely to avoid extinction, since the ESS is low enough to reside in the region of positive gradient, while a weakly coupled pathogen finds its ESS in the region of negative gradient. At first glance, once would be tempted to call the strongly coupled pathogen more deadly than the weakly coupled pathogen, but this is contradicted by the ESS. A weakly coupled pathogen can afford to evolve higher β^P while retaining the same virulence as a strongly coupled pathogen. Indeed, we see that the host is more likely to eradicate the weakly coupled pathogen as its ESS is more likely to lie in the region of negative gradient.

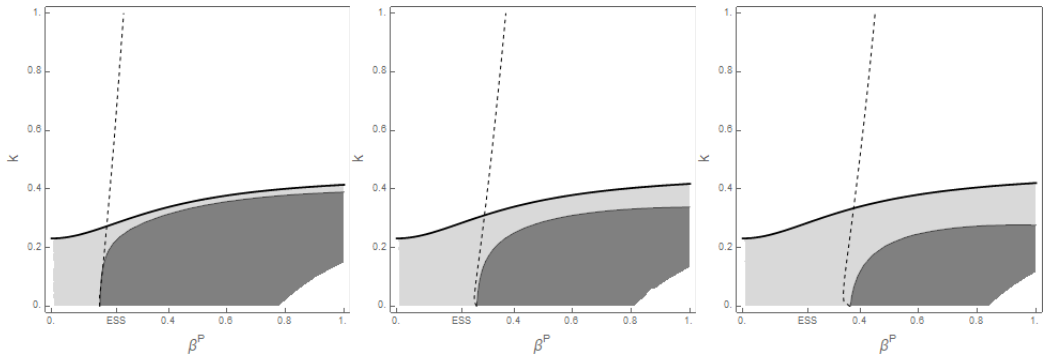

(a) $b_a = 0.002$, $v_\alpha = 0.1$ (b) $b_a = 0.006$, $v_\alpha = 0.1$ (c) $b_a = 0.01$, $v_\alpha = 0.1$

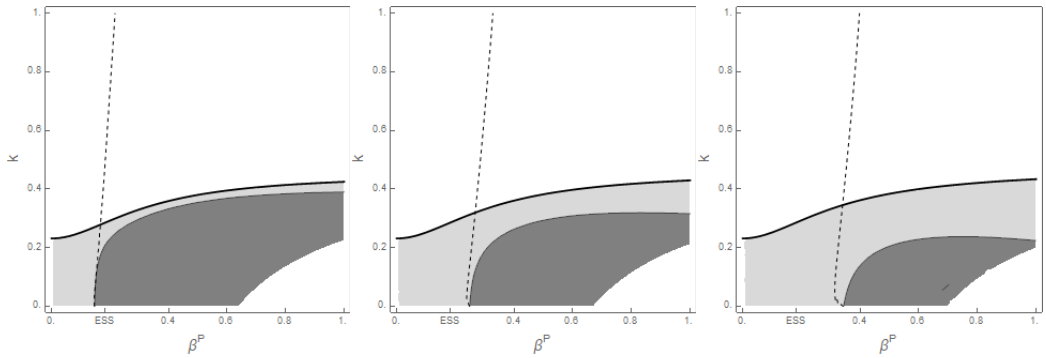

(d) $b_a = 0.002$, $v_\alpha = 0.15$ (e) $b_a = 0.006$, $v_\alpha = 0.15$ (f) $b_a = 0.01$, $v_\alpha = 0.15$

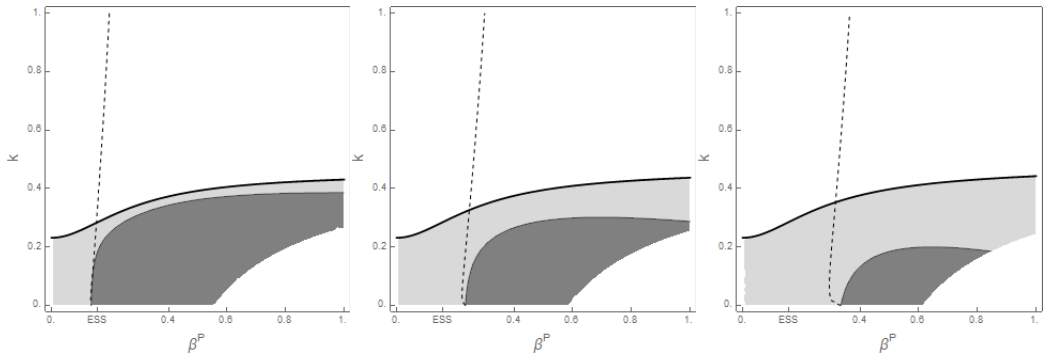

(g) $b_a = 0.002$, $v_\alpha = 0.2$ (h) $b_a = 0.006$, $v_\alpha = 0.2$ (i) $b_a = 0.01$, $v_\alpha = 0.2$

$$\nu_E = 0.05, \quad \nu_I = 0, \quad \mu = 0.005, \quad c = 0.05,$$
$$a = 0.04 + b_a \beta^H, \quad \alpha = v_\alpha (\beta^P)^2.$$

Figure 12: This figure depicts the selection gradient of β^H at the saddle-node bifurcation. As usual, the light gray regions indicate a positive gradient while the dark gray regions indicate a negative gradient. The dot-dashed line on the edge of the shaded region indicates $k_{\max}$. As expected, the edge of the region where the saddle-node bifurcation occurs coincides with $k_{\max}$. The unshaded region which appears at the lower right corner indicates that a Hopf bifurcation occurred here before the saddle-node could be reached.

7 Discussion

In this thesis, we showed that the demographic dynamics of the model described by the differential equations in (1) are very rich. In addition to endemic equilibria, we find limit cycles which give rise to cyclically occurring epidemics. Moreover, all the parameters are constant in time, hence we obtain cyclical epidemics in a model that is fairly simple in its formulation. Finally, we showed in section 6.2 that these limit cycles could be evolutionarily attracting, cementing their significance in the biological interpretation.

The model discussed in this thesis is not formulated with any specific disease in mind, and is as such not well-suited to simulate the real world. That said, due to its rich dynamics, the model provides an excellent basis for the further study of more targeted research questions.

Cyclic epidemics and seasonal variation. In Figures 2, 3 and 4, which present examples of the population dynamics following a pathogen invasion of the disease-free host, we saw that the cycles presented by the model seem to occur on a generational time-scale rather than a seasonal time-scale. Indeed, the periods of the cycles only begin to resemble that of seasonally occurring epidemics when k is very high, but in these cases the dynamics quickly converge to the endemic equilibrium, rather than a limit cycle.

Commonly, the seasonality of various diseases is modelled through a transmission rate, $\beta(t)$, that varies with time [1], [12]. As we discussed in the demographic example of section 4.4.1, the length of the period between epidemics depends on the replenishment of susceptible individuals following an epidemic. Adding a rate, γ, by which immunity is lost in order to facilitate the replenishment of susceptible individuals following an epidemic could be enough to capture cycles on a seasonal times-scale without the use of time dependent parameters. However, the effect of seasonality on disease dynamics can arguably not be denied, and as [14] shows, a system that would otherwise not oscillate, can exhibit significant oscillations when there is resonance between the intrinsic disease dynamics and seasonal variation, even when the seasonal variation is negligibly small.

In light of [14], the attempt to explain seasonal variation in terms of the cycles shown in our model is perhaps in vain. Instead, a better avenue for further research arises when one expands the questions posed in [14] to this model: what is the effect of seasonal variations on the intrinsic oscillations of our model? And can negligible seasonal variation bring about significant disturbances in the intrinsic oscillations? A particularly interesting question is whether or not seasonal variations can send the model into chaos. For example, linking seasonal variation with chaotic dynamics in an effort to provide insight into the irregularly occurring measles epidemics is something that has been studied in [15] and [16].

Predicting the long term dynamics from the short term. In addition to finding examples of indefinitely oscillating epidemics, we saw that a pathogen whose invasion leads to a stable endemic equilibrium looks very much like a cyclically occurring pathogen for at least a few generations after the initial epidemic. This property makes prediction from the observed dynamics rather weak; when a novel pathogen is introduced to a virgin host population it is practically impossible to deduce the long term dynamics simply by looking at how the epidemic proceeds. However, this problem is remedied by the fact that limit cycles hint at the existence of Hopf bifurcations. Hence, to predict the long term dynamics of a novel disease, one can measure the model parameters and see how the real world fits the bifurcation patterns of the model.

Unfortunately, here we need to point out a major shortcoming of the thesis. The fitting of real world data to the model was never the major consideration in this thesis, and is admittedly an afterthought. Nevertheless, one should always study a model as if it were to be applied to real world data. In this sense, ν_E has major importance for the analysis of the model as it is arguably the most difficult parameter to estimate. Hence, determining the sensitivity of the model to variations in ν_E would have been an important question to answer in this thesis.

Pathogen eradication through evolution. In the examples of section 6.1.3 we saw interesting cases where the pathogen committed evolutionary suicide when k was sufficiently low. In particular, Corollary 7 states that $k < k_{\max}$ at the ESS is a necessary condition for the evolutionary suicide of the pathogen. We deduced that, in a sense, the effort on the behalf of the pathogen to minimise $\hat{E}_0$ backfired at low k, due to the small fraction of susceptibles being immediately infectious. Conversely, although lowering β^H is detrimental to the pathogen as well, in this case pathogen suicide would not occur, provided that k remained high enough, since minimising $\hat{E}_0$ was always beneficial for the pathogen in this case. In addition to the pathogen, similar results were found for the host. Here Theorem 11 implies that $k < k_{\max}$ is a necessary condition for pathogen eradication through host evolution, the examples of which we saw in section 6.2.2. These properties of $k_{\max}$ make it an important predictor of the possible evolutionary outcomes. Moreover, it is a very practical quantity in the sense that it is entirely defined by the model parameters.

The eradication of the pathogen through evolutionary means is an interesting find that helps us further our understanding of the complex relationship between hosts and their pathogens as they have coevolved through the millennia. Indeed, the prospect of some regions of the parameter space being unable to support evolutionarily stable endemic demographic attractors suggests that not every kind of pathogen is to be expected to exist in any given host. The evolutionary predictions provide a basis for comparing and estimating the accuracies of our models to real-world data, hence enabling us to not only formulate better descriptive models but

also better predictive models.

In light of these considerations, an interesting further question is studying whether or not analogues of $k_{\max}$ can be found in more realistically formulated models. Recall that $k_{\max}$ was the threshold, below which a backward transcritical bifurcation would occur at β_1^H. Hence, any model that exhibits this bifurcation, and a subsequent biologically meaningful saddle-node bifurcation, should be expected to admit some kind of an analogue to $k_{\max}$.

8 Appendix

8.1 Disease-free dynamics

In the absence of a pathogen the demographic dynamics become one dimensional:

$$\frac{dN}{dt} = (a - \mu - cN)N. \tag{46}$$

This system has two equilibria, namely the trivial equilibrium, $\hat{N} = 0$, and the disease-free equilibrium, $\hat{N}_{\text{free}} = (a - \mu)/c$.

8.1.1 Stability analysis

It is easy to see that when $N < \hat{N}_{\text{free}}$, then

$$\frac{dN}{dt} = a - \mu - cN > a - \mu - c\hat{N}_{\text{free}} = 0,$$

hence the trivial equilibrium is unstable and repelling. On the other hand, suppose $N > \hat{N}_{\text{free}}$, then

$$\frac{dN}{dt} = a - \mu - cN < 0.$$

In conclusion $\hat{N}_{\text{free}}$ is a globally attracting equilibrium, and so it is stable as well.

8.1.2 Evolutionary analysis

Let us define the rare mutant host, N_{mut}, dynamics in an equilibrated resident host population, N_{res}.

$$\frac{dN_{mut}}{dt} = (a_m - \mu - c\hat{N}_{res})N_{mut}.$$

At equilibrium $\hat{N}_{res} = (a_r - \mu)/c$ and so the above becomes

$$\frac{dN_{mut}}{dt} = (a_m - a_r)N_{mut}.$$

Indeed, this is positive if and only if $a_m - a_r > 0$, hence the mutant can invade if and only if $\beta_m^H > \beta_r^H$.

Invasion implies substitution. Can the mutant and resident hosts coexist when the pathogen is absent?

Let us denote the total population density of the mutant and resident as $N_T = N_{mut} + N_{res}$. Moreover, for the sake of argument, suppose the mutant is invasive, that is, $a_m > a_r$. The full dynamics of the resident-mutant system are given by

$$\frac{dN_{mut}}{dt} = (a_m - \mu - cN_T)N_{mut}$$
$$\frac{dN_{res}}{dt} = (a_r - \mu - cN_T)N_{res}.$$

Now, notice that $\dot{N}_{mut} > 0$ whenever $N_T < \hat{N}_{\text{free}}(\beta_m^H)$. Furthermore, $\dot{N}_{res} < 0$ and $\dot{N}_{mut} = 0$ when $N_T = \hat{N}_{\text{free}}(\beta_m^H)$. This means that the set

$$\{(N_{res}, N_{mut}) \mid N_T \leq \hat{N}_{\text{free}}(\beta_m^H)\}$$

is forward invariant, the boundary is repelling when $N_{res} > 0$ and N_{mut} is always growing in the interior of this set. All that remains is to note that for a sufficiently small initial mutant population, the initial condition of the mutant invasion event satisfies $\hat{N}_{res} + N_{mut} < \hat{N}_{\text{free}}(\beta_m^H)$, in which case the orbit will begin at a point where N_{mut} is growing. Because N_{mut} is growing in the interior, the orbit must eventually reach the boundary of the forward invariant set, but the boundary is repelling for all points where $N_{res} > 0$, hence we conclude that the orbit eventually reaches the point $(\hat{N}_{mut}, \hat{N}_{res}) = (\hat{N}_{\text{free}}(\beta_m^H),\ 0)$; the mutant replaces the host as the new resident.

8.2 Stability of the disease-free equilibrium against pathogen invasion

In this section we show that the disease-free equilibrium, $\hat{N}_{\text{free}}$, is indeed unstable when $R_0^P > 1$ and stable when $R_0^P < 1$.

The Jacobian matrix, J, of the system (1) evaluated at $(N, E, I, R) = (\hat{N}_{\text{free}}, 0, 0, 0)$ is

$$J = \begin{bmatrix} -(a-\mu), & 0, & -\alpha, & 0 \\ 0, & -(\mu+\nu_E), & (1-k)\beta^T \hat{N}_{\text{free}}, & 0 \\ 0, & 0, & \beta^T k \hat{N}_{\text{free}} - (\alpha+\mu+\nu_I), & 0 \\ 0, & 0, & \nu_I, & -\mu \end{bmatrix}.$$

Thus, the characteristic equation $\det(J - \lambda\mathbb{I}) = 0$, where $\mathbb{I}$ is the identity matrix, is as follows:

$$-(a-\mu+\lambda)(\mu+\nu_E+\lambda)\left(\beta^T k \hat{N}_{\text{free}} - (\alpha+\mu+\nu_I) - \lambda\right)(\mu+\lambda) = 0.$$

Evidently, three of the four eigenvalues are always negative. The fourth eigenvalue obtains the value

$$\lambda_4 = \beta^T k \hat{N}_{\text{free}} - (\alpha + \mu + \nu_I).$$

The sign of which is equivalent to the sign of $R_0^P - 1$. Indeed, when $R_0^P < 1$, then $\lambda_4 < 0$ and the disease-free equilibrium is stable, while if $R_0^P > 1$, then $\lambda_4 > 0$ and the disease-free equilibrium is unstable.

8.3 Invasion implies substitution at the endemic equilibrium

In this section we show that our model fits the class of models considered in [11], which proves that an invasive mutant host replaces the resident host whenever the selection gradient at the resident strategy, $D^H(\beta_r^H)$, is non-zero and mutation steps are sufficiently small.

The class of models discussed in [11] are formulated as follows:

$$\begin{aligned}
\dot{n}_{i,t} &= F(\beta_i^H, e_t, \theta_t) n_{i,t}, \\
\dot{e}_{1,t} &= G_1(e_t, \theta_t) + \sum_i H_1(\beta_i^H, e_t, \theta_t) n_t, \\
e_{2,t} &= G_2(e_t, \theta_t) + \sum_i H_2(\beta_i^H, e_t, \theta_t) n_{i,t}, \\
\dot{\theta}_t &= A(\theta_t) + B(\theta_t)\dot{W}.
\end{aligned} \tag{47}$$

Indeed, at face value this formulation looks vastly different than our model formulation. However, as we will see this is not the case. Here we have indicated time dependency by the subscript t. The vector n_t is the vector of sub-population densities and $e_t = (e_{1,t}, e_{2,t})$ is an environmental feedback function. Note that $e_{2,t}$ is defined implicitly. The parameter θ_t is a stochastic driver function, which adds noise to the otherwise deterministic environment. F is a matrix that operates linearly on n_t once the environment has been fixed. The functions G_1 and G_2 are intrinsic dynamics of the virgin environment and H_1 and H_2 describe how a population with the strategy β_i^H impacts the environment. Furthermore, F, G_1, H_1, G_2 and H_2 are required to be sufficiently smooth (as per assumption **A2** in [11]), but we do not need to worry about this; it will be clear that our functions will be smooth in all variables.

Our model is completely deterministic, and so no stochastic drivers exist, thus $\theta_t = \dot{\theta}_t = 0$. We denote the vector of sub-population densities as $n_{i,t} = (S_{i,t}, E_{i,t}, I_{i,t}, R_{i,t})$, where the index i refers to the type of the host, the types being m for mutant and r for resident. We begin by writing our model in terms of a matrix operating on the

population vector. We obtain

$$\dot{n}_{i,t} = \begin{bmatrix} a_i - cN_{T,t} - \beta_i^T I_{T,t} - \mu, & (a_i - cN_{T,t}) + \nu_E, & (a_i - cN_{T,t}), & (a_i - cN_{T,t}) \\ (1-k)\beta_i^T I_{T,t}, & -(\beta_i^T I_{T,t} + \mu + \nu_E), & 0, & 0 \\ k\beta_i^T I_{T,t}, & \beta_i^T I_{T,t}, & -(\alpha + \mu + \nu_I), & 0 \\ 0, & 0, & \nu_I, & -\mu \end{bmatrix} n_{i,t}.$$

Here $N_{T,t} = N_{m,t} + N_{r,t}$ is the total combined population size of the mutant and resident, and $I_{T,t} = I_{m,t} + I_{r,t}$ is, correspondingly, the total size of the infectious sub-population. Now we need to choose a suitable environmental feedback function so that the the matrix above is independent of the population vector when the environment has been fixed. Let us choose $e_{1,t} = 0$ and $e_{2,t} = (N_{T,t}, I_{T,t})$. Since $e_{1,t} = 0$, we shorten the notation and denote $e_t = e_{2,t}$. Now we obtain

$$\dot{n}_{i,t} = \begin{bmatrix} a_i - ce_t^1 - \beta_i^T e_t^2 - \mu, & a_i - ce_t^1 + \nu_E, & a_i - ce_t^1, & a_i - ce_t^1 \\ (1-k)\beta_i^T e_t^2, & -(\beta_i^T e_t^2 + \mu + \nu_E), & 0, & 0 \\ k\beta_i^T e_t^2, & \beta_i^T e_t^2, & -(\alpha + \mu + \nu_I), & 0 \\ 0, & 0, & \nu_I, & -\mu \end{bmatrix} n_{i,t}.$$

$$e_t = (N_{T,t}, I_{T,t}) = \begin{bmatrix} 1, & 1, & 1, & 1 \\ 0, & 0, & 1, & 0 \end{bmatrix} (n_{m,t} + n_{r,t})$$

Here e_t^i is the i^{th} component of e_t. Indeed, our model has been shown to fit the description of (47), hence the successful invasion by a mutant host leads to the replacement of the resident, provided that the selection gradient is non-zero and mutations are sufficiently small.

References

[1] Diekmann, O., Heesterbeek, H. and Britton, T. (2013). Mathematical tools for understanding infectious diseases. Princeton University Press.

[2] Diekmann O., Heesterbeek J. A. P. and Roberts M. G. 2009. The construction of next-generation matrices for compartmental epidemic models. J. R. Soc. Interface. 7: 873–885

[3] Geritz, S., Kisdi, É., Meszéna, G. and Metz, J. A. J. Evolutionarily singular strategies and the adaptive growth and branching of the evolutionary tree. Evolutionary Ecology 12, 35–57 (1998).

[4] Durinx, M., (Hans) Metz, J.A.J. and Meszéna, G. Adaptive dynamics for physiologically structured population models. J. Math. Biol. 56, 673–742 (2008).

[5] Gyllenberg, M., Parvinen, K., and Dieckmann, U. (2002). Evolutionary suicide and evolution of dispersal in structured metapopulations. Journal of mathematical biology, 45(2), 79-105.

[6] Meszena et. al, 2001. Evolutionary Optimisation Models and Matrix Games in the Unified Perspective of Adaptive Dynamics.

[7] Boldin, Barbara. (2006). Introducing a Population into a Steady Community: The Critical Case, the Center Manifold, and the Direction of Bifurcation. SIAM Journal on Applied Mathematics. 66. https://doi.org/10.1137/050629082

[8] Reece, J. B. et al. (2011). Campbell Biology (9th edition). Benjamin Cummings / Pearson.

[9] V.I. Arnold (1973). Ordinary Differential Equations. MIT Press, Cambridge, MA.

[10] Kuznetsov, Yuri (1998). Elements of Applied Bifurcation Theory (2nd edition). Springer-Verlag New York, Inc.

[11] Cai, Y., Geritz, S. (2020). Resident-invader dynamics of similar strategies in fluctuating environments. Journal of mathematical biology. https://doi.org/10.1007/s00285-020-01532-8

[12] Buonomo, B., Chitnis, N. and d'Onofrio, A. Seasonality in epidemic models: a literature review. Ricerche mat 67, 7–25 (2018). https://doi.org/10.1007/s11587-017-0348-6

[13] W. J. W. Botzen and J. C. J. M. Van den Bergh, (2009). Managing natural disaster risks in a changing climate, Environmental Hazards, 8:3, 209-225, DOI: https://doi.org/10.3763/ehaz.2009.0023

[14] Dushoff, J. et al. Dynamical resonance can account for seasonality of influenza epidemics, (2004). Proceedings of the National Academy of Sciences (vol. 101). National Academy of Sciences. https://www.pnas.org/content/101/48/16915.full.pdf

[15] B. T. Grenfell, (1992). Chance and Chaos in Measles Dynamics, Journal of the Royal Statistical Society: Series B (Methodological), pp. 383-398. Royal Statistical Society. DOI: https://doi.org/10.1111/j.2517-6161.1992.tb01888.x

[16] B. T. Grenfell and B. M. Bolker, (1993). Chaos and biological complexity in measles dynamics. Proc. R. Soc. Lond. B.25175–81 http://doi.org/10.1098/rspb.1993.0011

[17] Buitrago-Garcia, D et al., (2020). Occurrence and transmission potential of asymptomatic and presymptomatic SARS-CoV-2 infections: A living systematic review and meta-analysis. PLOS Medicine (vol. 17). Public Library of Science. https://doi.org/10.1371/journal.pmed.1003346

[18] Mercatelli D and Giorgi F. M. (2020). Geographic and Genomic Distribution of SARS-CoV-2 Mutations. Frontiers in Microbiology (vol. 11). https://www.frontiersin.org/article/10.3389/fmicb.2020.01800

[19] https://www.cdc.gov/csels/dsepd/ss1978/lesson1/section10.html

[20] A. D. Luis et al. (2013). A comparison of bats and rodents as reservoirs of zoonotic viruses: are bats special? Proceedings of the Royal Society B: Biological Sciences (vol 280). https://doi.org/10.1098/rspb.2012.2753